Targeting the Hsp90 Molecular Chaperone and Resistant Pathways in *BRAF*-mutant Melanoma

by

Jaquelyn Nicole Sanchez

A dissertation submitted in partial fulfillment
of the requirements for the degree of
Doctor of Philosophy
(Pharmacology)
in the University of Michigan
2020

Doctoral Committee:

Professor Mark S. Cohen, Chair
Professor Yoichi Osawa
Professor Leslie Satin
Professor Shaomeng Wang

Jaquelyn Nicole Sanchez

jaquesan@umich.edu

ORCID iD: 0000-0001-8264-2688

Dedication

To my late grandmother, Mary Silva.

Acknowledgments

The past five years in Ann Arbor, as a Ph.D. student, have undoubtedly been some of the most challenging. Still, despite the adversity, there was a tremendous amount of personal growth and unforgettable memories. And for this, I am immensely grateful to my mentors, colleagues, family, and friends for their endless support and encouragement throughout the journey.

First, I would like to acknowledge my advisor, Dr. Mark Cohen. Thank you for giving me autonomy during graduate school and in the lab. The independence instilled several attributes in me, beyond the bench, that will set me up for success in the future. Your optimistic mindset is influential and taught me the importance of looking at the bigger picture, even and particularly when it came to my project. I would also like to acknowledge my thesis committee members. Dr. Yoichi Osawa, thank you for providing constructive and actionable feedback, especially with grant writing and 646 seminar presentations. Dr. Leslie Satin, thank you for being with me every step of the way as a rotation mentor, prelim committee chair, committee member, and of course, sharing a LA/SoCal connection. Dr. Shaomeng Wang, thank you for providing technical and knowledgeable advice on how to refine the therapeutic combination and mechanistic aspects of my project. Thank you all for your time and investment in me as a Ph.D. student. I appreciate your valuable insights during our meetings, and otherwise, to enhance my dissertation work and help me become the confident, Michigan-trained scientist I am today.

To the current and past members of the Cohen laboratory, thank you for always supporting me – technically in the lab and mentally. In particular, I would like to acknowledge Dr. Chitra Subramanian for helping plan experiments, teaching me new techniques, and providing solace when I needed it most. Additionally, thank you to Dr. Ton Wang for collaborating on manuscripts, discussing experiment results, and keeping me sane with banter in our office. Thank you to our collaborators, Drs. Brian Blagg (University of Notre Dame) and Barbara Timmerman (Kansas University), for providing me with novel Hsp90 inhibitors, without your compounds this dissertation would genuinely not be possible.

Thank you to the University of Michigan for providing me with the opportunity and a world-class academic community to not only achieve my goals but reshape and set new ones. Next, thank you to the Department of Pharmacology for giving me a scientific home and unmatched resources to grow into a poised pharmacologist. I would like to acknowledge Dr. Isom, our bold and spirited leader, thank you for your unbiased commitment to the success of each student. Thank you to the administrative staff for all of your work behind the scenes to make our department run smoothly. A big thank you to Lisa Garber and Liz Oxford for accommodating every student, often putting our needs before your own. Thank you to the Department of Surgery for your support and inclusion on the research team.

I am thankful for various funding sources throughout graduate school to support my dissertation research – the Program in Biomedical Sciences (University of Michigan Medical School), Rackham Merit Fellowship (University of Michigan Rackham Graduate School), Pharmacological Sciences Training Program (NIH National Institutes of General

Medical Sciences T32-GM007767) and Genetics Training Program (NIH National Institutes of General Medical Sciences T32-GM007544).

Next, I would like to thank my undergraduate mentor, Dr. Sylvine Deprele, at Mount St. Mary's University in Los Angeles, CA. Thank you for being a role model, inspiring me to pursue graduate school, and advocating for me. I will always cherish our conversations, scientific, and otherwise, trips to conferences, and lab group discussions. Drs. Luisa Nogaj, Stacey Peterson, and Eric Stemp thank you for also being catalysts in my graduate career and pursuit of becoming a scientist.

Finally, thank you to my family and friends. Debbie and Jerry Sanchez, I cannot begin to put into words what it means to have such loving and supportive parents as I do with you two. Thank you for giving me the mental and emotional support needed to preserve through graduate school and accomplish all that I have. To my sisters, Loni and Gina, thank you for always being a phone call or text away and visiting me in Michigan, especially to take care of me after ACL surgery. I would also like to acknowledge the empathetic and encouraging friendships I gained while in Michigan. Shout out to Margaret, Danny, Rossen, Kelly, Julie, Chiamaka, and Kelsey (among many others) that positively contributed to my mental health and overall well-being, enriching my dissertation work. Last, to Mike Isaacs, thank you for sharing your ambitious outlook and being a supportive significant other, even and mostly when you had no idea the premise of my scientific rants. You thought me to be resilient and the value of having a tenacious mindset in everything I do.

I was so fortunate to have you all along for the journey. Thank you!

Table of Contents

List of Tables

List of Figures

Abstract

Melanoma remains the most aggressive and fatal type of skin cancer. In greater than 50% of cases, patients present with an activating *BRAF* mutation ($BRAF^{+}$), leading to upregulated mitogen-activated protein kinase (MAPK) pathway signaling. Of these patients, 80-90% have a missense mutation at codon 600 (e.g., $BRAF^{V600E}$), making the mutant form of the protein an attractive and druggable target. In 2011, the FDA approved combination therapy of $BRAF^{+}$ and MEK inhibitors (BRAFi/MEKi), like vemurafenib and cobimetinib (Ve/Cb), for use in unresectable late-stage melanoma patients, drastically changing treatment options and initial outcomes. Still, the majority of patients become refractory to BRAFi/MEKi within the first year of treatment. The lack of treatment durability underscores the need for novel therapeutic strategies and drug candidate development, such as the utilization of molecular chaperone inhibitors.

The 90-kDa heat shock protein (Hsp90) is a molecular chaperone and responsible for stabilizing the protein folding of “client” proteins that interact with the heterochaperone complex that Hsp90 forms with the 70-kDa heat shock protein (Hsp70) and other co-chaperones. These clients are involved in several cellular signaling pathways and processes, highlighting the significance of chaperone function in eukaryotic cells. Interestingly, Hsp90 expression increases several-fold in cancer cells to compensate for cellular stress and client protein dependence on chaperone function. To-date 18 small molecule Hsp90 inhibitors (Hsp90i) entered clinical trials, of which 94.4% target the N-terminus (NT-Hsp90i) but failed to get FDA approval. The NT-Hsp90i are effective and

potent, but pan-inhibitors of all four Hsp90 isoforms. In clinical trials, patients require dose-escalation of NT-Hsp90i to reach a therapeutic effect, ultimately leading to dose-limiting toxicities (DTL). Studies suggest a link between DTLs and the activation of the heat shock response (HSR), especially the cytoprotective role of Hsp70. Previously, our lab, with collaborators, developed novel C-terminal Hsp90i (CT-Hsp90i) and showed efficacy in several cancer models *in vitro* and *in vivo* while mitigating the HSR, suggesting a decreased toxicity profile compared to NT-Hsp90i.

For this dissertation, I researched therapeutic resistance mechanisms in $BRAF_+$ melanoma through various preclinical *in vitro* studies that targeted Hsp90. Specifically, I tested the hypothesis that several resistance-promoting processes require Hsp90 function and, therefore, could be targeted with an Hsp90i to simultaneously knockdown resistance pathways and oncogenic processes. First, I showed effective melanoma cell death using the CT-Hsp90i KU758 at potent micromolar concentrations (e.g., IC_{50} = 0.36μM – 0.43μM). Next, I demonstrated robust synergy (e.g., CI<0.5) of KU758 when combined with either a BRAFi or MEKi to target two resistance pathways effectively (e.g., MAPK/Erk and PI3K/Akt), significantly mitigate melanocyte migration, and downregulate key Hsps involved in HSR activation. Finally, I accessed publicly available genomic data via the National Cancer Institute and The Cancer Genome Atlas (TCGA) program to identify additional genes of interest in $BRAF_+$ melanomas. Using a clustered heatmap of RNA expression data, I distinguished genes of interest based on common expression alterations amongst a subset of $BRAF_+$ melanoma patients to provide a genetic perspective in the context of Hsp90i use in melanoma patients.

Collectively, this work reviews the use of and development of several small

molecule inhibitors in melanomas (e.g., BRAFi/MEKi and Hsp90i), identifies a novel and effective KU758-combination approach in $BRAF_{+}$ melanomas, and gives insight into future therapeutic directions based on various translational and genetic signatures in these difficult-to-treat tumors.

Chapter 1
BRAF and MEK Inhibitors: Use and Resistance in BRAF-Mutated Cancers[1]

Abstract

The mitogen activated protein kinase/extracellular signal-related kinase (MAPK/ERK) signaling pathway serves an integral role in growth, proliferation, differentiation, migration, and survival of all mammalian cells. Aberrant signaling of this pathway is often observed in several types of hematologic and solid malignancies. The most frequent insult to this signaling cascade, leading to its constitutive activation, is to the serine/threonine kinase rapidly accelerating fibrosarcoma (RAF). Considering this, the development and approval of various small molecule inhibitors targeting the MAPK/ERK pathway has become a mainstay of treatment as either mono- or combination therapy in these cancers. Although effective initially, a major clinical barrier with these inhibitors is the relapse of patients due to drug resistance. Knowledge of the mechanisms of resistance to these drugs is still premature, highlighting the need for a more in-depth understanding of how patients become insensitive to these pharmacologic interventions. Herein, we will succinctly summarize the milestones in the approval of select MAPK/ERK pathway inhibitors, their use in patients, and major modes of resistance.

[1] This chapter was published in *Drugs* (PMID: 29488071) and completed in collaboration with the following authors: Ton Wang and Mark S. Cohen.

Introduction

The MAPK/ERK signaling pathway is evolutionarily conserved and critical in regulating cell growth, proliferation, differentiation, migration, and survival [1]. Unfortunately, in many cancers including melanoma, thyroid, colorectal, non-small cell lung cancer (NSCLC), and hairy cell leukemia (HCL) this signaling pathway is altered leading to uncontrolled cellular processes, constitutive activation and cancer cell growth. Given the strong link of aberrations in this pathway and cancer cell growth, targeted inhibition of this pathway has become a central focus of cancer therapeutic development in recent years [2]. This effort has led to the development and Food and Drug Administration (FDA) approval of several small molecule inhibitors targeting mitogen-activated protein kinase/extracellular-signal regulated kinase (MAPK/ERK) pathway tyrosine kinase proteins such as BRAF and MEK [3,4]. The MAPK/ERK pathway is activated by extracellular signaling molecule(s) that bind to their respective trans-membrane receptor tyrosine kinases (RTKs), such as epidermal growth factor (EGF) and its receptor (EGFR), respectively. Upon receptor activation, the extracellular signal is transduced inside the cell, subsequently activating the GTPase, rat sarcoma protein (RAS), via guanine nucleotide exchange from guanosine diphosphate (GDP) to guanosine triphosphate (GTP). The active GTP-bound- RAS can then initiate activation of the three-tier MAPK cascade – RAF → MEK → ERK (RAF, rapidly accelerated fibrosarcoma; MEK, mitogen activated protein kinase). As the final protein kinase in the pathway, activated ERK is then able to phosphorylate downstream cytoplasmic and/or nuclear effectors that regulate and ultimately alter cell growth, proliferation, differentiation, migration, and survival [1-3].

As mentioned previously, the MAPK/ERK pathway is frequently altered at its early stages. This includes overexpression/amplification of RTKs, activating mutations to RTKs, sustained production of signaling molecules, and point mutations of RAS or RAF. Although the MAPK/ERK signaling pathway can be altered at various places, many cancers present with mutations to RAF [5,6]. In melanoma, more than 50% of patients present with a point mutation to the BRAF isoform at codon 600, where a valine is substituted for glutamate (V600E) in almost 90% of cases [7]. A recent genomic analysis of melanomas through next-generation sequencing and the cancer genome atlas project demonstrated that BRAF hot-spot mutations are the most common mutation identified, with 52% harboring BRAF somatic mutations; the most common being V600E (75%), followed by V600K (11%), K601 (3%), and V600R (2%). Both BRAF V600 and K601 hot-spot mutations were anti-correlated with hot-spot NRAS mutations while BRAF non-hot-spot mutations co-occurred with RAS (N/H/K) hot-spot and NF1 mutations [8]. Similar to melanoma, approximately 45% of papillary thyroid cancers and 10% of colorectal cancer patients harbor similar BRAF mutations [9-11]. Interestingly, this same mutation has been found in 100% of HCL patients [12]. It has become apparent in the last few years that a large subset of patients with these cancers are affected by aberrations to the MAPK/ERK pathway, specifically BRAF, which has led to the development and approval of small molecule BRAF inhibitors for the treatment of these malignancies. While BRAF has been shown as an effective target in the MAPK/ERK pathway for several cancers where this pathway is aberrant, other selective small molecule inhibitors of MEK, the downstream effector of RAF, have also been recently developed and are now FDA approved for use in cancer patients [13]. Despite their initial efficacy, however, the biggest barrier faced in

the clinic with these selective small molecule inhibitors is the emergence of resistance following treatment in a majority of patients. This resistance can come from a myriad of escape mechanisms that cancer cells have developed to overcome this targeted drug effect. Given the multiple mechanisms of resistance that exist with these inhibitors, overcoming this resistance does not have a simple solution and is the ongoing work of many researchers and clinicians.

In this review, we will discuss landmark clinical trials investigating the use of MAPK/ERK pathway inhibitors as monotherapy and in combination for the treatment of melanoma, thyroid cancer, colorectal cancer, NSCLC, and HCL. Further discussion will also describe a detailed overview of the mechanisms of resistance to these inhibitors and the current clinical application of these inhibitors including their application in standard-of-care treatment regimens, costs, and side effects.

MAPK/ERK Pathway Inhibitors as Monotherapies

BRAF Inhibitors

Vemurafenib

Vemurafenib (formerly PLX4032; brand name Zelboraf; developed by Plexxikon and Genentech) was approved by the FDA in 2011 and by the European Commission in 2012 for the treatment of $BRAF_{V600E}$-mutated late-stage melanoma. This reversible, small molecule inhibitor is orally administered and causes apoptosis of melanoma cells by selectively targeting $BRAF_{V600E}$ mutations.

In 2009, a Phase I multicenter study was conducted in patients with metastatic cancer to identify the maximum tolerated dose and safety and pharmacokinetic profiles

of the selective BRAF inhibitor [14]. Of the 55 patients enrolled in the dose-escalation study, 49 patients had metastatic melanoma and 16 patients in this subset harbored the $BRAF_{V600E}$ mutation. Newly enrolled patients were administered PLX4032 at 160 mg twice daily followed by escalation. During the study, dose-limiting toxicities were first observed at 720 mg twice daily of PLX4032 with minor adverse effects (AEs) such as grade 2 or 3 rash, fatigue, and arthralgia. These AEs were also observed in patients given doses up to 1120 mg twice daily. Of the 16 patients with $BRAF_{V600E}$ mutant melanomas, partial and complete responses were seen in 11 patients (10 and 1, respectively). Following the dose-escalation phase of the study, an extension phase was completed in an additional 32 patients with $BRAF_{V600E}$-mutated metastatic melanoma. Patients were administered 960 mg twice daily and showed partial and complete responses in 24 and 2 patients, respectively. From this, the recommended Phase II dose (RP2D) was established as 960 mg twice daily. Overall, this study demonstrated that the use of vemurafenib as a targeted therapy in humans with metastatic melanoma harboring the activating $BRAF_{V600E}$ mutant is safe. Additionally, dosing for further clinical trials was determined.

In 2011, the Phase II clinical trial (BRIM-2) conducted by Ribas and colleagues was pivotal in showing the efficacy of vemurafenib in previously treated metastatic melanoma patients with the $BRAF_{V600E}$ mutation [15]. The primary endpoint of this open-label, multicenter study was overall response rate (ORR) to vemurafenib in stage IV melanoma patients who had previously received either one or more systemic therapies. Secondary endpoints included the duration of patient response to vemurafenib, progression-free survival (PFS), overall survival (OS), and safety. In BRIM-2, 53% of

patients demonstrated response overall, and the median duration of response was 6.8 months. The AEs observed in the study were similar to the Phase I trial of PLX4032, which included rash, fatigue, and arthralgia. In addition, investigators noted liver function abnormalities and the development of secondary skin tumors. These skin lesions were the most common Grade 3 AEs and are thought to be the result of paradoxical MAPK/ERK pathway activation [16]. Cells that harbor oncogenic RAS or upregulated RTKs are able to evade BRAF inhibition through feedback activation of the pathway [17,18]. In vemurafenib-treated patients, it is suggested that oncogenic RAS has a major role in bypassing direct pathway inhibition [17,18]. In these cells, despite BRAF inhibition, cell proliferation and growth are achieved through upstream activation by RAS. Most AEs were manageable and could be reversed with a simple dose reduction. Results from the BRIM-2 study, including the ORR of 53%, demonstrated the effectiveness of vemurafenib in $BRAF_{V600E}$ melanoma patients previously treated with other systemic agents.

Following these early Phase I and II clinical trials, a randomized Phase III clinical trial was performed directly comparing the efficacy of vemurafenib to dacarbazine in previously untreated metastatic melanoma patients with the $BRAF_{V600E}$ mutation [19]. The co-primary endpoints of the study were OS and PFS, whereas secondary endpoints were response rate, duration, and safety. In this trial, 675 patients were randomly assigned to receive either vemurafenib (960 mg orally twice daily) or dacarbazine (1000 mg per square meter of body surface area intravenously every 3 weeks). After 6 months of treatment, the OS was found to be higher in vemurafenib treated patients (84%) compared to dacarbazine treated patients (64%). Due to the significant benefit observed in the vemurafenib group, crossover from dacarbazine to vemurafenib was recommended

in patients not responding to dacarbazine. Common minor AEs to vemurafenib again included rash, fatigue, arthralgia, alopecia, photosensitivity, and nausea, and were typically managed with dose reduction. Eighteen percent of patients treated with vemurafenib developed secondary skin tumors, which were treated with simple excision. In addition to the increased OS, vemurafenib also improved median PFS in previously untreated $BRAF_{V600E}$ metastatic melanoma patients to 5.3 months versus 1.6 months in dacarbazine-treated patients.

Vemurafenib is FDA approved (August 2011) for use in unresectable metastatic melanoma harboring the $BRAF_{V600E}$ mutation, but on-going clinical trials are now testing this selective, small inhibitor in other cancer models, specifically those with the same activating BRAF mutation (V600E or V600K), such as thyroid cancer and HCL. In an ongoing pilot study, the efficacy of vemurafenib used alone or in combination with radioiodine in radioiodine refractory BRAF mutant thyroid cancers (ClinicalTrials.gov Identifier: NCT02145143) is being tested to determine treatment effects. Similarly, there are on-going clinical trials testing the efficacy of vemurafenib in HCL. Notably, there is one completed multicenter Phase II trial that reports >96% response rates in patients and a median of 23 months for response duration [20]. In 2017, the FDA approved vemurafenib in the treatment of Erdheim Chester Disease. As a whole, these studies show promising results for the possibility of vemurafenib approval in other cancers harboring activating BRAF mutations.

The approval for use of vemurafenib in metastatic melanoma has changed the current standard of care and patient prognosis. Both preclinical and clinical studies have shown the efficacy of selectively targeting a protein that plays a major role in a pathway

contributing to tumor progression. Although vemurafenib has dramatically altered the breadth of treatment options for patients, it is important to highlight that vemurafenib is rarely used as monotherapy and is instead more efficacious in combination therapy with MEK inhibitors. This is in large part due to the feedback activation of the MAPK/ERK pathway observed with single-agent treatment with vemurafenib. Combination strategies and why they are more effective than the use of vemurafenib alone will be discussed in a later section.

Dabrafenib

Dabrafenib (formerly GSK2118438; brand name Tafinlar; developed by GlaxoSmithKline) was approved by the FDA and the European Union for use in unresectable or metastatic $BRAF_{V600E}$ or $BRAF_{V600K}$ melanoma in 2013. Like vemurafenib, dabrafenib is a reversible, small molecule inhibitor of the kinase BRAF harboring the V600E or V600K mutation. The use of dabrafenib is contraindicated in patients with wild-type BRAF ($BRAF_{WT}$) due to the risk of tumor progression in these patients. Melanoma patients with $BRAF_{WT}$ have a unique response to selective BRAF inhibitors by demonstrating hyperactivation of the MAPK/ERK pathway. Although the exact mechanism has yet to be elucidated, there is evidence to suggest that selective BRAF inhibitors drive the dimerization of other RAF isoforms, like CRAF [21,22]. Alternatively, Holderfield and colleagues proposed a mechanism that interrupts inhibitory autophosphorylation of the protein [23]. This allows for paradoxical pathway activation independent of BRAF ultimately leading to cell proliferation.

During the initial Phase I study from 2009 to 2012, the tolerability and safety of dabrafenib was tested at multiple centers in Australia and the U.S.A. to ultimately

establish a standard recommended dose to be used in Phase II trials [24]. In this study, patients with the $BRAF_{V600E}$ mutation were treated with dabrafenib in a dose-escalation protocol. Dabrafenib was well-tolerated in patients with an activating $BRAF_{V600E}$ mutation, with most AEs as minor and these included fatigue, pyrexia, and cutaneous squamous cell carcinoma (SCC). Although dabrafenib administration was increased to 300 mg twice daily in this study, no maximum tolerated recorded dose was noted and 150 mg twice daily was established as the RP2D.

The clinical efficacy and safety of dabrafenib was tested in a multicenter Phase II (BREAK-2) trial in patients with metastatic BRAF-mutated melanoma [25]. Patients enrolled in the study received dabrafenib 150 mg twice daily orally until they experienced dose-limiting AEs, disease progression, or death. The primary endpoint of the BREAK-2 study was ORR, while PFS and OS were secondary endpoints. The study enrolled patients with $BRAF_{V600E}$ (76 patients) and $BRAF_{V600K}$ mutations (16 patients) with a confirmed response rate of 59 and 13%, respectively. Results from the trial supported that dabrafenib was an active agent in both $BRAF_{V600E}$ and $BRAF_{V600K}$ mutations, but more effective in patients with the V600E mutation. The median PFS was 6.8 months in $BRAF_{V600E}$ patients and 4.5 months in $BRAF_{V600K}$ patients. The most common AEs observed during the Phase II study were arthralgia, pyrexia, and hyperkeratosis; 10% of patients developed secondary skin tumors. Overall, BREAK-2 confirmed the safety and activity of dabrafenib in metastatic melanoma patients with $BRAF_{V600E}$ mutations.

FDA approval of dabrafenib in 2013 for unresectable or metastatic melanoma was based on results from a multicenter international, open label randomized, active control Phase III trial [26]. In this study, the improvement in PFS was observed in patients treated

with dabrafenib compared to systemic treatment with dacarbazine. In this study, 250 patients with previously untreated disease and $BRAF_{V600E}$ mutations were enrolled. The median PFS of dabrafenib-treated patients was 5.1 months compared to only 2.7 months with dacarbazine; patients from the dacarbazine treatment group were allowed to cross over to the dabrafenib treatment group. The AEs of dabrafenib in this study were similar to those observed in earlier Phase I and II trials, but also included erythrodysesthesia palmar plantar syndrome and papilloma. At the end of this study, dabrafenib was recommended for use in $BRAF_{V600E}$-positive unresectable or metastatic melanoma at a dose of 150 mg twice daily. Ongoing clinical efficacy trials of dabrafenib are currently enrolling in both papillary thyroid cancer (ClinicalTrials.gov Identifier: NCT01723202) and refractory leukemia (ClinicalTrials.gov Identifier: NCT03091257; NCT02551718).

Similar to vemurafenib, dabrafenib has improved treatment options for patients but has been shown to be most effective when used in combination with other therapies that target the MAPK/ERK pathway or immune response. These combinations will be discussed in the following section.

Encorafenib

Encorafenib (also known as LGX818; developed by Novartis), is a selective $BRAF_{V600E}$ inhibitor currently in Phase III trials to be approved for use in combination with a MEK inhibitor in BRAF-mutated melanoma. Despite sharing the same selectivity for mutant BRAF with the inhibitors mentioned in previous sections, encorafenib has some unique characteristics that distinguish it from other BRAF inhibitors, providing potential therapeutic benefit. In September 2017, Deloard and colleagues published preclinical and

clinical (Phase I) data on the potent small molecule inhibitor [27]. The preclinical data show that encorafenib is not only more potent than its counterparts (vemurafenib and dabrafenib), but also has a longer dissociation half-life. Moreover, encorafenib treatment results in less severe AEs than observed in vemurafenib- and dabrafenib-treated patients, including secondary skin tumors. The finding that encorafenib is more potent, has a longer dissociation half-life, and a lower incidence of secondary skin tumors makes it a promising drug in the pipeline for approval. In the Phase I clinical trial, the primary objective was to determine the maximum tolerated dose (MTD) and RP2D. BRAF inhibitor-naive and previously treated patients were enrolled in the study, where the former group of patients responded better. The ORR in BRAF inhibitor-naive patients was 60% and minimal in patients previously treated with a BRAF inhibitor. The MTD was determined to be 450 mg twice daily, but due to dose-limiting toxicities in the extension phase of the study the PR2D was declared as 300 mg twice daily. During Phase I of the trial, the standard of care for the metastatic melanoma shifted greatly to the use of BRAF and MEK inhibitors in combination. As a result, encorafenib clinical trials progressed forward to test its use in combination with the MEK inhibitor binimetinib. This combination treatment strategy will be discussed in subsequent sections.

Sorafenib

Sorafenib (brand name Nexavar; co-developed by Bayer and Onyx Pharmaceuticals), is a multi-targeted tyrosine kinase inhibitor (TKI) that is FDA and European Union approved for use in renal cell carcinoma (RCC), hepatocellular carcinoma (HCC), and radioactive-iodine refractive differentiated thyroid cancer (RAIR DTC) [28,29]. Although originally discovered as a Raf-1 inhibitor, sorafenib has since

been found to be a potent inhibitor of several other kinases including BRAF. In 2005 and 2007, the FDA approved the use of sorafenib in RCC and HCC, respectively. Its indication in RCC was based on the Phase III clinical trial, TARGET (Treatment Approaches in Renal Cancer Global Evaluation Trial), which determined the effect of sorafenib or placebo on OS and PFS in patients with advanced RCC [30]. In this study, the median OS was 19.3 and 15.9 months and PFS was 5.5 and 2.8 months in sorafenib- and placebo-treated groups, respectively. Sorafenib's approval for use in HCC was based on the Phase III clinical trial, SHARP (Sorafenib Hepatocellular Carcinoma Assessment Randomized Protocol), which compared the administration of sorafenib or placebo in previously untreated patients with unresectable disease [31]. In this international multicenter study, OS and time to symptomatic progression were the primary endpoints. Pharmacological intervention showed a significant increase in median OS from 7.9 months in placebo-versus 10.7 months in sorafenib-treated patients. There was no significant difference observed in time to symptomatic progression.

The 2013 FDA approval of sorafenib in RAIR DTC was based on the Phase III randomized control trial, DECISION [32]. In this study, 417 patients with RAIR DTC were randomized to undergo treatment with sorafenib or placebo; patients treated with sorafenib demonstrated median PFS of 10.8 versus 5.8 months with placebo [hazard ratio (HR) was 0.59; 95% CI, 0.45–0.76; p\0.0001], with a 41% decrease in risk of disease progression or death. There are numerous on-going clinical trials testing sorafenib in solid and hematological tumors including breast cancer, glioma, and acute myeloid leukemia. In these trials, the efficacy of sorafenib is being tested alone or in combination with the current standard of care, whether it be chemotherapy or targeted therapy, in each

respective malignancy. In addition to these on-going trials, there is work in chronic myelomonocytic leukemia (CMML) using sorafenib (ClinicalTrials.gov; Identifier: NCT01620216). In 2014, Zhang and colleagues showed that a subset of CMML patients with wild-type RAS harbor mutations in its downstream effector, BRAF [33]. This gives premise for the use of targeting BRAF in CMML since it is mutated and contributes towards pathway activation and subsequent tumor progression. Taken together, future work is warranted evaluating the use of selective BRAF inhibitors.

MEK Inhibitors

Trametinib

Trametinib (brand name Mekinist, GlaxoSmithKline Pharmaceuticals) was approved by the FDA in 2013 and by the European Union in 2014 for unresectable or metastatic melanoma with BRAF (V600E or V600K) mutations. Trametinib is an orally administered, reversible selective allosteric inhibitor of MEK1 and MEK2 [34]. MEK is a kinase downstream of both RAS and RAF in the MAPK pathway. Although approved for monotherapy, more recent treatment strategies recommend combining trametinib with dabrafenib for improved effect.

Initial Phase I studies, conducted from 2008-2010, recommended an oral dose of 2 mg daily for trametinib, which was well-tolerated in patients with minor AEs observed [34]. FDA approval was ultimately based on a multicenter Phase III trial of over 300 patients enrolled from 2010–2011 [35]. In this trial, patients were randomized to receive either 2 mg daily of oral trametinib or standard intravenous chemotherapy with dacarbazine or paclitaxel. The results of the trial showed a disease PFS of 4.8 months in

patients receiving trametinib versus only 1.5 months in patients receiving standard chemotherapy and a 56% risk reduction in mortality [35].

Notably, a 2012 Phase II study was conducted to determine whether there is a role for trametinib in patients with metastatic BRAF-mutated melanoma who have previously been treated with a BRAF inhibitor based on the hypothesis that inhibition of MEK, which is downstream from BRAF, may be a useful adjunct in patients who have developed resistance to BRAF inhibition [36]. In this study, patients were divided into two cohorts, those previously treated with a BRAF inhibitor (either dabrafenib or vemurafenib) and those previously treated with other systemic chemo- or immunotherapy. In the group of patients previously treated with a BRAF inhibitor, there was a significant decrease in disease response; no patients showed an objective response versus 25% of patients who were naive to BRAF inhibitor therapy who demonstrated either complete or partial responses. There was a median PFS period of only 1.8 months compared to 4.0 months in patients who had not previously been treated with a BRAF inhibitor. This study suggested that the mechanisms of resistance from BRAF inhibitor treatment confer similar resistance to treatment with MEK inhibitors.

In comparing trametinib with vemurafenib, a major finding of multiple studies has been the lack of development of cutaneous SCC with treatment of trametinib [35]. While dermatological side effects such as rashes are common in patients treated with both trametinib and vemurafenib, trametinib appears to avoid the concerning development of SCC found in up to one-quarter of patients who receive vemurafenib [37].

While currently only approved for treatment in patients with metastatic $BRAF_{V600E}$- or $BRAF_{V600K}$-mutated melanoma, there are some studies that suggest that trametinib

may have a role in the treatment of patients with rarer BRAF-mutations. Currently a Phase II study is in progress to determine the efficacy of trametinib in patients with non-$BRAF_{V600E}$ mutations (ClinicalTrials.gov; Identifier: NCT02296112).

The possible role of trametinib in the treatment of KRAS-mutated NSCLC treatment was investigated in a 2015 Phase II study, which enrolled 129 patients and randomized them to receive treatment with either trametinib or docetaxel [38]. The study was terminated early due to failure to demonstrate any difference in PFS between the groups.

Cobimetinib

Cobimetinib (GDC-0973 or brand-name Cotellic, developed by Exelixis and Genentech) was first introduced as a novel MEK inhibitor in 2012. *In vitro* studies indicated that this drug was particularly potent in BRAF or KRAS mutant cancer cell lines, a finding that was confirmed with *in vivo* human mutant xenograft tumor models [39]. In 2014, a Phase Ib study was performed evaluating cobimetinib in conjunction with vemurafenib in patients with BRAF-mutated melanoma. The 129 patients who were enrolled in the trial had either progressed on vemurafenib or had never been trialed on a BRAF inhibitor. The study was able to achieve its primary endpoint of demonstrating that cobimetinib was safe for use in conjunction with vemurafenib. Additionally, 15% of patients who had previously progressed on vemurafenib prior to being enrolled in the study and 87% of patients who had never been trialed on a BRAF-inhibitor demonstrated objective responses to therapy [40]. Based on promising trial results, in 2015 the FDA and the European Union approved cobimetinib in conjunction with vemurafenib for the

treatment of advanced stage $BRAF_{V600E}$ or $BRAF_{V600K}$-mutated melanoma. Cobimetinib is not approved for single-drug use [41].

Selumetinib

Selumetinib (study name AZD6244, ARRY-142886) was granted orphan drug status by the FDA in May 2016 for the treatment of patients with stage III or IV differentiated thyroid cancer. Similar to trametinib, selumetinib is an orally administered selective, allosteric inhibitor of MEK1 and MEK2. Initial Phase I trials recommended a dosing of 75 mg twice daily [42]. While studied in a number of different tumors, the best-supported application for selumetinib has been in patients with metastatic differentiated thyroid cancers that are refractory to radioiodine concentration. The inability of certain thyroid cancers to concentrate iodine has been linked to mutations in BRAF and RAS, both of which lead to activation of MAPK signaling [43]. A 2013 study demonstrated that selumetinib was able to sensitize patients with differentiated thyroid cancer who were previously immune to radioiodine concentration in order to allow for successful radioiodine treatment [44]. In this study, 20 patients with metastatic, radioiodine-resistant differentiated thyroid cancer were treated with selumetinib for 4 weeks. After 4 weeks of treatment, they underwent iodine-124 PET imaging to determine whether the tumor had improved iodine uptake. Of the 20 patients enrolled, selumetinib was able to increase the uptake of iodine in 12/20 patients [44]. The most notable response was in patients with NRAS mutations; 5/5 patients received radioiodine treatment with four patients demonstrating partial responses and one patient showing stable disease. A randomized, large-scale Phase III study with a goal recruitment of 400 patients is currently in progress to validate these results (ClinicalTrials.gov; Identifier: NCT01843062). This study,

expected to be completed in 2019, aims to compare the response of patients with differentiated thyroid cancer receiving selumetinib and radioactive iodine with those receiving a placebo and radioactive iodine treatment.

Selumetinib has been studied extensively for the treatment of KRAS-mutated NSCLC. There have been mixed findings supporting its efficacy in this disease. A 2010 Phase II study comparing selumetinib to standard-of-care treatment did not show any significant difference in outcomes [45]. However, a 2013 Phase II study showed that the combination of selumetinib and docetaxel acted synergistically, leading to an improved OS and PFS compared to placebo and docetaxel [46]. Based on these results, the large Phase III (SELECT-1) trial was conducted randomizing 500 patients with KRAS-mutated NSCLC to receive either selumetinib and docetaxel or placebo and docetaxel. The results, which were published in 2017, showed no significant difference in OS or PFS between both treatment groups [47].

Pimasertib

Pimasertib (AS-703026), from Santhera Pharmaceuticals and licensed by Merck Serono and Sanofi, is a selective, oral small-molecule MEK inhibitor, which was first introduced in 2009 with promising anti-tumor activity in *in vitro* models. A 2012 Phase I study established its safety and recommended a dose of 60 mg twice daily [48]. Combination therapy studies have been performed, including a 2015 Phase I study which evaluated the combination of pimasertib plus FOLFIRI in patients with KRAS-mutated metastatic colorectal cancer; however, the study was limited, as patients were only able to tolerate a maximum dose of 45 mg daily due to adverse events of mucositis [49]. More promisingly, results were recently published in 2016 of a multicenter Phase II clinical trial

evaluating pimasertib compared to dacarbazine in the treatment of cutaneous NRAS melanoma. One hundred and ninety-four patients were randomized to pimasertib 60 mg twice daily or dacarbazine infusion; the trial found that median PFS was significantly longer in patients treated with pimasertib (13.0 vs 6.9 weeks) [50].

Binimetinib

Binimetinib (ARRY-162, MEK-162) by Array BioPharma is a novel orally available small molecule MEK inhibitor that was accepted by the FDA in September 2017 for review of its New Drug Application [51]. Preliminary data published in 2010 indicated that binimetinib is a potent inhibitor of cell proliferation in mutant B-Raf and Ras cell lines and has anti-tumor activity in xenograft tumor models across a variety of cancer types including colorectal cancer and pancreatic cancer [52]. A Phase I trial was published in 2017 demonstrating safety and efficacy of binimetinib in 93 patients with biliary cancer, KRAS-mutant colorectal cancer, and BRAF-mutant colorectal cancer. The recommended treatment dose was 45 mg twice daily. The trial noted dose-limiting adverse events of dermatitis acneiform and ocular toxicity, including chorioretinopathy [53]. Further Phase I and II trials have evaluated binimetinib with a variety of targeted and chemotherapy agents; for example, a 2017 study demonstrated the safety of combined binimetinib and FOLFOX in 26 patients with colorectal cancer who previously progressed on standard therapies [54]. Currently, the COLUMBUS (encorafenib in combination with binimetinib in BRAF-mutant melanoma) and BEACON CRC (encorafenib, binimetinib and cetuximab in BRAF-mutant colorectal cancer) are major Phase III trials in progress to evaluate the role of binimetinib in advanced cancers [51].

MAPK/ERK Pathway Inhibitors as Combination Therapy by Malignancy

Melanoma

Although the use of a BRAF inhibitor as monotherapy in patients with BRAF-mutant unresectable or metastatic melanoma has been shown to improve OS and PSF compared to standard chemotherapy, there are major barriers in clinical use of these agents including the development of resistance and/or secondary skin tumors. Resistance to these inhibitors is likely due to reactivation of the MAPK/ ERK pathway [55-57], while the development of secondary skin tumors is the result of BRAF inhibitor-induced paradoxical MAPK/ERK pathway activation [21,27,58]. Similar to BRAF inhibitors, MEK inhibitors have also improved OS of these patients, but do not lead to same pitfalls. As a result, the use of MAPK/ERK pathway inhibitors in combination has overcome many of the limitations associated with the use of BRAF inhibitors as monotherapy.

Within the past half-decade, the use of BRAF and MEK inhibitors in combination therapy has been FDA and European Union approved for the treatment of metastatic melanoma patients. The advantage of using the two MAPK/ERK pathway inhibitors in combination was first seen with dabrafenib and trametinib in 2014. The approval of this combination treatment was based on the multicenter open-label randomized Phase III clinical trial enrolling patients with advanced (stage III or IV) BRAF mutant (V600E or V600K) melanoma [59]. Patients were randomly selected to receive one of three treatment regimens—trametinib 2 mg daily with dabrafenib 150 mg twice daily, trametinib 1 mg once daily with dabrafenib 150 mg twice daily, or dabrafenib as a single agent 150 mg twice daily. The patients treated with BRAF/MEK inhibitor combination therapy

experienced a higher ORR and PFS compared to the BRAF inhibitor alone. The combination-treated group had an ORR of 67% (complete 10%; partial 56%) compared to 51% (complete 9%; partial 43%) in the dabrafenib-alone group. The median PFS was 9.3 versus 8.8 months in the combination and monotherapy groups, respectively.

In 2015, vemurafenib was approved by the FDA and the European Union for use in combination with the MEK inhibitor cobimetinib. The approval of this combination therapy was based on the Phase III randomized clinical trial that tested the combination treatment on previously untreated patients with metastatic melanoma [60]. In this study, all patients first received vemurafenib and were then randomly selected to either receive cobimetinib, or placebo. The group receiving combination therapy experienced a prolonged PFS compared to the vemurafenib alone group—9.9 and 6.2 months after starting treatment, respectively. Additionally, patients who were treated with combination therapy lived longer and had complete or partial response to treatment compared to the patients treated with BRAF inhibitor monotherapy. The ORR was 68% in vemurafenib+cobimetinib treated patients, with a completed response in 10% of patients. In vemurafenib-placebo-treated patients, there was an ORR of 45%, with a complete response in 4% of patients. Additionally, there was an improvement in the survival rate at 9 months from 73% in the control group to 81% in the combination therapy group. From this study, it was determined that the administration of the BRAF and MEK inhibitors vemurafenib and cobimetinib in combination provides metastatic melanoma patients with increased efficacy over a BRAF inhibitor alone.

Since the approval of these MAPK/ERK pathway inhibitor combinations, the landscape for treatment of metastatic melanoma has shifted drastically. It is important to

emphasize that these trials not only show that BRAF and MEK inhibitors used together are effective, but also mitigate the AEs of these agents when used alone—specifically secondary skin tumors. In the 2014 Phase III trial, only 2% of patients given the dabrafenib-trametinib combination developed cutaneous SCCs compared to 9% of dabrafenib-only patients [59]. Similarly, the vemurafenib+cobimetinib combination resulted in fewer occurrences (2%) than vemurafenib alone (11%) [60].

In addition to these approved BRAF and MEK inhibitor combinations, another BRAF and MEK inhibitor combination in the pipeline for FDA approval is encorafenib and binimetinib. The two-part Phase III trial of these agents (COLUMBUS) demonstrated that the combination of encorafenib and binimetinib improves ORR and PFS of metastatic melanoma patients, as well as lowers the incidence of severe AEs. The first part of the study measured various endpoints (e.g. ORR, PFS, AEs) of encorafenib+binimetinib, encorafenib alone, and vemurafenib alone [61]. The ORR was highest in the combination group at 63% (complete 8%; partial 55%), followed by encorafenib alone at 51% (complete 5%; partial 45%), and lowest in vemurafenib alone at 40% (complete 6%; partial 35%). The PFS was 14.9 months in the combination group, whereas the BRAF inhibitors alone were 9.6 and 7.3 months in encorafenib and vemurafenib, respectively.

In addition to improved outcomes with BRAF/MEK inhibitor combination therapy, exposure time to the targeted agents was also extended (combination 51 weeks, encorafenib 31 weeks, and vemurafenib 27 weeks). The second part of the study focused on the contribution of binimetinib to the combination therapy [62]. At the end of the trial, PFS was extended from 7.4 months in encorafenib-alone to 12.9 months in encorafenib+binimetinib combination. The ORR was also improved from 50 to 66% in

encorafenib alone and encorafenib+binimetinib combination, respectively. With the recent publishing of the Part 2 results in September 2017, it is without question that BRAF/MEK inhibitor combinations are advantageous alternatives to MAPK/ERK pathway inhibitors as monotherapies. Additionally, the use of BRAF and MEK inhibitors in combination with immunotherapies has gained a substantial amount of support in the field [63].

Immunotherapy, such as anti-PD1 (programmed cell death protein 1) and CTLA-4 (cytotoxic T-lymphocyte associated antigen 4) antibodies, and BRAF/MEK inhibitors are currently considered first-line agents in the treatment of metastatic/advanced-stage melanoma. Consequently, there is interest in investigating whether these agents can be used safely and efficaciously in combination therapy. Unfortunately, a 2013 Phase I study on the combination of vemurafenib and the CTLA-1 antibody ipilimumab in 12 BRAF-mutated melanoma patients was terminated prior to Phase II investigations due to dose-limiting toxic elevations in hepatic enzymes in more than 50% of patients at both the full approved doses and at a lower dose of vemurafenib [64]. However, a more recent Phase I study (KEYNOTE-022 study) was released in 2017 evaluating the combination of the PD-L1 inhibitor pembrolizumab, dabrafenib, and trametinib, in 15 patients with metastatic BRAF-mutated melanoma. In these patients, there was a 20% rate of dose-limiting toxicities related to elevations in hepatic enzymes; in all patients, these elevations normalized with pauses in therapy. Overall, patients demonstrated promising responses, with one patient showing a complete response, nine patients showing partial responses, and two patients with stable disease. The trial is currently in Phase II [65]. An additional Phase II study evaluating the combination of cobimetinib, vemurafenib, and the PD-L1 inhibitor atezolizumab and a Phase III study evaluating the combination of dabrafenib,

trametinib, and the novel PD-1 inhibitor PDR001 are currently underway. If successful, these studies have the potential to dramatically alter the current paradigm of care in patients with advanced-stage melanoma (ClinicalTrials.gov Identifier: NCT02902029; NCT02967692).

Non-Small Cell Lung Cancer

In the last few years, many studies have been completed to establish the possible role of BRAF inhibitors in the treatment of NSCLC [66-68]. An estimated 2.6% of NSCLCs have BRAF mutations [67]. Key *in vitro* experiments first demonstrated that treatment with dabrafenib and trametinib significantly inhibited cell growth in BRAF-mutated NSCLC cells. This led to a 2016 Phase II multicenter international study to determine the efficacy of this combination therapy (dabrafenib and trametinib) in the treatment of patients with BRAF-mutated stage IV NSCLC [67]. In this study, 57 patients with $BRAF_{V600E}$-mutant metastatic NSCLC previously treated with platinum-based systemic therapy were enrolled and treated with the combination of dabrafenib (150 mg twice daily) and trametinib (2 mg once daily) for multiple 21-day cycles until disease progression was noted. The results of the study indicated that 63.2% of patients demonstrated complete or partial response to treatment with a median PFS of 9.7 months [67]. By comparison, literature evaluating the prior standard of care estimated the response rate and median PFS for this chemotherapy regimen in the treatment of BRAF-mutated NSCLC patients to be 9% and 3.1 months, respectively [66]. Of note however, in this combination trial more than half of patients (56%) experienced a more serious grade 3 or 4 adverse event (SAE) and nearly all patients experienced some AE. Despite these SAEs, only 12% of patients required discontinuation of the trial due to these toxicities [68]. Accordingly, in

2017, the FDA and the European Union approved the combination of dabrafenib and trametinib for treatment of patients with metastatic NSCLC with $BRAF_{V600E}$ mutations [69].

Colorectal Cancer

The use of BRAF inhibitors in the treatment of colorectal cancer has a long history of investigation. Unlike treatment of BRAF-mutated melanomas, very rapid resistance and reactivation of the downstream MAPK/ERK pathway occurs in BRAF-mutated colorectal cancer cells, rendering single-agent treatment with BRAF inhibitors virtually ineffective [70]. However, some evidence exists supporting the utility of combining vemurafenib with other chemotherapy agents. A 2015 study suggested some benefit of combination therapy with vemurafenib and panitumumab, an EGFR inhibitor approved by the FDA in 2006 for patients with metastatic colorectal cancer with disease progression despite prior treatment [71]. In this study, 15 metastatic colorectal cancer patients with $BRAF_{V600E}$ mutations were enrolled; all patients had previously failed standard chemotherapy treatment. The combination of vemurafenib and panitumumab initially resulted in tumor regression in 10 out of 12 patients; however, the authors noted that this response was modest with all patients having disease progression within one year [71].

However, a chemotherapy regimen that has shown more promise in the treatment of metastatic BRAF-mutated colorectal cancer is combining vemurafenib, irinotecan, and cetuximab. Similar to panitumumab, cetuximab is an EGFR inhibitor approved by the FDA for treatment of metastatic colorectal cancer in conjunction with standard chemotherapy such as irinotecan [72]. In preliminary *in vitro* studies, the combination of vemurafenib, cetuximab, and effect augmentation with irinotecan was more effective in the treatment of colorectal tumor cells with BRAF mutations than any of the individual drugs alone [73].

Based on these findings, a 2016 study enrolled 19 patients with mutated $BRAF_{V600E}$ metastatic colorectal cancer and treated them with the combination of cetuximab, irinotecan, and vemurafenib [74]. Results from this study demonstrated tumor regression radiographically in over one-third (35%) of patients. Based on these outcomes, a large Phase II study enrolled 106 patients with BRAF-mutated metastatic colorectal cancer who were randomized to receive irinotecan and cetuximab with or without vemurafenib (ClinicalTrials.gov; NCT02164916). Interim results of the study released in 2017 demonstrated that the addition of vemurafenib significantly increased PFS from 2.0 to 4.4 months and improved disease control rate from 22 to 67% [75].

Thyroid Cancer

To date, there are no approved MAPK/ERK pathway combination therapies for use in thyroid carcinomas. Despite this, there are some ongoing Phase I clinical trials testing the therapeutic potential of a MAPK/ERK pathway inhibitor used in combination with another therapeutic intervention. For example, a pilot study is testing the effect of vemurafenib plus the biological agent KTN3379 in BRAF-mutant radioiodine refractory thyroid carcinoma patients. The primary endpoint of this study will measure if the combination can increase tumoral radioiodine incorporation. In addition, standard safety and tolerability are outcomes that are being assessed in this early study (ClinicalTrials.gov Identifier: NCT02456701). Additionally, there is another ongoing Phase I study testing the use of dabrafenib and lapatinib, the dual HER2/neu and EGFR inhibitor, in unresectable radioiodine refractory thyroid cancer patients (ClinicalTrials.gov Identifier: NCT01947023).

Mechanisms of Resistance to MAPK/ERK Pathway Inhibitors

MAPK/ERK pathway inhibitors have proven to be effective treatments in various cancer types, but the major clinical problem faced with these targeted therapies is the emergence of resistance soon after the start of treatment. An initial strategy to overcome resistance to BRAF inhibitors involved adding another MAPK/ERK pathway inhibitor targeting the serine/threonine kinase, MEK. The rationale behind adding another MAPK/ERK pathway inhibitor to the treatment strategy is based on pathway reactivation [16,21-23]. When given alone, BRAF inhibitors can induce the pathway to become activated evading the blockade. By adding in an inhibitor of a downstream effector (e.g., MEK) you are targeting two nodes of the pathway increasing its inhibition. Since the preceding section focused extensively on the use of MAPK/ERK pathway inhibitor combination therapies in various cancers, we will review the postulated mechanisms of resistance to MAPK/ ERK pathway inhibitors, namely in inhibitors of BRAF. It is important to note that mechanisms of BRAF inhibitor resistance can vary within an individual type of cancer, as well as between different malignancies. For example, it cannot be assumed that all melanoma patients who develop resistance to a given BRAF inhibitor have the same underlying mechanism. There are various modes that can attribute towards resistance, but one thing that is shared amongst these patients is the median time to resistance — 6–8 months after the start of treatment [76,77]. As with any type of resistance, BRAF-inhibitor resistance can be primary (intrinsic) and/or secondary (acquired) (Figure 1-1).

Primary (Intrinsic) Resistance

Despite the large majority of metastatic melanoma patients who present with the activating *BRAF* mutation (V600E or V600K), 20% of these patients are initially refractory to selective BRAF inhibitors and do not respond [76]. Similarly, there is a subset of metastatic colorectal cancer patients who have the BRAF mutant (<10%) and do not respond to BRAF inhibitors [78]. In melanoma, mechanisms of intrinsic resistance can include, but are not limited to: *RAC1* mutations, loss of PTEN, dysregulation of cell-cycle proteins, and changes to the microenvironment. In colorectal cancers harboring the same BRAF mutation, intrinsic resistance to these inhibitors is primarily due to feedback activation of EGFR [79].

The $RAC1_{P29S}$ mutation is the third most common hotspot mutation present in metastatic melanoma patients, followed by the second most common $NRAS_{Q61}$, and the most common being $BRAF_{V600}$ [80]. *RAC1* is a member of the RAS GTPase superfamily and has an integral role in cell motility and growth. Its exact role in melanogenesis is not fully understood, but evidence supports that *RAC1* is a key player in epithelial mesenchymal transition (EMT) [81-84]. Unlike BRAF and NRAS mutations, the RAC1 hotspot mutation is recognized as a UVB (sunlight)-induced DNA damage (e.g. C → T transition in dipyrimidine). This mutation keeps the GTPase in a mostly active state—compared to mutant isoforms of RAS, which are constitutively active—through increased GDP → GTP exchange [80]. Moreover, melanoma cell lines that possess the $RAC1_{P29S}$ somatic mutation have been shown to be resistant to BRAF inhibitors [85]. In this study, Watson and colleagues showed that the expression of mutant RAC1 in melanoma cell lines lead to increased cell viability and decreased apoptosis *in vitro* and enhanced tumor

growth *in vivo* when treated with BRAF inhibitors constituting resistance. Interestingly, when the RAC1 mutant was silenced and cells still expressed mutant BRAF, sensitivity to the kinase inhibitors was increased [85].

Additionally, the loss of PTEN in melanoma not only contributes to tumorigenesis in melanoma patients, but can contribute to BRAF inhibitor resistance [86,87]. *PTEN* gene is a tumor suppressor gene that encodes a phosphatase responsible for dephosphorylating products of PI3K. Loss of this protein results in decreased apoptotic and increased mitogen pathway signaling due to increased phosphorylation of AKT. This can be reversed with the addition of PTEN to cells deficient of the protein [88,89]. In 2011, Paraiso and colleagues showed that the loss of PTEN contributed to BRAF-inhibitor resistance through changes in expression of BIM, a pro-apoptotic regulator [90,91]. When a BRAF inhibitor was used to treat melanoma cells without PTEN there is an increase in AKT signaling compared to cells that do express the phosphatase. This increase led to decreased apoptosis, which was determined to be mediated by expression of BIM. The increased expression of BIM correlated to cells that expressed PTEN, whereas BIM expression was suppressed in cells not expressing PTEN. To confirm the contribution of BIM, knockdown studies of the protein were conducted and in cells expressing PTEN, the siRNA of BIM led to abrogated apoptosis [91]. Not only can loss of PTEN contribute to intrinsic BRAF-inhibitor resistance, but it has also been shown that loss-of-function mutations can also be a mechanism of resistance [92].

The dysregulation of a critical cell-cycle regulator, CDK4, is suggested to be another intrinsic mode of resistance to BRAF inhibitors [93]. More specifically, this positive regulator of cell-cycle progression is found to have activating mutations in a large subset

of metastatic melanoma patients, therefore rendering them nonresponsive to targeted treatment. The active CDK4 protein phosphorylates RB (retinoblastoma protein), which promotes the transition of a cell from the G1 phase to S phase of the cell cycle. CDK4 is also responsible for phosphorylating other proteins critical in cell-cycle progression and inhibition of apoptosis and/or cell senescence [92]. Interestingly, when another cell-cycle regulator, cyclin D1, is overexpressed in cells also expressing mutated CDK4, BRAF inhibitor resistance is seen [94].

A unique feature of CRC patients with BRAF mutants is their primary resistance to BRAF inhibitors. Despite these patients carrying the activating $BRAF_{V600}$ mutation, the selective inhibitors are not effective as they are in melanoma patients carrying the same mutant [95]. The general mechanism is the feedback activation of the MAPK/ERK pathway through EGFR. Studies using a BRAF inhibitor in combination with an antibody or small-molecule inhibitor targeting this growth-factor receptor have shown optimal synergism compared to the BRAF inhibitor alone in CRC patients [54]. It is also important to emphasize that CRC patients generally have higher expression levels of EGFR than melanoma patients, lending some reasoning for the difference in response to BRAF inhibitors. Since melanoma patients express a smaller amount of EGFR than CRC patients, feedback activation through a growth-factor receptor is not a mode of resistance to the BRAF inhibitor [79,95].

Secondary (Acquired) Resistance

For the patients who do initially respond to a BRAF inhibitor but show disease progression a few months after the start of treatment, the resistance mechanisms can be generally classified as MAPK/ERK pathway dependent or independent. In the two

following subsections, we will discuss various modes of resistance that fall into each of these categories focusing on those most prevalent in melanomas.

MAPK/ERK Pathway Dependent

Resistance mechanisms that are dependent on this signaling pathway include somatic activating mutations of NRAS, an isoform of the GTPase upstream of BRAF. As mentioned previously, activating mutations of NRAS contribute to paradoxical MAPK/ERK pathway activation through dimerization of CRAF [2,3,6]. Additionally, there are alterations made directly to BRAF itself such as truncation, amplification, or fusion of the protein kinase. In the instance of the latter, it has been reported that the AGAP3-BRAF or various other fusion genes are strong contributors to acquired resistance in melanoma patients [96,97]. Moreover, it has been shown that despite having BRAF fusion genes, these melanomas are still sensitive to MEK inhibitors in combination with a PI3K inhibitor or CDK4/6 inhibitor [96]. When changes are made to BRAF, it develops the ability to ‘‘escape’’ inhibition by selective small molecules such as vemurafenib, dabrafenib, and encorafenib. Downstream of BRAF, modifications can be made to the MAPK/ERK pathway that ultimately lead to resistance against BRAF inhibitors. In some instances, MEK mutations can occur that render the kinase constitutively active and can subsequently activate ERK [98]. There have been some reported cases that show the activation of ERK in a MEK-independent manner by another protein kinase, COT (MAP3K8; mitogen activated protein kinase 8) [99]. In the MAPK/ERK pathway-dependent modes of resistance, cellular processes like immune response, cell-cycle regulation, and angiogenesis are affected in a manner that promotes tumor cell maintenance. Although this drug-resistance favors cancer progression, it also provides

researchers with the opportunity to develop therapies that target these aberrant cellular processes. Examples of this include application of cutting-edge immunotherapies such as the immune checkpoint inhibitors of PD-L1 and CTLA-4, as well as cyclin dependent kinase 4 (CDK4) and vascular endothelial growth factor receptor (VEGFR) inhibitors to antagonize cell-cycle progression and angiogenesis, respectively [100-102].

MAPK/ERK Pathway Independent

Alternatively, resistance to BRAF inhibitors can occur in a MAPK/ERK pathway-independent manner. In such instances, RTKs can be overexpressed or other signaling pathways can be upregulated [103]. Overexpression of RTKs and their respective RTK ligands (e.g. EGF and EGFR, PDGF and PDGFR) are commonly observed [104]. The PI3K/AKT signaling pathway is most often upregulated to compensate for the blockade of the MAPK/ERK pathway [105,106]. In this pathway, various insults can be made that promote its increased signaling. The activity of AKT is tightly regulated by the phosphatase, PTEN. Upon phosphorylation by PI3K, AKT becomes activated and acts on its downstream effectors such as mTOR and GSK. Activity of Akt can be reversed via phosphate removal by PTEN. In a resistant state, PTEN has been reported to harbor inactivating mutations that lead to the phosphorylation of AKT and subsequent pathway activation [89]. This signaling cascade can also be altered to promote BRAF inhibitor resistance with the amplification of AKT. Due to the crosstalk to the MAPK/ERK and PI3K/AKT pathways, one approach to overcome resistance is the combination of inhibitors of each pathway. There is a breadth of preclinical and clinical data supporting this approach [107,108].

Novel Approach to Overcoming BRAF Resistance

As resistance to BRAF inhibitors has developed into a more clinically relevant problem, deciphering these resistance mechanisms has become a critically important strategy to identify novel methods to overcome them. Given the many pathways for BRAF inhibitor resistance, simultaneously targeting of these multiple pathways at once to ultimately overcome resistance would be an ideal strategy. A representative example of this multi-pathway approach is the use of novel heat shock protein 90 (Hsp90) inhibitors. Hsp90 is a molecular chaperone that functions as the hub of proteostasis for many cellular proteins. The activity of this chaperone assures proper protein folding and stability, therefore playing a major role in their function [109]. The substrates of Hsp90 are referred to as ‘‘clients’’ and are involved in a vast range of cellular processes. Interestingly, many of the proteins involved not only in cancer development and maintenance, but also BRAF inhibitor resistance are all clients of Hsp90 chaperone function [110]. This highlights the prospect of simultaneously targeting multiple signaling pathways through the inhibition of this molecular chaperone. While early Hsp90 inhibitors such as geldanamycin and 17-AAG were trialed in melanoma and thyroid cancer (ClinicalTrials.gov Identifier: 00087386) patients in Phase II, they never progressed to Phase III given the hepatotoxicity observed with treatment [111]. This toxicity was believed to be due to a dose-escalation effect resulting from upregulation of Hsp70 as a secondary effect of the heat shock response induced by Hsp90 inhibition. Given the pro-survival processes Hsp70 regulates, it counteracted the inhibitory effects of Hsp90 inhibition requiring higher doses to maintain the inhibitory effect until a dose-limiting toxicity had occurred. Novel Hsp90 inhibitors in more advanced clinical and preclinical studies that do not induce this significant heat

shock effect may be on the horizon as a novel strategy to overcome BRAF resistance in several tumors [112,113]. Some of these have moved into Phase III trials such as retaspimycin and ganetespib as combination therapies but have not been FDA approved. Other preclinical and early clinical strategies in development involve combinations of immunotherapy agents with BRAF or MEK inhibitors, histone deacetylase inhibitors with BRAF inhibitors, and check-point inhibitors combined with BRAF/MEK inhibition [114,115]. Further translational and clinical testing will be needed to define which of these strategies may be the most successful in overcoming this resistance problem.

Clinical Applications of BRAF and MEK Inhibitors

Standard of Care

Melanoma

The current National Comprehensive Cancer Network (NCCN) guidelines for the treatment of unresectable metastatic melanoma offer patients and clinicians a wide range of options. For patients with brain metastases, treatment historically involved radiation therapy with or without palliative resection. However, this paradigm has been rapidly shifting due to the development of BRAF inhibitors and immunotherapy. Emerging evidence suggests that BRAF inhibitors may have an important role in the treatment of patients with brain metastases as an adjunct to radiation. A 2012 Phase II study treated 172 patients with metastatic BRAF-mutated melanoma and at least one brain metastases with dabrafenib; of patients with $BRAF_{V600E}$ mutations who had never received local treatment for brain metastases, 40% achieved and overall intracranial response. Of the patients who had previously received local treatment (surgery, whole-brain radiotherapy,

or stereotactic radiosurgery), the overall intracranial response rate was 31% [116]. To further investigate this potential therapeutic strategy, an upcoming Phase II trial will aim to investigate the concurrent roles of dabrafenib and trametinib with stereotactic radiation (ClinicalTrials.gov Identifier: NCT02974803). For patients without brain metastases, options include systemic therapy, intralesional injections, palliative surgical resection, radiation, or palliative supportive care. First-line systemic therapies for non-resectable metastatic melanoma include immunotherapy, clinical trials, and for the large subset of patients with $BRAF_{V600E}$ mutations, treatment includes either the combination of dabrafenib and trametinib or vemurafenib and cobimetinib. Other systemic therapies are broader and include traditional cytotoxic agents such as dacarbazine and paclitaxel, high-dose IL-2, imatinib (if a c-Kit mutation is present), temozolomide, vinblastine, nitrosourea, and interferon alpha-2b; all of these options are very rarely used in current clinical practice and only if no other options including clinical trials are available to the patient. In general, patients are nearly always treated with immunotherapy or targeted therapy [117].

Differentiated Thyroid Cancer

The current NCCN guidelines for the treatment of metastatic differentiated thyroid cancer relies heavily on radioactive iodine treatment. However, there are a subset of patients with persistent disease, locoregional recurrence, or distant metastases that do not uptake iodine. In these patients, the recommendation is to suppress TSH levels with levothyroxine treatment. Additionally, options include resection or treatment with radiation therapy, surveillance only in asymptomatic patients with slow disease progression, treatment with non-FDA-approved small molecule inhibitors, or treatment with lenvatinib or sorafenib for disease that has failed these other options. Cost and side-effect profiles

of these inhibitors must be weighed as part of the risk/benefit analysis and treatment should always be performed on an individual basis [118].

Metastatic Colorectal Cancer

The current NCCN guidelines offer many chemotherapy options for the treatment of metastatic colorectal cancer. First-line or initial therapy includes FOLFOX, CAPEOX, FOLFIRI, FOLFOXIRI, 5FU/leucovorin, or capecitabine, all plus or minus bevacizumab. In patients with KRAS/NRAS wild-type and left-sided tumors, treatment options expand to include FOLFOX or FOLFIRI plus cetuximab or panitumumab. To date, there are no NCCN-recommended chemotherapy regimens that include BRAF or MEK inhibitors [119].

NSCLC

The current NCCN guidelines for the treatment of stage IV metastatic NSCLC depend on the initial determination of EGFR, ALK, ROS1, and PD-L1 tumor markers. If the patient is found to have a sensitizing EGFR mutation, first-line treatment is with erlotinib, afatinib, or gefitinib. If the patient has ALK rearrangement, first-line treatment is with crizotinib or ceritinib, and if the patient has ROS1 rearrangement, first-line therapy is with crizotinib. If the patient is PD-L1 expression positive, first-line therapy is with pembrolizumab. For all other patients or those who demonstrate disease progression with the above therapies, first-line therapy is with doublet chemotherapy (typically cisplatin or carboplatin-based). Very recently in 2017, the combination therapy of dabrafenib and trametinib has been approved by the FDA for the treatment of BRAF-mutated NSCLC [120].

Hairy Cell Leukemia

The current NCCN guidelines for the treatment of patients with HCL recommend initial chemotherapy with the purine analogs cladribine or pentostatin. If there is less than complete response or relapse at less than a year, options include treatment with a purine analog plus or minus rituximab, interferon alpha, or rituximab alone. The current recommendation for any progression despite these therapies is treatment with vemurafenib plus or minus rituximab, or ibrutinib [121].

Common or Noted Side Effects of BRAF and MEK Inhibitors

Vemurafenib

The most common side effects are dermatological, including skin rash and photosensitivity [122]. Cutaneous SCC or keratoacanthomas develop in 15–30% of patients; in the 2011 Phase III trial conducted by Chapman et al., 18% of patients developed SCC or keratoacanthomas or both; and all could be treated by simple excision [19]. Other adverse events include arthralgia, fatigue, nausea, vomiting, diarrhea, neutropenia, peripheral edema, and alopecia [122].

Dabrafenib

The most common side effects are dermatological, including hyperkeratosis, papillomas, or palmar-plantar erythrodysesthesia. Between 5 to 20% of patients develop cutaneous SCC or keratoacanthoma. Other adverse events include fatigue, headache, arthralgia, peripheral edema, nausea, vomiting, diarrhea, and hyperglycemia [123].

Sorafenib

The most common side effects are hypertension, headache, peripheral neuropathy, palmar-plantar erythrodysesthesia, alopecia, rash with desquamation,

hypocalcemia, fatigue, and weight loss [124]. In the 2014 Phase III study by Brose et al., serious adverse effects included secondary malignancy in 4.3% of patients, dyspnea, and pleural effusion [32].

Trametinib

The most common side effects are hypertension, cardiomyopathy (7–11%), skin rash (8% with grade 3 or 4 rash), dermatitis acneiform, diarrhea, minor bleeding (<1% grade 3–4), and peripheral edema. Rare events include ocular events such as a blurred vision, reversible chorioretinopathy, and retinal-vein occlusion/retinal detachment. Of note, there are no findings of cutaneous SCC or keratoacanthomas as seen with vemurafenib and dabrafenib [32,35,125].

Cobimetinib

The adverse effects of cobimetinib are reported in conjunction with vemurafenib treatment. The most common side effects are diarrhea, nausea, vomiting, elevated liver enzymes, elevated creatine kinase levels, and central serous retinopathy, as reported in the 2014 study by Larkin et al. [60]. Other adverse events include decreased ejection fraction, hypertension, dermatologic side effects (rare cutaneous SCC or keratoacanthomas), minor hemorrhage (<1% grades 3 or 4), and visual impairment, including blurred vision, chorioretinopathy, and retinal detachment (12% overall, 2% grades 3 or 4) [126].

Selumetinib

The most common side effects are fatigue, rash, and elevated liver enzymes. Other side effects events include nausea, diarrhea, peripheral edema, oral mucositis, electrolyte abnormalities, and dyspnea. Most adverse events are grade 1 or 2 [42].

Average Monthly Costs of Selective Inhibitors (Medicare Data)

Annual monthly costs for selective inhibitors can be seen in **Table** 1-1.

Conclusion

The development and approval of BRAF and MEK inhibitors in BRAF-mutant cancers has dramatically changed the landscape of treatment options and clinical outcomes of cancer patients, especially those with metastatic melanoma. While the initial response to these inhibitors is robust, long-term complete responses are rare and most patients will develop resistance, leading to disease progression. Additionally, the side-effect profiles to BRAF inhibitors are of concern due to the risk of developing secondary skin tumors, such as cutaneous SCCs. The advent of combination therapy with BRAF and MEK inhibitors has eliminated many of the initial concerns associated with BRAF inhibitor monotherapy; evidence demonstrates both improved side-effect profiles and prolonged clinical endpoints like ORR and PFS. Future treatment strategies involving BRAF and MEK inhibitors will aim to overcome currently recognized mechanisms of resistance and provide synergistic anti-tumor activity. Excitingly, Hsp90 small-molecule inhibitors—especially C-terminal targeted—are on the horizon of being an alternative to overcome resistance, and new research supports the role of MAPK/ERK pathway inhibitors in combination with other protein or system targets, like CDK4/6 and PI3K or immunotherapy, respectively.

Tables

Table 1-1 Average monthly costs for selective inhibitors (Medicare data)

Drug	Cost (US$)
Vemurafenib	$13,021 for 30 day
Dabrafenib	$11,581 for 30 days
Sorafenib	$19,775 for 30 days
Trametinib	$12,753 for 30 days
Cobimetinib	$7,856 for 28 days
Selumetinib	Average wholesale price unavailable

Figures

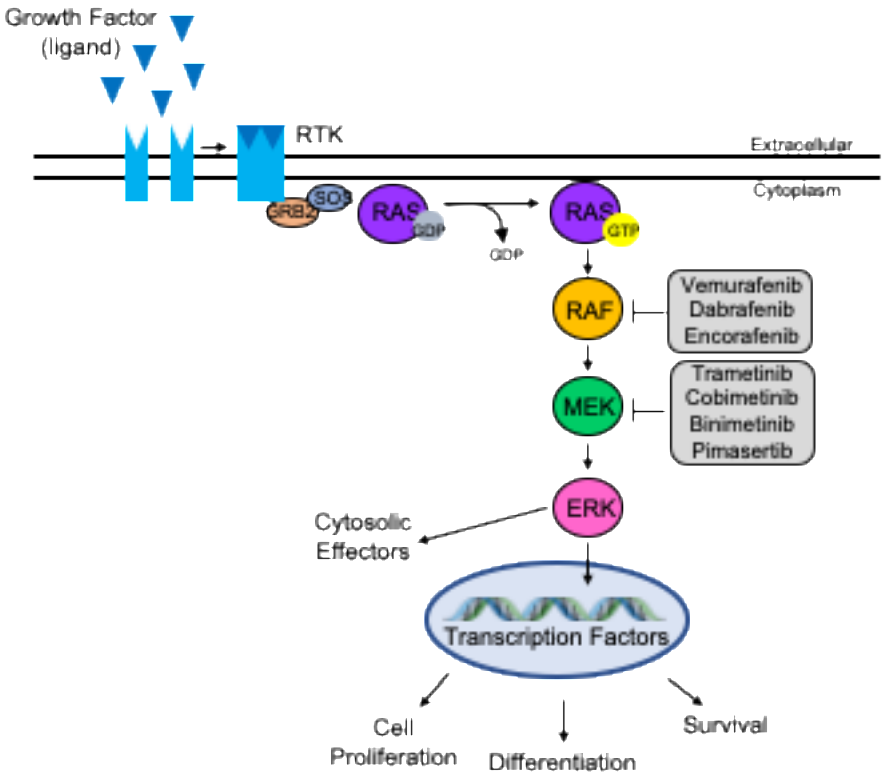

Figure 1-1 MAPK/ERK Pathway

This signaling pathway is activated when a growth factor (ligand) binds to its respective growth factor receptor. Once activated, the RTK transmits the extracellular signal inside the cell via the adaptor protein GRB2. The membrane bound GTPase, RAS, then becomes activated by the exchange of GDP for GTP. This is facilitated by the nucleotide exchange factor, SOS. Activated RAS then initiates the signaling cascade of MAP kinases. Finally, activated ERK can phosphorylate its cytosolic or nuclear effectors. The latter results in changes to transcription and ultimately cell proliferation, differentiation, and survival. GRB2: growth factor receptor bound protein 2, ERK (MAPK): extracellular signal related kinase, MEK (MAPKK), RAF (MAPKKK): rapidly accelerated fibrosarcoma, RAS: rat sarcoma protein, RTK: receptor tyrosine kinase, SOS: son of sevenless.

Abbreviations

AE	adverse events
AKT	protein kinase B
ALK	anaplastic lymphoma kinase
BIM	Bcl-2-like protein 11
$BRAF_{WT}$	BRAF wild-type
CAPEOX	capecitabine oxaliplatin
CDK4	cyclin dependent kinase 4
CMML	chronic myelomonocytic leukemia
COT	MAP3K8; mitogen activated protein kinase 8
CRC	colorectal cancer
CTLA-4	cytotoxic T-lymphocyte associated antigen 4
DTC	differentiated thyroid cancer
EGF	epidermal growth factor
EGFR	Epidermal growth factor receptor
EMT	epithelial mesenchymal transition
ERK	extracellular signal-related kinase
FDA	Food and Drug Administration
FOLFIRI	folinic acid fluorouracil irinotecan hydrochloride
FOLFOX	folinic acid fluorouracil oxaliplatin
FOLFOXIRI	folinic acid fluorouracil oxaplatin irinotecan
FU	fluorouracil
GDP	guanosine diphosphate

GSK	glycogen synthesis kinase 3
GTP	guanosine triphosphate
HCL	hairy cell leukemia
Hsp70	70 kDa heat shock protein
Hsp90	90 kDa heat shock protein
IL-2	interleukin-2
MAPK	mitogen activated protein kinase
MEK	mitogen activated protein kinase
MTD	maximum tolerated dose
mTOR	mammalian target of rapamycin
NCCN	National Comprehensive Cancer Network
NSCLC	non-small cell lung cancer
ORR	overall response rate
OS	overall survival
PD-L1	programmed death ligand 1
PD1	programmed cell death protein 1
PDGF	platelet derived growth factor
PDGFR	platelet derived growth factor receptor
PET	positron emission tomography
PFS	progression free survival
PI3K	phosphoinositide 3-kinase
PTEN	phosphatase and tensin homolog
RAC1	Ras-related C3 botulinum toxin substrate 1

RAF	rapidly accelerating fibrosarcoma
RAF (A/B/C)	RAF isoforms
RAIR	radioactive iodine refractive
RAS	rat sarcoma protein
RAS (H/K/N)	RAS isoforms
RB	retinoblastoma protein
RCC	renal cell carcinoma
RP2D	recommended Phase II dose
RTK	receptor tyrosine kinase
SAE	serious adverse events
SCC	squamous cell carcinoma
TKI	tyrosine kinase inhibitor
TSH	thyroid stimulating hormone
VEGFR	vascular endothelial growth factor receptor

References

1. Zhang W and Liu HT. MAPK signal pathways in the regulation of cell proliferation in mammalian cells. *Cell Res* 2002;**12**(1): 9-18.
2. Dhillon AS, Hagan S, Rath O and Kolch W. MAP kinase signalling pathways in cancer. *Oncogene* 2007;**26**(22): 3279-3290.
3. Roberts PJ and Der CJ. Targeting the Raf-MEK-ERK mitogen-activated protein kinase cascade for the treatment of cancer. *Oncogene* 2007;**26**(22): 3291-3310.
4. Seshacharyulu P, Ponnusamy MP, Haridas D, Jain M, Ganti AK and Batra SK. Targeting the EGFR signaling pathway in cancer therapy. *Expert Opin Ther Targets* 2012;**16**(1): 15-31.
5. Davies H, Bignell GR, Cox C, Stephens P, Edkins S, Clegg S*, et al.* Mutations of the BRAF gene in human cancer. *Nature* 2002;**417**(6892): 949-954.
6. Prior IA, Lewis PD and Mattos C. A comprehensive survey of Ras mutations in cancer. *Cancer Res* 2012;**72**(10): 2457-2467.
7. Ascierto PA, Kirkwood JM, Grob JJ, Simeone E, Grimaldi AM, Maio M*, et al.* The role of BRAF V600 mutation in melanoma. *J Transl Med* 2012;**10**(85.
8. Genomic Classification of Cutaneous Melanoma. *Cell* 2015;**161**(7): 1681-1696.
9. Clarke CN and Kopetz ES. BRAF mutant colorectal cancer as a distinct subset of colorectal cancer: clinical characteristics, clinical behavior, and response to targeted therapies. *J Gastrointest Oncol* 2015;**6**(6): 660-667.
10. Tang KT and Lee CH. BRAF mutation in papillary thyroid carcinoma: pathogenic role and clinical implications. *J Chin Med Assoc* 2010;**73**(3): 113-128.
11. Yarchoan M, LiVolsi VA and Brose MS. BRAF mutation and thyroid cancer recurrence. *J Clin Oncol* 2015;**33**(1): 7-8.
12. Tiacci E, Trifonov V, Schiavoni G, Holmes A, Kern W, Martelli MP*, et al.* BRAF mutations in hairy-cell leukemia. *N Engl J Med* 2011;**364**(24): 2305-2315.
13. Regad T. Targeting RTK Signaling Pathways in Cancer. *Cancers (Basel)* 2015;**7**(3): 1758-1784.
14. Flaherty KT, Puzanov I, Kim KB, Ribas A, McArthur GA, Sosman JA*, et al.* Inhibition of mutated, activated BRAF in metastatic melanoma. *N Engl J Med* 2010;**363**(9): 809-819.
15. Ribas A, Kim KB, Schuchter LM, Gonzalez R, Pavlick AC, Weber JS*, et al.* BRIM-2: An open-label, multicenter phase II study of vemurafenib in previously treated patients with BRAF V600E mutation-positive metastatic melanoma. *Journal of Clinical Oncology* 2011;**29**(15_suppl): 8509-8509.
16. Zhang C, Spevak W, Zhang Y, Burton EA, Ma Y, Habets G*, et al.* RAF inhibitors that evade paradoxical MAPK pathway activation. *Nature* 2015;**526**(7574): 583-586.
17. Oberholzer PA, Kee D, Dziunycz P, Sucker A, Kamsukom N, Jones R*, et al.* RAS mutations are associated with the development of cutaneous squamous cell tumors in patients treated with RAF inhibitors. *J Clin Oncol* 2012;**30**(3): 316-321.
18. Su F, Viros A, Milagre C, Trunzer K, Bollag G, Spleiss O*, et al.* RAS mutations in cutaneous squamous-cell carcinomas in patients treated with BRAF inhibitors. *N Engl J Med* 2012;**366**(3): 207-215.

19. Chapman PB, Hauschild A, Robert C, Haanen JB, Ascierto P, Larkin J*, et al.* Improved survival with vemurafenib in melanoma with BRAF V600E mutation. *N Engl J Med* 2011;**364**(26): 2507-2516.
20. Tiacci E, Park JH, De Carolis L, Chung SS, Broccoli A, Scott S*, et al.* Targeting Mutant BRAF in Relapsed or Refractory Hairy-Cell Leukemia. *N Engl J Med* 2015;**373**(18): 1733-1747.
21. Hatzivassiliou G, Song K, Yen I, Brandhuber BJ, Anderson DJ, Alvarado R*, et al.* RAF inhibitors prime wild-type RAF to activate the MAPK pathway and enhance growth. *Nature* 2010;**464**(7287): 431-435.
22. Heidorn SJ, Milagre C, Whittaker S, Nourry A, Niculescu-Duvas I, Dhomen N*, et al.* Kinase-dead BRAF and oncogenic RAS cooperate to drive tumor progression through CRAF. *Cell* 2010;**140**(2): 209-221.
23. Holderfield M, Merritt H, Chan J, Wallroth M, Tandeske L, Zhai H*, et al.* RAF inhibitors activate the MAPK pathway by relieving inhibitory autophosphorylation. *Cancer Cell* 2013;**23**(5): 594-602.
24. Falchook GS, Long GV, Kurzrock R, Kim KB, Arkenau TH, Brown MP*, et al.* Dabrafenib in patients with melanoma, untreated brain metastases, and other solid tumours: a phase 1 dose-escalation trial. *Lancet* 2012;**379**(9829): 1893-1901.
25. Ascierto PA, Minor D, Ribas A, Lebbe C, O'Hagan A, Arya N*, et al.* Phase II trial (BREAK-2) of the BRAF inhibitor dabrafenib (GSK2118436) in patients with metastatic melanoma. *J Clin Oncol* 2013;**31**(26): 3205-3211.
26. Hauschild A, Grob JJ, Demidov LV, Jouary T, Gutzmer R, Millward M*, et al.* Dabrafenib in BRAF-mutated metastatic melanoma: a multicentre, open-label, phase 3 randomised controlled trial. *Lancet* 2012;**380**(9839): 358-365.
27. Delord JP, Robert C, Nyakas M, McArthur GA, Kudchakar R, Mahipal A*, et al.* Phase I Dose-Escalation and -Expansion Study of the BRAF Inhibitor Encorafenib (LGX818) in Metastatic BRAF-Mutant Melanoma. *Clin Cancer Res* 2017;**23**(18): 5339-5348.
28. (2016). "Hematology/Oncology (Cancer) Approvals and Safety Notifications." Retrieved September, 2016, from https://www.fda.gov/drugs/resources-information-approved-drugs/hematologyoncology-cancer-approvals-safety-notifications.
29. Ali SM, He J, Carson W, Stephens PJ, Fiorillo J, Lipson D*, et al.* Extended Antitumor Response of a BRAF V600E Papillary Thyroid Carcinoma to Vemurafenib. *Case Rep Oncol* 2014;**7**(2): 343-348.
30. Escudier B, Eisen T, Stadler WM, Szczylik C, Oudard S, Siebels M*, et al.* Sorafenib in advanced clear-cell renal-cell carcinoma. *N Engl J Med* 2007;**356**(2): 125-134.
31. Llovet JM, Ricci S, Mazzaferro V, Hilgard P, Gane E, Blanc JF*, et al.* Sorafenib in advanced hepatocellular carcinoma. *N Engl J Med* 2008;**359**(4): 378-390.
32. Brose MS, Nutting CM, Jarzab B, Elisei R, Siena S, Bastholt L*, et al.* Sorafenib in radioactive iodine-refractory, locally advanced or metastatic differentiated thyroid cancer: a randomised, double-blind, phase 3 trial. *Lancet* 2014;**384**(9940): 319-328.

33. Zhang L, Singh RR, Patel KP, Stingo F, Routbort M, You MJ*, et al.* BRAF kinase domain mutations are present in a subset of chronic myelomonocytic leukemia with wild-type RAS. *Am J Hematol* 2014;**89**(5): 499-504.
34. Falchook GS, Lewis KD, Infante JR, Gordon MS, Vogelzang NJ, DeMarini DJ*, et al.* Activity of the oral MEK inhibitor trametinib in patients with advanced melanoma: a phase 1 dose-escalation trial. *Lancet Oncol* 2012;**13**(8): 782-789.
35. Flaherty KT, Robert C, Hersey P, Nathan P, Garbe C, Milhem M*, et al.* Improved survival with MEK inhibition in BRAF-mutated melanoma. *N Engl J Med* 2012;**367**(2): 107-114.
36. Kim KB, Kefford R, Pavlick AC, Infante JR, Ribas A, Sosman JA*, et al.* Phase II study of the MEK1/MEK2 inhibitor Trametinib in patients with metastatic BRAF-mutant cutaneous melanoma previously treated with or without a BRAF inhibitor. *J Clin Oncol* 2013;**31**(4): 482-489.
37. Gençler B and Gönül M. Cutaneous Side Effects of BRAF Inhibitors in Advanced Melanoma: Review of the Literature. *Dermatol Res Pract* 2016;**2016**(5361569.
38. Blumenschein GR, Jr., Smit EF, Planchard D, Kim DW, Cadranel J, De Pas T*, et al.* A randomized phase II study of the MEK1/MEK2 inhibitor trametinib (GSK1120212) compared with docetaxel in KRAS-mutant advanced non-small-cell lung cancer (NSCLC)†. *Ann Oncol* 2015;**26**(5): 894-901.
39. Hoeflich KP, Merchant M, Orr C, Chan J, Den Otter D, Berry L*, et al.* Intermittent administration of MEK inhibitor GDC-0973 plus PI3K inhibitor GDC-0941 triggers robust apoptosis and tumor growth inhibition. *Cancer Res* 2012;**72**(1): 210-219.
40. Ribas A, Gonzalez R, Pavlick A, Hamid O, Gajewski TF, Daud A*, et al.* Combination of vemurafenib and cobimetinib in patients with advanced BRAF(V600)-mutated melanoma: a phase 1b study. *Lancet Oncol* 2014;**15**(9): 954-965.
41. (2015). "FDA approves Roche's Cotellic (cobimetinib) in combination with Zelboraf (vemurafenib) in advanced melanoma." Retrieved December, 2015, from https://www.roche.com/media/releases/med-cor-2015-11-11.htm.
42. Banerji U, Camidge DR, Verheul HM, Agarwal R, Sarker D, Kaye SB*, et al.* The first-in-human study of the hydrogen sulfate (Hyd-sulfate) capsule of the MEK1/2 inhibitor AZD6244 (ARRY-142886): a phase I open-label multicenter trial in patients with advanced cancer. *Clin Cancer Res* 2010;**16**(5): 1613-1623.
43. Chakravarty D, Santos E, Ryder M, Knauf JA, Liao XH, West BL*, et al.* Small-molecule MAPK inhibitors restore radioiodine incorporation in mouse thyroid cancers with conditional BRAF activation. *J Clin Invest* 2011;**121**(12): 4700-4711.
44. Ho AL, Grewal RK, Leboeuf R, Sherman EJ, Pfister DG, Deandreis D*, et al.* Selumetinib-enhanced radioiodine uptake in advanced thyroid cancer. *N Engl J Med* 2013;**368**(7): 623-632.
45. Hainsworth JD, Cebotaru CL, Kanarev V, Ciuleanu TE, Damyanov D, Stella P*, et al.* A phase II, open-label, randomized study to assess the efficacy and safety of AZD6244 (ARRY-142886) versus pemetrexed in patients with non-small cell lung cancer who have failed one or two prior chemotherapeutic regimens. *J Thorac Oncol* 2010;**5**(10): 1630-1636.
46. Jänne PA, Shaw AT, Pereira JR, Jeannin G, Vansteenkiste J, Barrios C*, et al.* Selumetinib plus docetaxel for KRAS-mutant advanced non-small-cell lung

cancer: a randomised, multicentre, placebo-controlled, phase 2 study. *Lancet Oncol* 2013;**14**(1): 38-47.
47. Jänne PA, van den Heuvel MM, Barlesi F, Cobo M, Mazieres J, Crinò L*, et al.* Selumetinib Plus Docetaxel Compared With Docetaxel Alone and Progression-Free Survival in Patients With KRAS-Mutant Advanced Non-Small Cell Lung Cancer: The SELECT-1 Randomized Clinical Trial. *Jama* 2017;**317**(18): 1844-1853.
48. Awada A, Delord JP, Houédé N, Lebbe C, Lesimple T, Schellens JHM*, et al.* Safety and Recommended Phase II Dose (RP2D) of the Selective Oral MEK1/2 Inhibitor Pimasertib (MSC1936369B/AS703026): Results of a Phase I Trial. *European Journal of Cancer* 2012;**48**(Supplemental 6): 2.
49. Macarulla T, Cervantes A, Tabernero J, Roselló S, Van Cutsem E, Tejpar S*, et al.* Phase I study of FOLFIRI plus pimasertib as second-line treatment for KRAS-mutated metastatic colorectal cancer. *Br J Cancer* 2015;**112**(12): 1874-1881.
50. Lebbe C, Dutriaux C, Lesimple T, Kruit W, Kerger J, Thomas L*, et al.* Pimasertib (PIM) versus dacarbazine (DTIC) in patients (pts) with cutaneous NRAS melanoma: a controlled, open-label phase II trial with crossover. *Annals of Oncology* 2016;**27**(Supplemental 6): 21.
51. Biopharma A. (2017). "Binimetinib (MEK-162)." Retrieved December, 2017, from www.arraybiopharma.com/product-pipeline/binimetinib.
52. Lee AP, Wallace E, Marlow A, Yeh T, Marsh V, Anderson DJ*, et al.* Preclinical Development of ARRY-162, A Potent and Selective MEK 1/2 Inhibitor. *Cancer Res* 2010;**70**(Supplemental 8):
53. Bendell JC, Javle M, Bekaii-Saab TS, Finn RS, Wainberg ZA, Laheru DA*, et al.* A phase 1 dose-escalation and expansion study of binimetinib (MEK162), a potent and selective oral MEK1/2 inhibitor. *Br J Cancer* 2017;**116**(5): 575-583.
54. Cho M, Gong J, Frankel P, Synold TW, Lim D, Chung V*, et al.* A phase I clinical trial of binimetinib in combination with FOLFOX in patients with advanced metastatic colorectal cancer who failed prior standard therapy. *Oncotarget* 2017;**8**(45): 79750-79760.
55. Rizos H, Menzies AM, Pupo GM, Carlino MS, Fung C, Hyman J*, et al.* BRAF inhibitor resistance mechanisms in metastatic melanoma: spectrum and clinical impact. *Clin Cancer Res* 2014;**20**(7): 1965-1977.
56. Shi H, Hugo W, Kong X, Hong A, Koya RC, Moriceau G*, et al.* Acquired resistance and clonal evolution in melanoma during BRAF inhibitor therapy. *Cancer Discov* 2014;**4**(1): 80-93.
57. Van Allen EM, Wagle N, Sucker A, Treacy DJ, Johannessen CM, Goetz EM*, et al.* The genetic landscape of clinical resistance to RAF inhibition in metastatic melanoma. *Cancer Discov* 2014;**4**(1): 94-109.
58. Poulikakos PI, Zhang C, Bollag G, Shokat KM and Rosen N. RAF inhibitors transactivate RAF dimers and ERK signalling in cells with wild-type BRAF. *Nature* 2010;**464**(7287): 427-430.
59. Long GV, Stroyakovskiy D, Gogas H, Levchenko E, de Braud F, Larkin J*, et al.* Combined BRAF and MEK inhibition versus BRAF inhibition alone in melanoma. *N Engl J Med* 2014;**371**(20): 1877-1888.

60. Larkin J, Ascierto PA, Dréno B, Atkinson V, Liszkay G, Maio M*, et al.* Combined vemurafenib and cobimetinib in BRAF-mutated melanoma. *N Engl J Med* 2014;**371**(20): 1867-1876.
61. Dummer R, Ascierto PA, Gogas HJ, Arance AM, Mandala M, LIszkay, G., Grabe C*, et al.* (2016). Results of COLUMBUS Part 1: A phase 3 trial of encorafenib (enco) plusbinimetinib (bini) versus vemurafenib (vem) or enco in BRAF mutant melanoma. Society for Melanoma Research Congress. Boston, MA, doi.
62. Dummer R, Ascierto PA, Gogas HJ, Arance AM, Mandala M, LIszkay, G., Grabe C*, et al.* (2017). Results of COLUMBUS Part 2: a phase 3 trial of encorafenib (enco) plus binimetinib (bini) versus encorafenib in BRAF-mutant melanoma. European Society for Medical Onoclogy. Mardrid, Spain, Annals of Oncology. **28:** 20.
63. Luke JJ, Flaherty KT, Ribas A and Long GV. Targeted agents and immunotherapies: optimizing outcomes in melanoma. *Nat Rev Clin Oncol* 2017;**14**(8): 463-482.
64. Ribas A, Hodi FS, Callahan M, Konto C and Wolchok J. Hepatotoxicity with combination of vemurafenib and ipilimumab. *N Engl J Med* 2013;**368**(14): 1365-1366.
65. Ribas A, Hodi FS, Lawrence D, Atkinson V, Agarwal R, Carlino MS*, et al.* (2017). KEYNOTE-022 update: phase 1 study of first of first-line pembrolizumab plus dabrafenib and trametinib for BRAF-mutant advanced melanoma. European Society for Medical Oncology. Madrid, Spain, Annals of Oncology. **28:** 20.
66. Barlesi F, Mazieres J, Merlio JP, Debieuvre D, Mosser J, Lena H*, et al.* Routine molecular profiling of patients with advanced non-small-cell lung cancer: results of a 1-year nationwide programme of the French Cooperative Thoracic Intergroup (IFCT). *Lancet* 2016;**387**(10026): 1415-1426.
67. Cui G, Liu D, Li W, Fu X, Liang Y, Li Y*, et al.* A meta-analysis of the association between BRAF mutation and nonsmall cell lung cancer. *Medicine (Baltimore)* 2017;**96**(14): e6552.
68. Planchard D, Besse B, Groen HJM, Souquet PJ, Quoix E, Baik CS*, et al.* Dabrafenib plus trametinib in patients with previously treated BRAF(V600E)-mutant metastatic non-small cell lung cancer: an open-label, multicentre phase 2 trial. *Lancet Oncol* 2016;**17**(7): 984-993.
69. (2017, June 2017). "FDA grants regular approval to dabrafenib and trametinib combination for metastatic NSCLC with BRAF V600E mutation." Retrieved December, 2017, from https://www.fda.gov/drugs/resources-information-approved-drugs/fda-grants-regular-approval-dabrafenib-and-trametinib-combination-metastatic-nsclc-braf-v600e.
70. Cohen R, Cervera P, Svrcek M, Pellat A, Dreyer C, de Gramont A*, et al.* BRAF-Mutated Colorectal Cancer: What Is the Optimal Strategy for Treatment? *Curr Treat Options Oncol* 2017;**18**(2): 9.
71. Yaeger R, Cercek A, O'Reilly EM, Reidy DL, Kemeny N, Wolinsky T*, et al.* Pilot trial of combined BRAF and EGFR inhibition in BRAF-mutant metastatic colorectal cancer patients. *Clin Cancer Res* 2015;**21**(6): 1313-1320.
72. Geng F, Wang Z, Yin H, Yu J and Cao B. Molecular Targeted Drugs and Treatment of Colorectal Cancer: Recent Progress and Future Perspectives. *Cancer Biother Radiopharm* 2017;**32**(5): 149-160.

73. Yang H, Higgins B, Kolinsky K, Packman K, Bradley WD, Lee RJ*, et al.* Antitumor activity of BRAF inhibitor vemurafenib in preclinical models of BRAF-mutant colorectal cancer. *Cancer Res* 2012;**72**(3): 779-789.
74. Hong DS, Morris VK, El Osta B, Sorokin AV, Janku F, Fu S*, et al.* Phase IB Study of Vemurafenib in Combination with Irinotecan and Cetuximab in Patients with Metastatic Colorectal Cancer with BRAFV600E Mutation. *Cancer Discov* 2016;**6**(12): 1352-1365.
75. Kopetz S, McDonough SL, Lenz HJ, Magliocco AM, CAtreya CE, Diaz LA*, et al.* Randomized trial of irinotecan and cetuximab with or without vemurafenib in BRAF-mutant metastatic colorectal cancer. *Journal of Clinical Oncology* 2017;**35**(Supplemental 15): 1.
76. Manzano JL, Layos L, Bugés C, de Los Llanos Gil M, Vila L, Martínez-Balibrea E*, et al.* Resistant mechanisms to BRAF inhibitors in melanoma. *Ann Transl Med* 2016;**4**(12): 237.
77. Solit DB and Rosen N. Resistance to BRAF inhibition in melanomas. *N Engl J Med* 2011;**364**(8): 772-774.
78. Mao M, Tian F, Mariadason JM, Tsao CC, Lemos R, Jr., Dayyani F*, et al.* Resistance to BRAF inhibition in BRAF-mutant colon cancer can be overcome with PI3K inhibition or demethylating agents. *Clin Cancer Res* 2013;**19**(3): 657-667.
79. Prahallad A, Sun C, Huang S, Di Nicolantonio F, Salazar R, Zecchin D*, et al.* Unresponsiveness of colon cancer to BRAF(V600E) inhibition through feedback activation of EGFR. *Nature* 2012;**483**(7387): 100-103.
80. Halaban R. RAC1 and melanoma. *Clin Ther* 2015;**37**(3): 682-685.
81. Liu B, Xiong J, Liu G, Wu J, Wen L, Zhang Q*, et al.* High expression of Rac1 is correlated with partial reversed cell polarity and poor prognosis in invasive ductal carcinoma of the breast. *Tumour Biol* 2017;**39**(7): 1010428317710908.
82. Rajendran V, Gopalakrishnan C and Purohit R. Impact of point mutation P29S in RAC1 on tumorigenesis. *Tumour Biol* 2016;**37**(11): 15293-15304.
83. Watson IR, Li L, Cabeceiras PK, Mahdavi M, Gutschner T, Genovese G*, et al.* The RAC1 P29S hotspot mutation in melanoma confers resistance to pharmacological inhibition of RAF. *Cancer Res* 2014;**74**(17): 4845-4852.
84. Zhou Y, Liao Q, Han Y, Chen J, Liu Z, Ling H*, et al.* Rac1 overexpression is correlated with epithelial mesenchymal transition and predicts poor prognosis in non-small cell lung cancer. *J Cancer* 2016;**7**(14): 2100-2109.
85. Stahl JM, Cheung M, Sharma A, Trivedi NR, Shanmugam S and Robertson GP. Loss of PTEN promotes tumor development in malignant melanoma. *Cancer Res* 2003;**63**(11): 2881-2890.
86. Kennedy SG, Wagner AJ, Conzen SD, Jordán J, Bellacosa A, Tsichlis PN*, et al.* The PI 3-kinase/Akt signaling pathway delivers an anti-apoptotic signal. *Genes Dev* 1997;**11**(6): 701-713.
87. Wu H, Goel V and Haluska FG. PTEN signaling pathways in melanoma. *Oncogene* 2003;**22**(20): 3113-3122.
88. Cheney IW, Johnson DE, Vaillancourt MT, Avanzini J, Morimoto A, Demers GW*, et al.* Suppression of tumorigenicity of glioblastoma cells by adenovirus-mediated MMAC1/PTEN gene transfer. *Cancer Res* 1998;**58**(11): 2331-2334.

89. Paraiso KH, Xiang Y, Rebecca VW, Abel EV, Chen YA, Munko AC*, et al.* PTEN loss confers BRAF inhibitor resistance to melanoma cells through the suppression of BIM expression. *Cancer Res* 2011;**71**(7): 2750-2760.
90. Catalanotti F, Chang DT, Shoushtari AN, Johnson DB, Panageas KS, Momtaz P*, et al.* PTEN Loss-of-Function Alterations Are Associated With Intrinsic Resistance to BRAF Inhibitors in Metastatic Melanoma. *JCO Precision Oncology* 2017, doi: 10.1200/PO.16.00054 JCO
91. Gogada R, Yadav N, Liu J, Tang S, Zhang D, Schneider A*, et al.* Bim, a proapoptotic protein, up-regulated via transcription factor E2F1-dependent mechanism, functions as a prosurvival molecule in cancer. *J Biol Chem* 2013;**288**(1): 368-381.
92. Sheppard KE and McArthur GA. The cell-cycle regulator CDK4: an emerging therapeutic target in melanoma. *Clin Cancer Res* 2013;**19**(19): 5320-5328.
93. Smalley KS, Lioni M, Dalla Palma M, Xiao M, Desai B, Egyhazi S*, et al.* Increased cyclin D1 expression can mediate BRAF inhibitor resistance in BRAF V600E-mutated melanomas. *Mol Cancer Ther* 2008;**7**(9): 2876-2883.
94. Tol J, Nagtegaal ID and Punt CJ. BRAF mutation in metastatic colorectal cancer. *N Engl J Med* 2009;**361**(1): 98-99.
95. Kopetz S, Desai J, Chan E, Hecht JR, O'Dwyer PJ, Lee RJ*, et al.* PLX4032 in metastatic colorectal cancer patients with mutant BRAF tumors. *Journal of Clinical Oncology* 2010;**28**(Supplemental 15): 1.
96. Kim HS, Jung M, Kang HN, Kim H, Park CW, Kim SM*, et al.* Oncogenic BRAF fusions in mucosal melanomas activate the MAPK pathway and are sensitive to MEK/PI3K inhibition or MEK/CDK4/6 inhibition. *Oncogene* 2017;**36**(23): 3334-3345.
97. Kulkarni A, Al-Hraishawi H, Simhadri S, Hirshfield KM, Chen S, Pine S*, et al.* BRAF Fusion as a Novel Mechanism of Acquired Resistance to Vemurafenib in BRAF(V600E) Mutant Melanoma. *Clin Cancer Res* 2017;**23**(18): 5631-5638.
98. Emery CM, Vijayendran KG, Zipser MC, Sawyer AM, Niu L, Kim JJ*, et al.* MEK1 mutations confer resistance to MEK and B-RAF inhibition. *Proc Natl Acad Sci U S A* 2009;**106**(48): 20411-20416.
99. Johannessen CM, Boehm JS, Kim SY, Thomas SR, Wardwell L, Johnson LA*, et al.* COT drives resistance to RAF inhibition through MAP kinase pathway reactivation. *Nature* 2010;**468**(7326): 968-972.
100. Goel HL and Mercurio AM. VEGF targets the tumour cell. *Nat Rev Cancer* 2013;**13**(12): 871-882.
101. O'Leary B, Finn RS and Turner NC. Treating cancer with selective CDK4/6 inhibitors. *Nat Rev Clin Oncol* 2016;**13**(7): 417-430.
102. Postow MA, Callahan MK and Wolchok JD. Immune Checkpoint Blockade in Cancer Therapy. *J Clin Oncol* 2015;**33**(17): 1974-1982.
103. Nazarian R, Shi H, Wang Q, Kong X, Koya RC, Lee H*, et al.* Melanomas acquire resistance to B-RAF(V600E) inhibition by RTK or N-RAS upregulation. *Nature* 2010;**468**(7326): 973-977.
104. Shi H, Kong X, Ribas A and Lo RS. Combinatorial treatments that overcome PDGFRβ-driven resistance of melanoma cells to V600EB-RAF inhibition. *Cancer Res* 2011;**71**(15): 5067-5074.

105. Perna D, Karreth FA, Rust AG, Perez-Mancera PA, Rashid M, Iorio F*, et al.* BRAF inhibitor resistance mediated by the AKT pathway in an oncogenic BRAF mouse melanoma model. *Proc Natl Acad Sci U S A* 2015;**112**(6): E536-545.
106. Vivanco I and Sawyers CL. The phosphatidylinositol 3-Kinase AKT pathway in human cancer. *Nat Rev Cancer* 2002;**2**(7): 489-501.
107. Sweetlove M, Wrightson E, Kolekar S, Rewcastle GW, Baguley BC, Shepherd PR*, et al.* Inhibitors of pan-PI3K Signaling Synergize with BRAF or MEK Inhibitors to Prevent BRAF-Mutant Melanoma Cell Growth. *Front Oncol* 2015;**5**(135.
108. Temraz S, Mukherji D and Shamseddine A. Dual Inhibition of MEK and PI3K Pathway in KRAS and BRAF Mutated Colorectal Cancers. *Int J Mol Sci* 2015;**16**(9): 22976-22988.
109. Schopf FH, Biebl MM and Buchner J. The HSP90 chaperone machinery. *Nat Rev Mol Cell Biol* 2017;**18**(6): 345-360.
110. Miyata Y, Nakamoto H and Neckers L. The therapeutic target Hsp90 and cancer hallmarks. *Curr Pharm Des* 2013;**19**(3): 347-365.
111. Pacey S, Gore M, Chao D, Banerji U, Larkin J, Sarker S*, et al.* A Phase II trial of 17-allylamino, 17-demethoxygeldanamycin (17-AAG, tanespimycin) in patients with metastatic melanoma. *Invest New Drugs* 2012;**30**(1): 341-349.
112. Byrd KM, Subramanian C, Sanchez J, Motiwala HF, Liu W, Cohen MS*, et al.* Synthesis and Biological Evaluation of Novobiocin Core Analogues as Hsp90 Inhibitors. *Chemistry* 2016;**22**(20): 6921-6931.
113. White PT, Subramanian C, Zhu Q, Zhang H, Zhao H, Gallagher R*, et al.* Novel HSP90 inhibitors effectively target functions of thyroid cancer stem cell preventing migration and invasion. *Surgery* 2016;**159**(1): 142-151.
114. Chai RC, Vieusseux JL, Lang BJ, Nguyen CH, Kouspou MM, Britt KL*, et al.* Histone deacetylase activity mediates acquired resistance towards structurally diverse HSP90 inhibitors. *Mol Oncol* 2017;**11**(5): 567-583.
115. Raveendran S, Rao A and Storkus W. Combination Immunotherapy of Melanoma by inhibiting HSP90 and targeting its client proteins. (TUM7P.934). *The Journal of Immunology* 2014;**192**(1):
116. Long GV, Trefzer U, Davies MA, Kefford RF, Ascierto PA, Chapman PB*, et al.* Dabrafenib in patients with Val600Glu or Val600Lys BRAF-mutant melanoma metastatic to the brain (BREAK-MB): a multicentre, open-label, phase 2 trial. *Lancet Oncol* 2012;**13**(11): 1087-1095.
117. Network NCC. (2017). "Melanoma NCCN Guidelines with NCCN Evidence Blocks." Retrieved July, 2017, from https://www.nccn.org/professionals/physician_gls/pdf/melanoma_blocks.pdf.
118. Network NCC. (2017). "Thyroid Carcinoma NCCN Guidelines with NCCN Evidence Blocks." Retrieved July, 2017, from https://www.nccn.org/professionals/physician_gls/pdf/thyroid_blocks.pdf.
119. Network NCC. (2017). "Colon Cancer NCCN Guidelines with NCCN Evidence Blocks." Retrieved July, 2017, from https://www.nccn.org/professionals/physician_gls/pdf/colon_blocks.pdf.
120. Network NCC. (2017). "Non-Small Cell Lung Cancer NCCN Guidelines with NCCN Evidence Blocks." Retrieved July, 2017, from https://www.nccn.org/professionals/physician_gls/pdf/nscl_blocks.pdf.

121. Network NCC. (2017). "Hairy Cell Leukemia NCCN Guidelines with NCCN Evidence Blocks." Retrieved July, 2017, from https://www.nccn.org/professionals/physician_gls/pdf/hairy_cell.pdf.
122. Lexicomp. (2017). "Vemurafenib: Drug Information." Retrieved July, 2017, from https://www.uptodate.com/contents/molecularly-targeted-therapy-for-metastatic-melanoma?search=vemurafenib-drug-information&source=search_result&selectedTitle=2~49&usage_type=default&display_rank=2.
123. Lexicomp. (2017). "Dabrafenib: Drug Information." Retrieved July, 2017, from https://www.uptodate.com/contents/dabrafenib-druginformation?source=search_result&search=dabrafenib&selectedTitle=1*33.
124. Lexicomp. (2017). "Sorafenib: Drug Information." Retrieved July, 2017, from https://www.uptodate.com/contents/sorafenib-druginformation?source=search_result&search=sorafenib&selectedTitle=1*107.
125. Lexicomp. (2017). "Trametinib: Drug Information." Retrieved July, 2017, from https://www.uptodate.com/contents/trametinib-druginformation?source=search_result&search=trametinib&selectedTitle=1*28.
126. Lexicomp. (2017). "Cobimetinib: Drug Information." Retrieved July, 2017, from https://www.uptodate.com/contents/cobimetinib-druginformation?source=search_result&search=cobimetinib&selectedTitle=1*18.

Chapter 2
Old and New Approaches to Target the Hsp90 Chaperone[2]

Abstract

The 90-kDa heat shock protein (Hsp90) is a molecular chaperone that ensures cellular proteostasis by maintaining the folding, stabilization, activation, and degradation of over 400 client proteins. Hsp90 is not only critical for routine protein maintenance in healthy cells, but also during states of cellular stress, such as cancer and neurodegenerative diseases. Due to its ability to affect phosphorylation of numerous client proteins, inhibition of Hsp90 has been an attractive anticancer approach since the early 1990's, when researchers identified a druggable target on the amino terminus of Hsp90 for a variety of cancers. Since then, 17 Hsp90 inhibitors that target the chaperone's N-terminal domain, have entered clinical trials. None, however, have been approved thus far by the FDA as a cancer monotherapy. In these trials, a major limitation observed with Hsp90 inhibition at the N-terminal domain was dose-limiting toxicities and relatively poor pharmacokinetic profiles. Despite this, preclinical and clinical research continues to show that Hsp90 inhibitors effectively target cancer cell death and decrease tumor progression supporting the rationale for the development of novel Hsp90 inhibitors. Here, we present an in-depth overview of the Hsp90 inhibitors used in clinical trials. Finally, we present current shifts in the field related to targeting the carboxy-terminal domain of Hsp90 as well

[2] This chapter was published in *Current Cancer Drug Targets* (PMID: 31793427) and completed in collaboration with the following authors: Trever R. Carter, Mark S. Cohen, and Brian S.J. Blagg.

as to the development of isoform-selective inhibitors as a means to bypass the pitfalls of current Hsp90 inhibitors and improve clinical trial outcomes.

Introduction

A vital characteristic of all eukaryotic cells is the requirement for proper molecular chaperone function. These chaperone proteins serve as part of a cell's "quality control system" to ensure proteostasis. Specifically, chaperones maintain the folding, stability, activation, and degradation of intracellular proteins, ultimately contributing to overall cellular homeostasis [1]. Proteins that depend upon and/or interact with these molecular chaperones are called clients. Chaperone function is not only important for routine client maintenance, but also in response to cellular stress. In certain disease states, like cancer and neurodegenerative diseases, proteins are often misfolded, leading to aggregation, which increases the cellular dependence upon chaperone function [2]. In light of this, there is a significant amount of interest to design and develop novel therapeutics that target molecular chaperones, specifically the heat shock protein (Hsp) family.

The Hsp family of molecular chaperones was first observed in *Drosophila melanogaster* by Ritossa in the early 1960s as a result of a heat-induced change to chromosome appearance [3]. In the *D. melanogaster* cells, certain regions of chromosomes gained "puff sites" where there was an increase of RNA synthesis and subsequent changes to the pattern of protein expression [4-6]. Interestingly, a small subset of these proteins accounted for the majority of proteins with increased expression and was accordingly named heat shock proteins [7]. Since their discovery and characterization, expression levels of these chaperones are not only increased in response to heat, but other environmental stressors as well, such as inflammation, hypoxia, infection, and/or nutrient deprivation. This increase in Hsp expression is the result of the heat shock response (HSR) that is mediated by the transcription factor heat

shock factor-1 (HSF1) binding to its transcriptional element, the heat shock element (HSE) [8]. The Hsp family consists of a multitude of chaperones named according to molecular weight. In regard to novel therapeutic agents, inhibitors that disrupt the 90-kDa Hsp (Hsp90) function are at the forefront of development and exhibit high potential for clinical use in humans and more specifically, the treatment of cancer.

Hsp90 accounts for 1-2% of total protein concentration in unstressed cells, whereas chaperone expression levels increase to ~4-6% in response to cellular stress as a means to handle the increased demand for client protein stabilization [1,9]. Regardless of cellular state, Hsp90 clientele includes a variety of proteins involved in several cellular processes and pathways, such as protein kinases, cell cycle regulators, transcription factors, and steroid hormone receptors, to name a few [10]. Interestingly, in the stressed state, which is common to malignancies, Hsp90 serves as a chaperone to numerous proteins that maintain the ten hallmarks of cancer [11,12]. Taken together, these points highlight the opportunity that Hsp90 chaperone inhibition simultaneously targets multiple oncogenic pathways and proteins.

In the early 1990s, Whitesell and colleagues demonstrated Hsp90's crucial role in oncogenic transformation by serendipitously inhibiting chaperone function with a benzoquinone ansamycin, geldanamycin (GDA), which initiated the concept of chaperone inhibition [13]. Prior to this finding, it was mechanistically unclear how oncogenic gene products, like tyrosine kinases and more specifically *v-src*, promoted the transformation of healthy cells into malignant ones [14]. GDA was presumed to be a tyrosine kinase inhibitor until Whitesell and colleagues showed that it bound to Hsp90 in a stable and specific manner. This binding not only disrupted the formation of the Hsp90-src

heteroprotein complex, but it also inhibited transformation, highlighting the dependence of the cell on Hsp90 during oncogenesis [15]. Since this pivotal finding, Hsp90's function and role in oncogenesis have been more well-defined, leading to the development of several compounds that target and inhibit the chaperone. Of these inhibitors, a handful have entered clinical trials for the treatment of cancer, but none yet have been approved for use as anti-neoplastic agents [16].

Although the need for Hsp90's function has mostly been recognized in cancer, the molecular chaperone also plays an integral role in the pathogenesis of neurodegenerative diseases characterized by protein aggregation, such as Alzheimer's disease (AD) and Parkinson's disease (PD) [17]. Interestingly, the proteins most implicated in protein aggregation in AD and PD are Hsp90 clients – β-amyloid (Aβ) peptide and tau and α-synuclein, respectively. For example, two hallmark indicators of AD are extracellular plaque deposits of Aβ and hyperphosphorylated tau [17,18]. In PD, α-synuclein is recognized as a genetic and pathological link to disease progression. More specifically, this protein is found deposited in Lewy bodies which are abnormal aggregates formed in presynaptic nerve terminals [19,20]. Unlike malignancies, where inhibition of Hsp90's function is ideal for treatment, it has been suggested that neurodegenerative diseases would benefit most from the upregulation of chaperone function to increase its cytoprotective role and ultimately decrease protein aggregation [17]. While the development of Hsp90 treatments for AD and PD is warranted, we will focus the remainder of our insights on Hsp90 therapeutic approaches in the context of malignancies.

Here, we provide a comprehensive, up-to-date evaluation of the Hsp90 inhibitors that have entered clinical trials, specifically in malignancies, as well as some observations as to why they have not yet achieved FDA approval. From these observations in trials, researchers have now shifted to alternative approaches to Hsp90 inhibition, including targeting the carboxy terminal domain as well as characterizing and developing isoform specific Hsp90 inhibitors that can then be selectively targeted in certain disease states.

Hsp90 Family of Proteins

The mammalian Hsp90 family of proteins is highly conserved and includes four members or isoforms. These proteins are indirectly involved in several cellular processes and found in distinct cellular compartments. In addition to Hsp90's function as a molecular chaperone, it serves an essential role in overall cellular homeostasis [10,21,22]. The majority of Hsp90 isoforms are located in the cytoplasm and in the HSP90A subfamily, which includes inducible Hsp90α and constitutively expressed Hsp90β isoforms. Also, there are the HSP90B and TRAP subfamilies that include the Grp94 isoform in the endoplasmic reticulum and TRAP1 isoform in the mitochondria, respectively [22]. The three Hsp90 subfamilies, their five gene products, and respective cellular locations are listed in **Table** 2-1. Despite occupying different cellular compartments, all isoforms share a very similar sequence and structural homology, which are important to understand in order to better evaluate and critique the challenges of current Hsp90 inhibitors.

The family of molecular chaperones is biologically active as homodimers with each monomer made up of three structurally and functionally distinct domains: N-terminal, middle, and C-terminal domains (**Figure** 2-1) [21]. The N-terminal domain (NTD) is the

site for nucleotide binding and ATPase activity [23]. The middle domain (MD) also plays an important role in the hydrolysis of ATP to ADP – namely, the Arg380 residue, which is part of the catalytic loop for hydrolysis [24]. The NTD and MD are connected or tethered to each other via a charged linker region. Lastly, the C-terminal domain (CTD) is the site for protein dimerization and additional ATP binding [25]. The CTD contains a tetratricopeptide repeat (TPR) motif that increases binding specificity for its substrates, especially co-chaperones with similar TPR-motifs. All three regions have been reported to bind clients and co-chaperones.

All inhibitors that have undergone clinical investigation as anticancer drugs, target the NTD and bind competitively to its ATP binding site. Although effective and potent at killing cancer cells preclinically, in clinical trials detrimental dose-limiting toxicities (DLTs) and dose scheduling limitations have prevented NTD Hsp90 inhibitors from gaining FDA approval [26]. One speculation in the field regarding the failure of NTD compounds in clinical trials due to DLTs is that NTD targeting leads to a “pan-inhibitory” effect against all Hsp90 isoforms and induces the HSR, leading to a pro-survival effort by the cell that in turn requires a higher dose of inhibition of Hsp90 to achieve the same cancer cell suppressive effect thereby resulting in progressive dose escalation, and over time, DLTs [21,27,28]. Although this remains a major obstacle in the clinic, recent findings at the 9th International Conference on the Hsp90 Chaperone Machine (ICHCM) suggest a new approach to target the chaperone which could decrease DLTs. At the conference, Dr. Brian Blagg presented two newly designed scaffolds of Hsp90β isoform-selective inhibitors that promoted degradation of HSF1 and ultimately led to no HSR induction [29]. This novel approach will be revisited in a subsequent section of the manuscript. As of

February 2019, more than 170 clinical trials have taken place to test 18 different Hsp90 inhibitors and their potential uses as therapeutic agents in humans [see ClinicalTrials.gov]. Although the majority of trials are seen through to completion, more than half do not progress past Phase I (**Figure** 2-2). In the following section, we present a comprehensive description of these chaperone inhibitors in clinical trials to date, in order to highlight their strengths and weaknesses. Additionally, we provide insight and recommendations to improve the development of novel Hsp90 inhibitors as anticancer agents.

Clinical Landscape of Hsp90 Inhibitors

For over 25 years, the development of Hsp90 inhibitors has predominantly centered around the design of drug com- pounds that competitively bind the N-terminal ATP-binding sites to disrupt molecular chaperone function [21,30]. Moreover, all four Hsp90 isoforms share high sequence identity in this region, which decreases the potential to selectively target a specific isoform. This form of pan-inhibition, wherein all isoforms are non-selectively inhibited, has been thought to represent a major limitation in the clinical development and approval of these inhibitors as anticancer agents. For cancer cells, optimal inhibitors should selectively target the cytosolic isoforms Hsp90α and Hsp90β, however this has been very difficult as these isoforms share >95% sequence identity in the NTD. Perhaps by gaining a better understanding of the chaperone's enzyme kinetics, it could help to distinguish each isoform and lead to the generation of more durable and effective Hsp90 inhibitors. Lee et al. eloquently present Hsp90 as being a "perfect enzyme" due to the chaperone having an ATP hydrolysis rate of ~1 s^{-1}. Although demonstrated in *Escherichia coli*, this work emphasizes the indispensable value

of gaining a mechanistic understanding of the ATPase activity, especially before optimizing inhibitors that disrupt its function [31]. The 18 Hsp90 inhibitors are characterized by five chemical structure-based categories: (i) natural products and their derivatives, (ii) purine-based, (iii) benzamide, (iv) resorcinol-containing, and (v) miscellaneous. The following five sections give an in-depth evaluation of Hsp90 inhibitors that have entered clinical trials.

Natural Products and their Derivatives

As mentioned above, in the early 1990s Whitesell and colleagues identified GDA as a ligand of Hsp90, and years later, demonstrated its binding to the N-terminal ATP-binding site. Upon GDA binding, ATPase activity of the molecular chaperone is disrupted and subsequently client-protein stabilization, which results in client protein degradation and an attack on multiple cellular processes [32]. GDA is a 1,4-benzoquinone ansamycin antibiotic derived from *Streptomyces hygroscopicus* (**Figure** 2-3) [33]. Although GDA effectively and potently kills cancer cells, it is not a good clinical candidate due to *in vivo* toxicity, instability, and poor solubility [34]. Specifically, GDA contains a reactive quinone that produces superoxide radicals causing cell death independent of Hsp90 inhibition [35]. Because of this, various groups have put forth a substantial amount of effort and resources to modify this compound and eliminate its redox potential. In addition to GDA, another natural product, radicicol (RDC), is isolated from the fungus *Monosporium bonorden* (**Figure** 2-3) [33]. Similar to GDA, RDC competitively binds Hsp90 at the ATP-binding site. Although GDA and RDC do not have clinical utility, the two natural products support the rationale that inhibiting Hsp90 represents a multi-pronged anticancer therapeutic approach. This resulted in the design and development of several semi-

synthetic GDA derivatives. Upon further investigation, it was determined that the C-17 position of GDA was critical for its mechanism of action and toxic reactivity. As a result, 17-N-allylamino-17-dimethoxygeldanamycin (17-AAG; tanespimycin), 17-AAGH$_2$ (IPI-504; retaspimycin), 17-AG (IPI-493), and 17-dimethylamino-17-dimthoxygeldanamycin (17-DMAG; alvespimycin) were designed and synthesized (**Figure** 2-3) [32].

By the end of 2003, the first GDA derivative 17-AAG, which adds an allylamine substituent to the C-17 position, entered eight Phase I clinical trials. Since then, there have been a total of 35 (23% terminated). Of these trials, none progressed past Phase II, which decreased enthusiasm for the development of GDA derivatives. Despite being reasonably effective against cancer tumor growth in early clinical trials, 17-AAG exhibited poor bioavailability. In order to improve this, Infinity Pharmaceuticals designed and synthesized the compound 17-AAGH$_2$ (IPI-504; retaspimycin) [36]. This hydroquinone hydrochloride salt analog improves the metabolic profile of 17-AAG by eliminating the requirement for reduction. Another benefit of this analog was its increased potency of Hsp90 inhibition. The development of 17-AAGH$_2$ resulted in 13 clinical Phase I or II trials with approximately half terminated or withdrawn. Another semi-synthetic benzoquinone ansamycin derivative developed by the same pharmaceutical company is 17-AG (IPI-493) [37]. At the time, 17-AG was a promising clinical candidate since it is the major metabolite of all GDA derivatives and was effective in preclinical xenograft models [38]. There have been only two reported 17-AG clinical trials, which ran simultaneously with retaspimycin trials, both of which were terminated due to superior effect of retaspimycin. Kosan Biosciences designed and developed 17-dimethylamino-17-dimthoxygeldana-mycin (17-DMAG; alvespimycin) which improved the physiochemical profile of GDA by

remaining protonated at physiological pH. 17-DMAG entered six Phase I clinical trials (17% terminated) and one Phase II that was terminated.

Purine-based Inhibitors

Similar to all ATPases, Hsp90 binds and hydrolyzes ATP, but the chaperone does so in a unique way. The molecular chaperone belongs to the Gyrase, Hsp90, Histidine kinase, MutL (GHKL) ATPase family, all of which share a special β-α-β fold containing four motifs I-IV. A pair of motifs within the fold interact with a different moiety of the ATP molecule; motifs I and III interact with the phosphate groups while motifs II and IV with the adenine component [39]. Taking advantage of this unique interaction with ATP, Chiosis and colleagues at Memorial Sloan Kettering designed the first reported fully synthetic small molecule Hsp90 inhibitor, PU-3 (**Figure** 2-4) [34,40]. After successfully arresting growth and differentiation in breast cancer cells, researchers began to enhance the purine chemical scaffold in PU-3 and generate derivatives [41]. To-date, there are five purine or purine-like compounds that entered clinicals trials, with none progressing past Phase II. These inhibitors include: BIIB021, BIIB028, MPC-3100, PU-H71, and Debio0932 (**Figure** 2-4). Two defining characteristics of inhibitors in this class are a purine (or purine-like) scaffold with amine and aryl substituents.

Biogen, Inc. developed BIIB021 and BIIB028, wherein the latter is an optimization of the former (**Figure** 2-4) [34,41-44]. In 2006, two Phase I clinical trials tested BIIB021 in chronic lymphocytic leukemia and advanced solid tumors. Although BIIB021 eventually progressed to two Phase II clinical trials by 2009, major limitations kept it from moving through the clinical pipeline. BIIB021 is an effective small molecule inhibitor, but lacks potency requiring higher doses to achieve biological effects. Additionally, the chemicals

needed to synthesize the molecule on a large scale are toxic and an acceptable intravenous formulation is difficult to obtain. Due to these setbacks, Biogen, Inc. designed and developed BIIB028. In an effort to improve potency, tolerability, and physical properties, the pharmaceutical company used X-ray crystal structure analysis to identify the N-7 position on the purine scaffold as an optimal site for modification [42]. After developing a series of alkynol analogs, BIIB028 was designed as a prodrug and identified as a lead second generation clinical candidate. Although seen through to completion, it entered only one trial in 2008.

MCP-3100 and Debio0932, inhibitors developed by Myrexis and Curtis Pharma respectively, entered three trials collectively, and did not demonstrate any clinical promise to move beyond Phase II [34]. Conversely, a newer compound, PU-H71, discovered by the Chiosis group at Memorial Sloan Kettering, is now listed in five clinical trials as either active, recruiting, or terminated (80% active or recruiting) [45]. The Phase I trial that was terminated resulted from a drug supply shortage and not a dose limiting toxicity.

Benzamide Inhibitors

Serenx Inc. discovered the pyrazole-containg Hsp90 inhibitor, SNX-5422, using an ATP-affinity column (**Figure** 2-5) [34,46,47]. In 2007, the first clinical trial testing SNX-5422 was posted. To-date there have been 13 trials, with one currently ongoing. This compound shows clinical promise due to its bioavailability as a prodrug, but a major limitation is its pan-inhibitory activity against all Hsp90 isoforms, with the induction of the HSR and resulting dose escalation challenges.

Resorcinol Containing Inhibitors

Using a high-throughput screen, Chueng and colleagues at The Institute for Cancer Research in London were the first to identify resorcinol-containing small molecule Hsp90 inhibitors [48]. In an effort to optimize this class of molecules, scientists at Vernalis and Novartis used structure-based drug design to improve compound solubility by adding substituents, which led to the discovery of AUY922 (luminespib) (**Figure** 2-6) [34,49]. Preclinical studies show that this Hsp90 inhibitor is active against tumor growth, angiogenesis, and metastasis in a xenograft mouse model [50,51]. In fact, AUY922 entered 25 clinical trials, both Phase I and II, with two trials currently on-going and one recruiting as of February 2019. Similarly, scientists at Synta Pharmaceuticals modified the resorcinol scaffold to discover STA-9090 (**Figure** 2-6) [52]. The Synta group first presented this novel inhibitor at the AACR-NCI-EORT International Conference on Molecular Targets and Cancer Therapeutics. In 2010, they presented preclinical and clinical data at another international cancer conference showing that the second-generation Hsp90 inhibitor demonstrates higher potency in downregulating oncoproteins and pathways than first-generation ansamycin-derived inhibitors. Interestingly, this Hsp90 inhibitor progressed into Phase III trials and entered nearly 40 trials in total, making it the most clinically evaluated Hsp90 inhibitor on record. Around the same time, scientists at Astex Therapeutics in the UK discovered another resorcinol containing Hsp90 inhibitor, AT13387 (**Figure** 2-6) [53]. This compound was discovered as part of a fragment-based drug design approach by combining NMR and X-ray crystallography. Optimization of the compound series led to a resorcinol scaffold that has both high potency and ideal ligand efficacy [54]. AT13387 is currently in three active and four recruiting clinical trials. Finally,

KW-2478 is an Hsp90 inhibitor discovered by scientists at Kyowa Hakko Kirin in Japan (**Figure** 2-6) [55]. The drug was tested in two clinical trials, one of which was completed in 2014 in combination with bortezomib, a proteasome inhibitor, in multiple myeloma. The primary objectives of the study were to establish safety of the combination therapy and assess overall response rates [56].

Miscellaneous

Other research groups have also designed and developed inhibitors of the molecular chaperone but are unique or do not have publicly available structures and therefore do not fall into one of the general classes of Hsp90 inhibitors above. These compounds include XL888, HSP990, DS2248, and TAS-116 discovered by Exelixis, Inc., Novartis, Daiichi Sankyo, Inc., and Taiho Pharmaceutical Co., respectively (**Figure** 2-7) [57-59]. Interestingly, all of these inhibitors manifest the same mechanism of action as the aforementioned inhibitors—binding Hsp90's NTD—except for TAS-116. This drug is unique, as it is the first reported compound to enter clinical trials that selectively binds to the cytosolic isoforms of Hsp90 (Hsp90α and Hsp90β) [34,60]. Between 2014 and 2017, 61 patients with advanced solid tumors in Japan and the United Kingdom were enrolled in the first-in-human clinical trial testing of TAS-116. The primary objectives of the study aimed to identify the maximum tolerated dose, safety, and overall response rates in patients with advanced solid tumors taking TAS-116 as a monotherapy intervention [61]. In March 2019, results from the study revealed minor adverse events (e.g. Grade 1 or 2) related to Hsp90 inhibition and a positive antitumor effect against solid tumors including KIT wild-type gastrointestinal stromal tumors (GIST). Additionally, the study identified three oral dosing schedules for future trials testing TAS-116. There are two on-going trials

in Japan evaluating this cellular compartment selective Hsp90 inhibitor. The trials are testing TAS-116 in combination with nivolumab, an immune checkpoint PD-1 inhibitor, in metastatic solid tumors or alone in GIST patients (Phase I and Phase II, respectively) [62].

Since the early 2000s, all Hsp90 inhibitors, except for TAS-116, that have entered clinical trials target the NTD of Hsp90. Clinical observations and trial data interpretation indicate that this approach carries antitumor efficacy but suffers from toxicities and adverse effects including hepatic, cardio, and ocular toxicities, as well as dose-scheduling limitations after induction of the HSR. Given the clinical efficacy potential Hsp90 inhibition carries, it would be ideal to develop novel Hsp90 inhibitors that can improve upon the pharmacodynamic and toxicity profiles of this therapeutic approach. Various efforts have been put forth to circumvent these setbacks, such as optimizing the approach to inhibit Hsp90's function. Specifically, certain groups, like Taiho Pharmaceutical Co. and our research group, hypothesize that selectively targeting the cytosolic isoforms (Hsp90α and Hsp90β) will lead to better clinical outcomes and have the potential to be FDA approved. In the following sections we elaborate upon the rational for employing a more selective approach to inhibit Hsp90's function and provide examples to demonstrate recent advancements in the field.

Inhibiting the Hsp90 C-terminal Domain

Although GDA and RDC bind to the N-terminal ATP binding motif of Hsp90, recent studies have demonstrated the existence of a C-terminal ATP binding region as well [63-65]. Similarly, Hsp90 contains two different binding sites for proteins, allowing the chaperone to bind both cochaperones and unfolded client proteins at the C- and N-

terminal regions [10,24,63,64]. Unlike the NTD, inhibitors that competitively bind at the nucleotide binding site to abrogate ATPase activity, small molecules that target and bind the CTD disrupt the association of co-chaperones containing TPR-motifs. This ultimately leads to aberrant chaperone function [17]. A hallmark example of a CTD Hsp90 inhibitor is novobiocin, a DNA gyrase ATP-binding site inhibitor, and its subsequent analogue KU-174 (**Figure** 2-8). Inhibition of the Hsp90 protein folding machinery by novobiocin also leads to destabilization of the multiprotein complex (**Figure** 2-9), which results in ubiquitinylation of the client protein, proteasome mediated hydrolysis and in many cases, induction of apoptosis in numerous cancer cell types [63,66]. A desirable characteristic of novobiocin is the lack of HSR induction, which is a major clinical drawback to all NTD Hsp90 inhibitors [67]. It is important to note that although novobiocin and most of its derivatives inhibit Hsp90's function, there has been recent evidence supporting paradoxical ATPase activation. Chatterjee et al. report that the novobiocin derivative, KU-32, binds the CTD which in turn leads to a global change in chaperone structure. This structural shift not only promotes ATP binding, but increases ATPase activity [68]. In this context, KU-32 is viewed as a positive allosteric modulator of Hsp90 function and could be used as a tool to develop AD and PD therapies. In addition to disrupting protein-protein interactions (PPIs) between Hsp90 and co-chaperones with distinct chemical scaffolds, such as novobiocin, Rahimi et al. demonstrated blockade of heterocomplex chaperone PPIs with a unique small molecule, LB76 [69]. This molecule was designed de novo using an amino acid sequence specific to the MEEVD region of the TPR-motif on the CTD.

Prior to studies by Prodromou and coworkers in 2006, no crystal structure of full-length Hsp90 protein had been solved [23]. Two binding sites for ligands are suggested

by this structure. One is located in the NTD and the other appears proximal to the dimerization domain. Clearly, a co-crystal structure of Hsp90 bound to novobiocin would be helpful towards further elucidation of the CTD binding site. However, the affinity of novobiocin for the CTD is too low for co-crystallization studies [63,67,70].

In 2004, Cox and coworkers demonstrated that the Hsp90-dependent transcription factor, aryl hydrocarbon receptor (AhR), was preferentially sensitive to the effects of NTD inhibitors and p23 concentration, whereas inhibition of the CTD with novobiocin remained unaffected by p23 concentration. Through subsequent studies, they determined that GDA and RDC were unable to overcome the effects of overexpressed p23, because NTD inhibitors competed for the same region. In contrast, they found that inhibition of the CTD with novobiocin was independent of p23 concentration [71].

Our group has since demonstrated these inhibitors have potent *in vitro* and *in vivo* efficacy in human xenograft tumors and do not initiate the HSR with Hsp70 upregulation [72-77]. These preclinical proof of concept studies provide supportive evidence that alternatives to NTD Hsp90 inhibition may have the ability to overcome the limitations of prior inhibitors in clinical trials and should be further validated [72-77].

Isoform-Selective Inhibition

As aforementioned, the mammalian Hsp90 family of molecular chaperones is comprised of three subfamilies, with a total of four distinct isoforms – Hsp90α, Hsp90β, Grp94, and TRAP1 (**Table** 2-1). To better understand the rationale for selective inhibition of Hsp90, the following subsection will provide information on the biological relevance of each isoform.

Biological Functions of Hsp90 Isoforms

Hsp90α and Hsp90β

As the two most abundant isoforms, Hsp90α and Hsp90β are predominantly found in the cytoplasm of mammalian cells. Despite this, there have also been reports of nuclear localization, albeit minor amounts [78]. A major distinction between the two isoforms is their expression profile. Hsp90α is the induced isoform, whereas Hsp90β is constitutively expressed. The major functions of the cytoplasmic isoforms are to aid in protein folding and prevent protein aggregation; in line with that of the Hsp90 family. Reported client proteins of Hsp90α and Hsp90β are involved in several cellular processes such as signaling pathways, survival, cell cycle, energy metabolism, and epigenetics – to name a few – making cytoplasmic Hsp90 isoforms indirectly involved in the regulation of these processes [79]. Moreover, several of these processes, if not all, are recognized as a hallmark of cancer [80]. Lastly, an extracellular form of Hsp90α (eHsp90), which is secreted from the cell, is implicated in invasion and migration or wound healing [29,81]. Since eHsp90 has been reported to play a role in wound healing, this extracellular form of the chaperone could be an alternative target for novel anticancer therapeutics.

Grp94

Unlike its cytoplasmic family members, Grp94, also known as endoplasmin, is found exclusively in the endoplasmic reticulum (ER) [82]. Here, it functions to orchestrate protein quality control on a small subset of proteins either secreted and/or membrane proteins [83]. Proteins that are misfolded in the ER are typically triaged to the Grp94 molecular chaperone machinery for proper refolding. On the contrary, if an ER protein is not properly folded it is translocated to the cytoplasm, where it can be marked for

degradation. In addition to serving as a chaperone for a large number of ER-specific proteins, Grp94 also plays an important role as a Ca^{2+} binding protein [84,85].

TRAP1

The last Hsp90 isoform, TRAP1 or tumor necrosis factor (TNF) receptor associated protein 1, is located in the mitochondria and was initially reported as the chaperone for TNF receptor 1, hence its name [86,87]. In recent years, researchers have shown TRAP1's function in the mitochondria to extend much further than proteostasis, and in fact, play a major role in mitochondrial homeostasis. For example, TRAP1 has been shown to be involved in the regulation of the organelle's redox state [88]. Additionally, TRAP1's involvement in diseases, such as cancer, has been speculated to result in the disruption of energy metabolism, which ties into the fact that Hsp90 is the chaperone for two proteins involved in the citric acid cycle [79,89-91]. Additionally, this alteration or "metabolic rewiring" has been suggested to have an intimate interplay with epigenetics and Condelli et al. provide thorough perspectives on the matter [79]. In fact, Dr. Oliver Kramer, from Johannes Gutenberg University, presented work at the 9th ICHCM that detailed the use of Hsp90 inhibitors in combination with histone deacetylase 6 (HDAC6), an epigenetic "eraser" of acetyl groups from histones, in acute myeloid leukemia [29]. While the exact mechanism(s) in which Hsp90 is involved in altered metabolism and epigenetics has yet to be elucidated, we further emphasize here, the critical and indirect role the chaperone has in various cellular processes.

Rationale for Selective Inhibition

Now with a fundamental understanding of all four isoforms biological functions, it is apparent there is some overlap between them, but more importantly, it underscores the

necessity to move away from “pan-inhibitors” and develop isoform-selective compounds. Moreover, this highlights an opportunity to target a specific isoform whose function is much more crucial in a given a disease state than another isoform. As previously mentioned, Hsp90 is responsible for the conformational maturation of a myriad of client proteins associated with all ten hallmarks of cancer, various neurodegenerative diseases, infections, and other disease states. Many of these client proteins depend upon a single Hsp90 isoform for their maturation, activation, and/or trafficking. Hsp90 has been shown to play an important role in tumorigenesis through the folding/activation of signaling kinases, steroid hormone receptors, tumor suppressors, and more [2]. For example, the mitogen activated protein kinase (MAPK) pathway kinase, B-Raf, is not only mutated in 60% of melanoma patients, but also is a client protein of the Hsp90 heterochaperone complex, suggesting that chaperone function helps to facilitate stabilization of this kinase which ultimately contributes in the mutated and overexpressed state to oncogenesis [92]. As mentioned previously, Hsp90 plays a critical role in neurodegenerative disorders such as AD and PD. In AD, Hsp90 exacerbates the formation of neurofibrillary tangles through the promotion of tau hyperphosphorylation; in PD, pharmacological induction of the chaperone machinery has been shown to prevent the self-assembly of Aβ aggregates [93,94]. Recall that Hsp90α and Hsp90β are two of the four Hsp90 isoforms that primarily reside in the cytoplasm to fold nascent polypeptides. Grp-94, the Hsp90 isoform localized to the endoplasmic reticulum, has a much smaller client list and includes Toll-like Receptors (TLRs), integrins, insulin-like growth factors, and has been shown to play a role in tumor immunogenicity [95,96]. TRAP1 is the mitochondrial isoform of Hsp90 that

plays a role in the transition to aerobic glycolysis, accumulation of reactive oxygen species, and the maintenance of protein homeostasis [97].

While the mechanism of Hsp90 has been well explored and a variety of inhibitors have been developed, most inhibitors manifest pan-inhibitory activity against all four Hsp90 isoforms. Not only do pan-inhibitors serve little utility for the elucidation of the biological roles played by each Hsp90 isoform, but most have been removed from clinical evaluation due to toxicity concerns including hepatic, cardio, and/or ocular toxicities, as well as induction of the HSR [35,98,99]. Recent work has demonstrated that the human Ether a-go-go Related Gene (hERG) product, which is responsible for repolarization of the cardiac action potential, is dependent upon Hsp90α for its maturation and trafficking [98]. Furthermore, pan-inhibition of Hsp90 also induces the pro-survival HSR by activating HSF1, which then induces the transcription of Hsp27, Hsp70, Hsp90, and other heat shock proteins [100]. The upregulation of Hsp90 requires an escalation in drug-dosing as well as significant scheduling difficulties. As a result of these observations, it was proposed that isoform-selective inhibition of Hsp90 may provide a viable way to mitigate the detriments and complications observed in clinical trials with pan-inhibition of all four Hsp90 isoforms. Furthermore, isoform-selective inhibitors provide a mechanism to elucidate the biological role played by each isoform in various diseases. Given the aforementioned dependence of clients upon individual isoforms, isoform-selective inhibitors could be used to target specific disease states in which one isoform may play a presiding role.

GRP94-Selective Inhibitors

Differences between the N-terminal ATP-binding pockets of Grp94 and Hsp90 were first elucidated using N-ethylcarboxamidoadenosine (NECA) as a competitive inhibitor in an adenosine-based ligand binding assay (**Figure** 2-10) [101]. Despite structural similarities between Grp94 and Hsp90, and the large abundance of Hsp90 as compared to Grp94 within cells, NECA was able to selectively bind suggesting that Grp94 could be selectively targeted [101]. Grp94 was the first Hsp90 isoform for which isoform-selective inhibitors were pursued.

One approach used to develop pan-Hsp90 inhibitors combined the structural features of GDA and RDC, two well established natural product Hsp90 inhibitors, to form chimeric molecules. These chimeric molecules retained the key binding features of each natural product, but reduced the structural complexity associated with their preparation. The first three chimeric inhibitors produced were radanamycin, radamide, and radester. All three of these chimeric inhibitors manifested anti-proliferative activity against MCF-7 human breast cancer cells and induced the degradation of Hsp90-dependent client proteins, HER2 and Raf (**Figure** 2-10) [102-104]. Co-crystallization of radamide bound to both Grp94 and Hsp90 revealed a unique 5'-extension pocket that was present only in Grp94, which was produced by a five amino acid insertion into the primary sequence that led to formation of this unique pocket. Otherwise, Grp94 and other Hsp90 isoforms share ~85% identity in this region [105]. The co-crystal structures demonstrated that selectivity was conferred through isomerization of the radamide bond, resulting in formation of the cis-amide, which highlighted the need to incorporate a cis-amide bioisostere into the structure of radamide to develop Grp94-selective inhibitors [105].

BnIm was produced by replacement of the cis-amide with a bioisoteric imidazole ring that mimicked the amide heteroatoms, while projecting the two appendages into a cis-orientation (**Figure** 2-10) [106]. A functional assay was developed to evaluate the effect of BnIm on TLR trafficking to the cell surface, which is Grp94-dependent [106,107] No cytotoxic effects were observed with BnIm and no degradation of Hsp90α/Hsp90β client proteins were observed at concentrations that affected TLR trafficking, which demonstrated a considerable selectivity of BnIm for Grp94 versus the cytosolic isoforms [106]. Second generation Grp94-selective inhibitors established structure-activity relationships for the BnIm scaffold and replaced the imidazole ring with other heterocycles to improve affinity, while modifying the benzyl appendage to improve selectivity and affinity. It was determined that meta-substitutions were not tolerated, while ortho- and para-substitutions improved selectivity [108]. For example, the incorporation of a bromine at the para-position demonstrated efficacy in animal studies for the treatment of glaucoma, as the accumulation of mutant myocilin levels is Grp94-dependent [109,110]. Modification of the imidazole ring via replacement with a phenyl group resulted in a 2-fold improvement in affinity versus BnIm and manifested an apparent Kd of 0.63 μM along with a 32-fold selectivity for Grp94 versus Hsp90α [108]. Fluorination of this molecule at the para-position yielded a compound that manifested an apparent Kd of 0.54 μM along with 73-fold selectivity for Grp94 [111]. Resorcinol-based Grp94 inhibitors also took advantage of the hydrophobic S2 sub-pocket and ultimately led to compounds that manifested low nanomolar affinity, but unfortunately only ~10-fold selectivity for Grp94 [112].

Because of Grp94's distinct extension pockets, it accommodated a wide variety of purine-based chemical tools that are also selective for this isoform. Chiosis and coworkers evaluated an in-house library of ~130 purine analogs in a fluorescence polarization assay to identify compounds that bind Grp94 with higher affinity than Hsp90α. While many of the compounds displayed a model of the purine-scaffold ligand PU-H54 bound to both Hsp90 and Grp94, the team demonstrated that the ligand bound to each isoform in a different orientation and caused Phe199 to swing away and expose a major hydrophobic cleft in Grp94 that is not available in Hsp90α [113]. While a similar cleft exists in Hsp90α, access to Hsp90α's binding pocket is blocked by Phe138. Compounds were found to engage this site and stabilize binding, which conferred Grp94 selectivity [113]. PU-WS13, a Grp94-selective purine derivative bound to this pocket and was shown to be nontoxic in *in vivo* assays for target modulation (**Figure** 2-10). Furthermore, PU-WS13 disrupted the architecture of the oncoprotein, HER2, at the cell surface. Treatment of HER2-overexpressing SKBr3 human breast cancer cells with PU-WS13 led to a substantial decrease in HER2 levels, highlighting a new role for Grp94 in disease states that are dependent on mutated, modulated, or otherwise modified cell surface receptors. These Grp94-selective inhibitors do not induce the HSR, unlike the pan-inhibitors [113].

Recently, a Grp94 selective inhibitor, Compound 54, with an IC_{50} of 2 nM and over 1000-fold selectivity for Grp94 versus Hsp90α was developed by Xu and coworkers [114]. In order to exploit the aforementioned Phe199 shift and to confer Grp94 selectivity, the group began with the benzamide moiety and introduced a phenyl ring at the meta-position as their lead compound. SAR investigations led to the introduction of an isopropyl appendage at the four-position of the benzene ring and a cyclohexanol with an amine

linker at the ortho-position of the benzamide scaffold. The compound was shown to induce the “ligand-induced” Phe199 shift, validating the mechanism for Grp94 selective inhibition. The compound was found to be efficacious in mouse models of ulcerative colitis and did not affect Hsp70 expression levels [114].

Hsp90α and Hsp90β-Selective Inhibitors

Cytosolic Hsp90 includes the inducible Hsp90α isoform and constitutively expressed Hsp90β, which are the most conserved among the four isoforms. In an attempt to avoid the profile exhibited by pan-inhibitors, compounds with selectivity toward the cytosolic isoforms of Hsp90 have been pursued with the intent of narrowing the list of clients in an effort to reduce on-target side effects that are observed with pan-Hsp90 inhibitors. Previous studies investigated the efficacy of Hsp90α/β inhibition in Huntington’s Disease and demonstrated that selective siRNA knockdown of cytosolic Hsp90 is sufficient to decrease mutant Huntington protein (mHtt) levels in HEK cells, which illustrates that isoform-selective inhibition leads to the clearance of disease-promoting aggregates, without affecting the function of the endoplasmic reticulum and mitochondrial chaperones [115]. The cytosolic Hsp90 inhibitor, SNX-0723, demonstrated about 100-fold selectivity for cytosolic Hsp90 isoforms versus Grp94 and about 300-fold selectivity versus TRAP1 (**Figure** 2-11). However, SNX-0723 manifests a similar affinity for both Hsp90α and Hsp90β [115,116]. Ernst and Conor revealed SNX-0723 as a promising lead compound for further optimization due to its CNS permeability as well as its selectivity for both cytosolic Hsp90 isoforms. Subsequent work by these researchers led to the identification of compound 31, a benzolactam-hydroindolone derivative that contains a cyclopentyl substituent and exhibits similar pharmacokinetics as SNX-0723, but less

cellular toxicity as a result of the 1,000-fold selectivity for cytosolic Hsp90s versus Grp94 and TRAP1 [117]. Similarly, TAS-116, which was prepared by researchers at Taiho Pharmaceuticals, Co. Ltd., was shown to be a cytosolic Hsp90 inhibitor that manifested a large selectivity over the non-cytosolic isoforms (**Figure** 2-11). TAS-116 induced the degradation of Hsp90 clients and reduced tumor burden in human xenograft mouse models, indicating that inhibition of cytosolic Hsp90 alone has the potential to exhibit promising anticancer activity. TAS-116 moved into Phase I clinical trials to define the maximum tolerated dose, pharmacokinetics, pharmacodynamics and preliminary antitumor activity of this orally available and selective inhibitor. While ocular disturbances are common with Hsp90 inhibitors, those observed in this trial were limited to grade 1 and a partial response was observed in patients with various tumors and mutation statuses [61]. While compounds have been prepared to manifest selectivity for both cytosolic Hsp90 isoforms as compared to Grp94 and TRAP1, the generation of compounds that are selective for either Hsp90α or Hsp90β proved to be a more challenging task. Hsp90α and Hsp90β share approximately 95% identity within the N-terminal ATP binding pocket and differ by only two amino acids; Hsp90β replaces Hsp90α's serine and isoleucine residues at positions 52 and 91 with alanine and leucine residues, respectively [118]. It has been demonstrated that there are three conserved water molecules that play different roles in Hsp90α versus Hsp90β due to the replacement of serine with alanine in Hsp90β. Based on this observation, this differential hydrogen bonding network was exploited to develop the first Hsp90β-selective inhibitors. KUNB31 was the first Hsp90β-selective N-terminal inhibitor produced and was shown to manifest low micromolar anti-proliferative activity, induce the degradation of Hsp90β-dependent clients, and did not induce the pro-

survival HSR (**Figure** 2-11) [118]. Studies have also suggested that Grp94-selective compounds based on the purine scaffold (PU) also exhibit a 3- to 5-fold selectivity for Hsp90α versus Hsp90β [113]. The proposed mechanism for selectivity of the PU compounds is based on a conserved N-terminus that is intercepted during quaternary transitions between isoforms, suggesting that selectivity must be conferred through a region outside the N-terminus. Further work toward the development of Hsp90α- and Hsp90β-selective inhibitors is ongoing.

TRAP1-Selective Inhibition

Typical pan-inhibitors of Hsp90 have not shown efficient inhibition of TRAP1 in the mitochondria due to a lack of permeability and drug accumulation within this organelle. The long-standing strategy for TRAP1 inhibition has been to use pan-inhibitors of Hsp90 that are targeted to the mitochondria. Shepherdin, a cell-permeable peptidomimetic, was the first rationally designed molecule to enter the mitochondria and target TRAP1 (**Figure** 2-12) [119]. When a highly positively charged moiety was placed at the N-terminus of shepherdin, it enabled mitochondrial penetration and induced extensive cell death through compromising mitochondrial integrity, which caused swelling, membrane depolarization and subsequent release of cytochrome c [120]. Given the peptidomimetic nature of shepherdin, it manifested a short half-life and was capable of inducing an immunogenic response. Shepherdin also targets cytosolic Hsp90s and induces the degradation of several Hsp90 clients [113,121]. Limitations associated with shepherdin opened the door for alternative TRAP1 inhibitors that contain a moiety to target pan-inhibitors of Hsp90, such as GDA, to the mitochondria. The first inhibitors of this class were formed by the inclusion of a triphenylphosphonium (TPP) or cyclic guanidinium

moiety onto GDA. These compounds disrupted mitochondrial function, induced cell death in cancer cell lines, and affected tumor growth in xenograft mouse models [122]. Other compounds soon followed and utilized inhibitors attached to cationic species, including SMTIN-P01 (**Figure** 2-12). SMTIN-P01 replaced the corresponding ammonium group on PU-H71 with the mitochondrial permeating TPP moiety [123]. SMTIN-P01 induced membrane depolarization and demonstrated cytotoxicity in cancer cells, which implicated TRAP1's role in carcinogenesis. While this method of inhibitor development can traffic pan-inhibitors to the mitochondria, it is not truly an isoform-selective process. TRAP1 and other isoforms of Hsp90 are highly conserved, but there are still significant differences within the ATP-binding regions that make TRAP1-selective inhibitors possible. However, compounds may not target TRAP1 with the same affinity observed for the cytosolic Hsp90s. A lack of selectivity may also lead to off target effects as compounds may interact with cytosolic chaperones. Kang and co-workers sought to minimize the binding to cytosolic Hsp90 and to maximize affinity for TRAP1 by the incorporation of guanine mimics that contain a piperonyl side chain. Modification of the pyridine ring to provide the pyrazolopyrimidine scaffold with a pyridinyl appendage demonstrated stronger inhibitory activities against TRAP1 than the corresponding piperonyl-containing side chains, but comparable inhibitory activity against cytosolic Hsp90. Further modification of the pyridinyl group led to potent inhibitors of TRAP1 (79 nM) as compared to Hsp90 (698 nM). In fact, DN401, which exhibited ~9-fold selectivity for TRAP1 versus Hsp90, is the most selective TRAP1 inhibitor reported to date (**Figure** 2-12) [124].

Conclusion

Hsp90 and its isoforms are shown to play a critical role in cancer, neurodegenerative disorders, and other disease states, illustrating that its pharmacological targeting can have profound implications for the treatment of these illnesses. Most attempts at Hsp90 inhibition have not seen success in clinical trials. Despite innovative chemistry and targeting these compounds all target the N-terminal binding site and therefore are pan-inhibitors of all four Hsp90 isoforms. These inhibitors—including natural products and their derivatives, purine-based inhibitors, benzamide inhibitors and resorcinol containing inhibitors—have time-and-again failed progression in clinical trials due to the detrimental toxicities associated with Hsp90 pan-inhibition. In fact, over half of the clinical trials with these Hsp90 Inhibitors did not progress past Phase I due to the cardiac, hepatic, and ocular toxicities commonly associated with Hsp90 pan-inhibition, making progress through in-human clinical trials difficult thus far.

Although Hsp90 pan-inhibitors may not be the key to a combinatorial attack on a variety of disease-causing pathways, non-traditional modulation of Hsp90, namely C-terminal inhibition or isoform-selective inhibition, remain a viable method to achieve the desired anticancer effect without harmful side effects seen with pan-inhibition. Inhibition of the cytosolic Hsp90 isoforms maintains the integrity of the endoplasmic reticulum and the mitochondria by leaving Grp94 and TRAP1, respectively, unaffected. Inhibition of Hsp90β in particular leaves the hERG channel unaffected and avoids induction of the pro-survival HSR. Grp94 and TRAP1 inhibition allow for the targeting of particular disease states in which their isoforms are implicated. Further, preclinical validation and advancement of these novel C-terminal and isoform-selective inhibitors will generate

exciting new anticancer compounds to move into clinical trials that could overcome the challenges of prior Hsp90 inhibitors, providing much needed novel anti-cancer drug compounds for patients.

Tables

Table 2-1 Hsp90 family members, gene products, and cellular locations

There are three Hsp90 subfamilies and each located in different cellular compartments. The majority of isoforms are in the cytoplasm and include Hsp90α and Hsp90β. The endoplasmic reticulum and mitochondria isoforms are Grp94 and TRAP1, respectively.

Subfamily	Gene(s)	Protein Isoform(s)	Cellular Location
HSP90A	HSP90AA1, HSP90AA2	Hsp90α1, Hsp90α2	Cytoplasm
	HSP90B1	Hsp90β	Cytoplasm
HSP90B	HSP90B1	Grp94	Endoplasmic reticulum
TRAP	TRAP1	TRAP1	Mitochondria

Figures

Figure 2-1 Structure of Hsp90

A schematic of Hsp90's homodimer structure. Each monomer has a N-terminal (NTD; grey), middle (MD; blue), and C-terminal (CTD; orange) domains. The NTD and MD are connected by a charged linker region (black line).

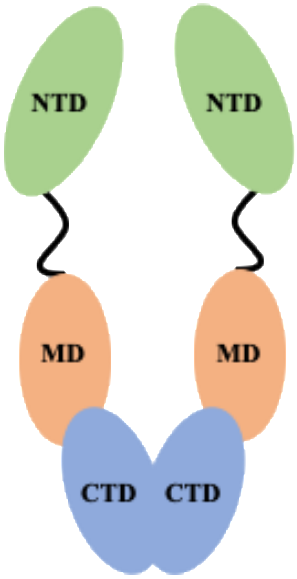

Figure 2-2 Clinical trial overview of Hsp90 inhibitors

18 Hsp90 inhibitors have entered the clinical pipeline totaling over 170 trials. A) There are currently 7 inhibitors in active or recruiting trials (green or orange, respectively). B) The majority of inhibitors have not progressed past Phase I. Note: active trials testing TAS-116 are in Japan.

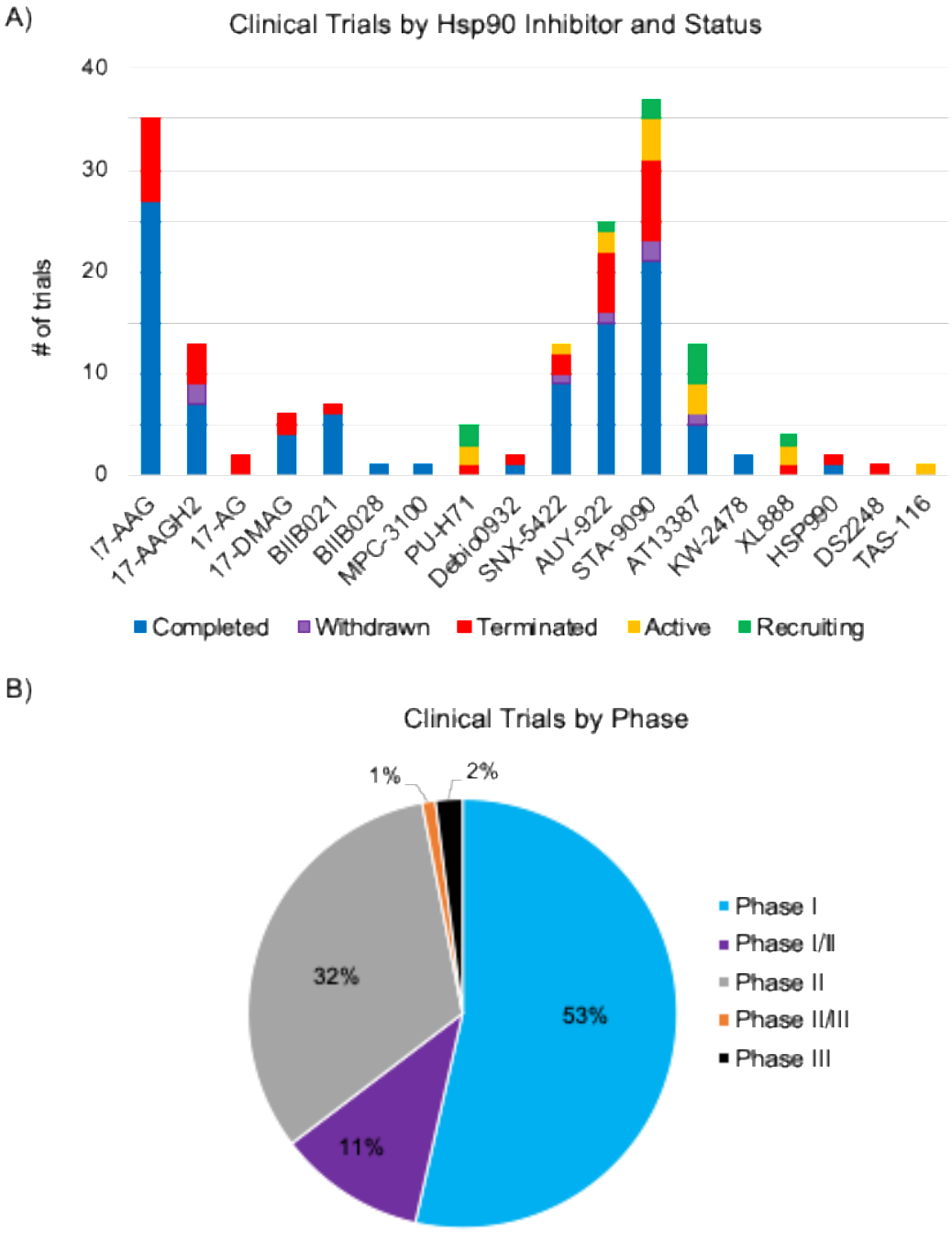

Figure 2-3 Hsp90 inhibitors derived from natural products

A) Geldanamycin is a benzoquinone ansamycin antibiotic. Three of its derivatives (tanespimycin, IPI-493, and alvespimycin) make substitutions to the C-17 position. B) In addition to a C-17 substitution, retaspimycin is the reduced derivative of GDA. C) Radicicol is an antifungal natural product.

A)

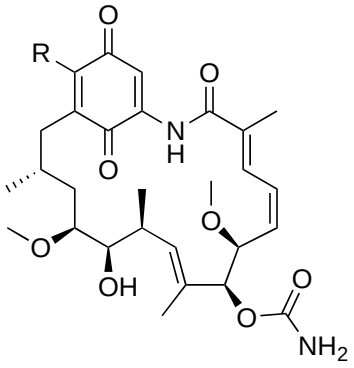

Geldanamycin (GDA) R = OMe
Tanespimycin (17-AAG) R = $NHCH_2CHCH_2$
IPI-493 (17-AG) R = NH_2
Alvespimycin (17-DMAG) R = $NHCH_2CH_2N(Me)_2$

B)

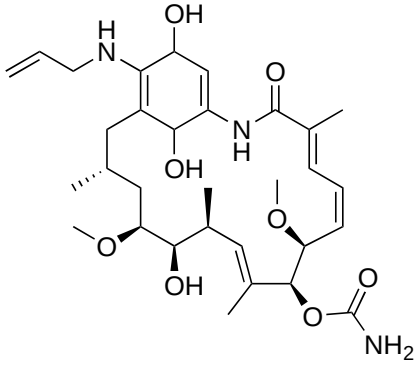

Retaspimycin (17-AAGH_2)

C)

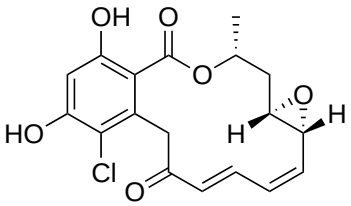

Radicicol (RDC)

Figure 2-4 Purine-based Hsp90 inhibitors

A) PU-3 was the first fully synthetic Hsp90 inhibitor and first of the purine-based class. B) BIIB021 and BIIB028 modify the N-7 and N-9 positions of the purine base. C-E) PU-H71, MPC-3100, Debio0932 each add a unique 1,3- benzodioxole moiety to the N-8 position via a thioether bond and a variable substituent to the N-9 position.

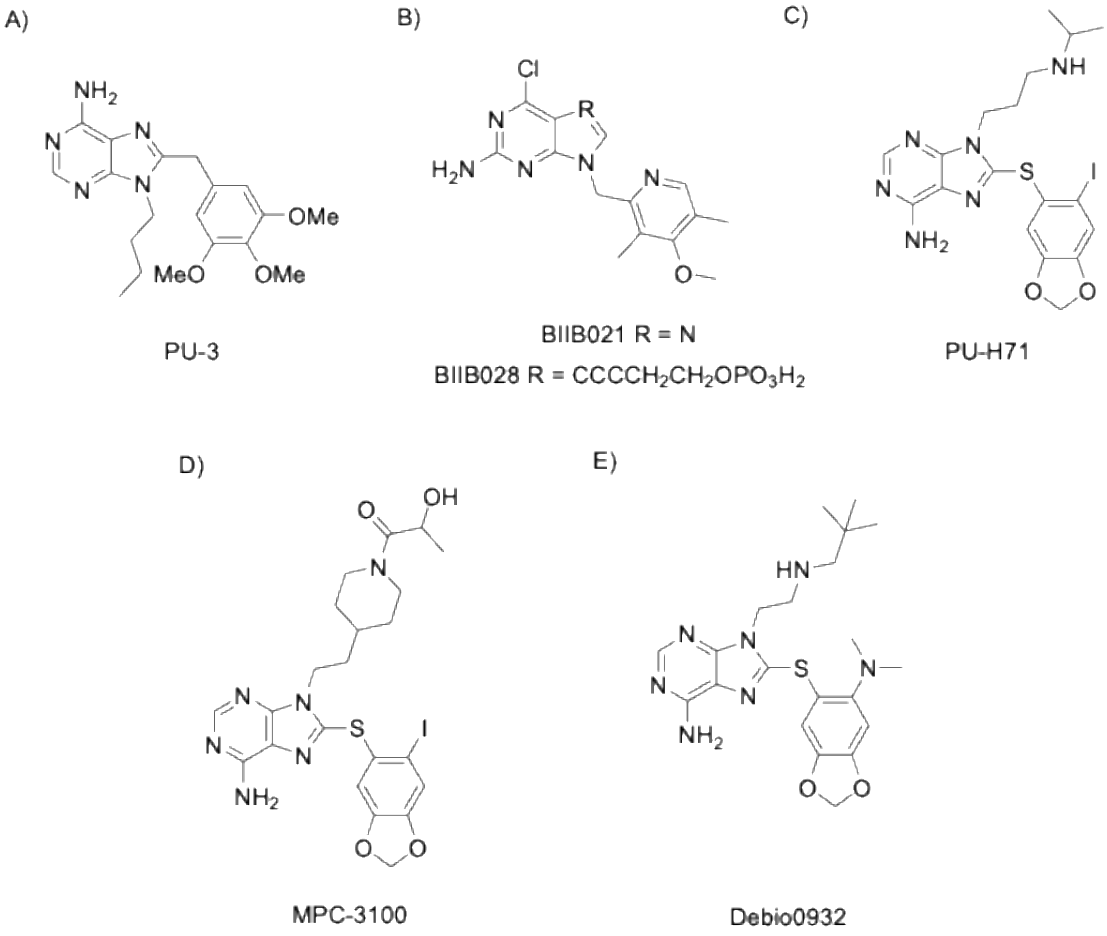

Figure 2-5 Benzamide Hsp90 inhibitor

SNX-5422 is a pyrazole-containing inhibitor and the only of its class.

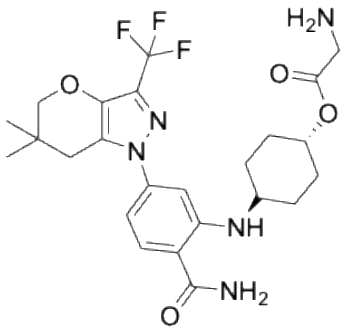

SNX-5422

Figure 2-6 Resorcinol-containing Hsp90 inhibitors

All inhibitors in this class contain a resorcinol moiety. A-C) Luminespib, ganetespib, and onalespib add two substituents to the resorcinol ring at ortho-positions to the hydroxyl groups; one is an isopropanol moiety and the other is unique to each compound. D) KW-2478 adds three substituents to the resorcinol moiety – two ortho and one meta to the hydroxyl groups.

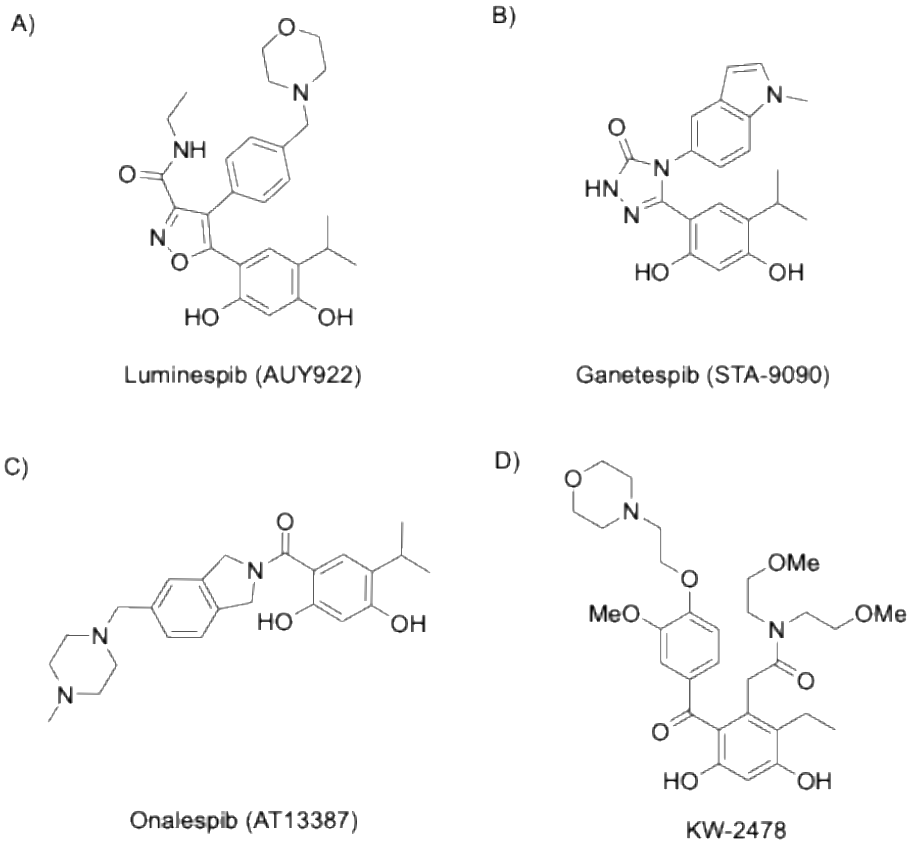

Figure 2-7 Miscellaneous Hsp90 inhibitors

HSP990 and XL888 do not fall into any of the chemical structure categories listed previously, but still target the N-terminal ATP-binding site. TAS-116 is a Hsp90α/β isoform-selective inhibitor.

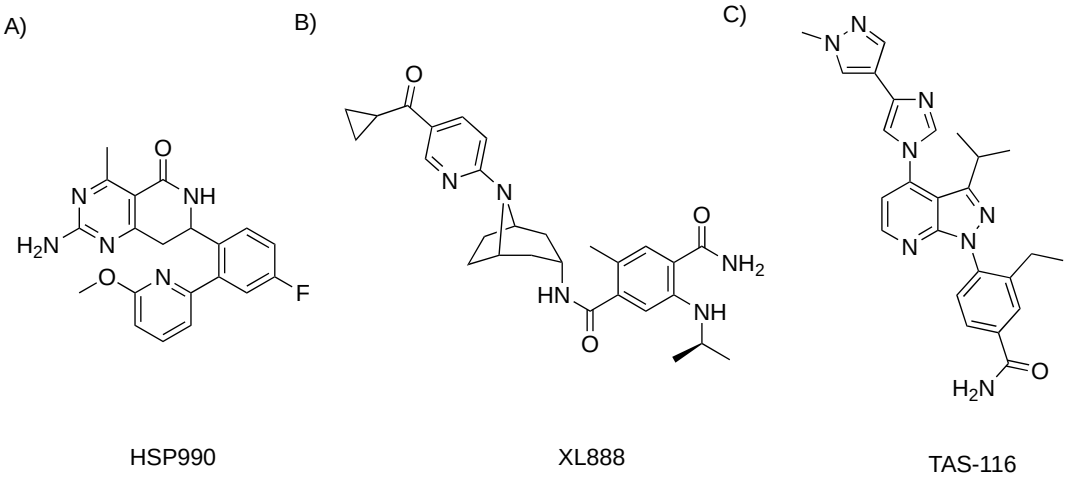

Figure 2-8 Structures of C-terminal Hsp90 inhibitors

The aminocoumarin antibiotic A) novobiocin derived from *Steptomyces niveus* and its analogue B) KU174. Compounds in this class share three common moieties: benzoic acid derivative, coumarin residue, and sugar novobiose.

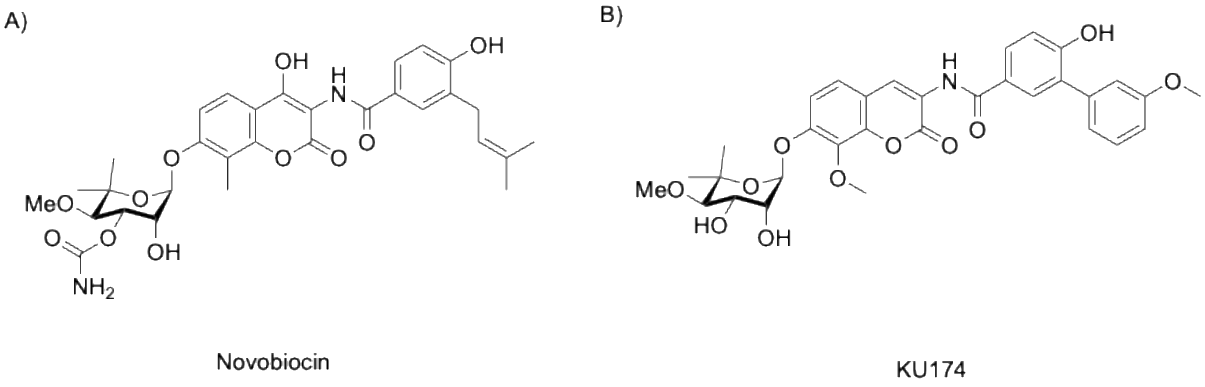

Figure 2-9 Hsp90 C-terminal inhibition

From upper left: Hsp90 chaperone and HSF1 transcription factor interaction is destabilized by C- terminal Hsp90 inhibitor binding. Once HSF1 is phosphorylated it associates with other phosphorylated HSF1 proteins and binds to DNA at its transcription element, HSE. After a tightly regulated process with several steps, this leads to ubiquitinylation of client proteins.

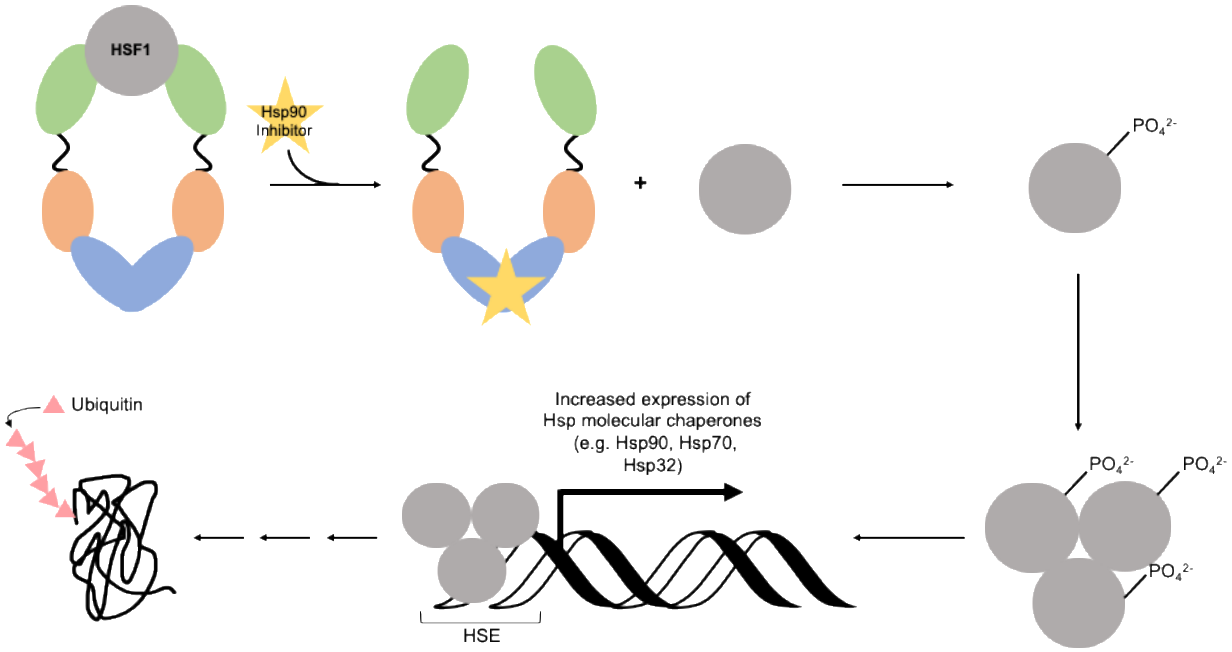

Figure 2-10 Structures representing various Grp94-selective inhibitors

Radanamycin, radamide, and radester are natural product derived. BnIm maintains the resorcinol moiety but introduces an imidazole ring. The PU compounds represent the purine class, and 54 is a novel inhibitor of the benzamide class.

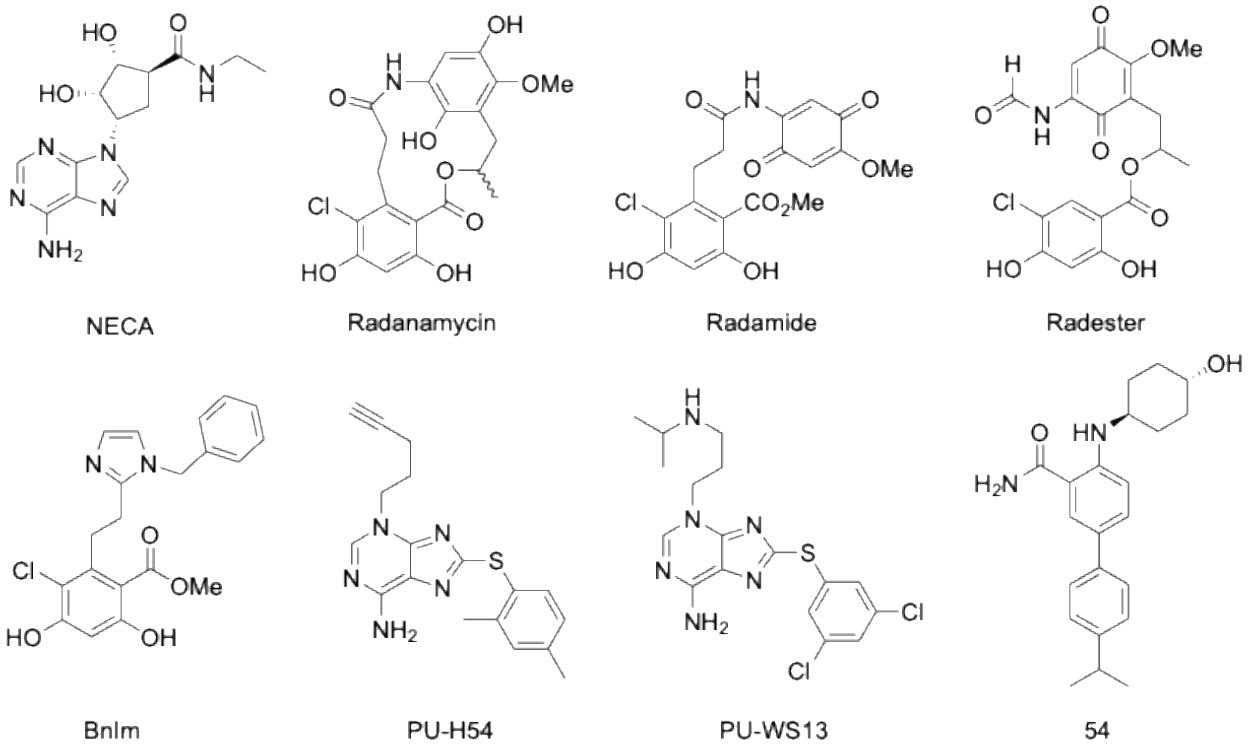

Figure 2-11 Hsp90 isoform-selective inhibitors

TAS-116 and KUNB31, the first N-terminal, Hsp90α/β and Hsp90β isoform-selective inhibitors, respectively.

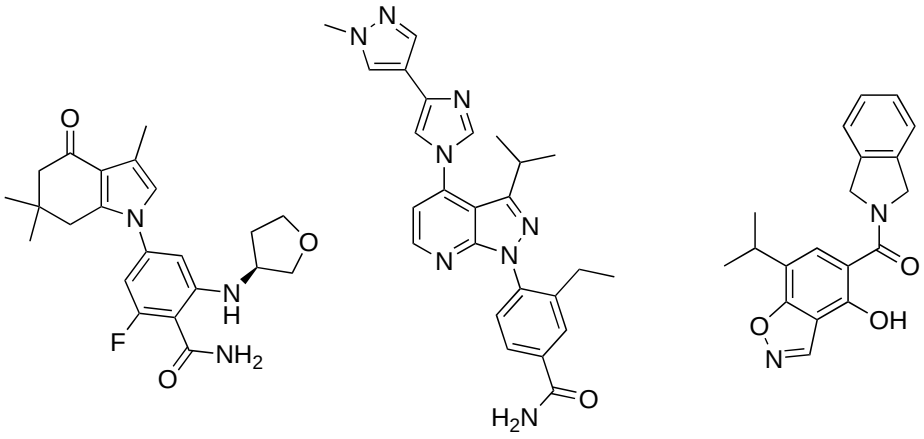

SNX-0723 TAS-116 KUNB31

Figure 2-12 TRAP1-selective inhibitors.

Shepherdin is the minimal nine amino acid sequence of survivin named for its binding to the “shepherding” protein Hsp90. SMTIN-PO1 represents compounds conjugated to mitochondrial targeting moieties, and DN401 is the most potent and selective TRAP1 inhibitor reported.

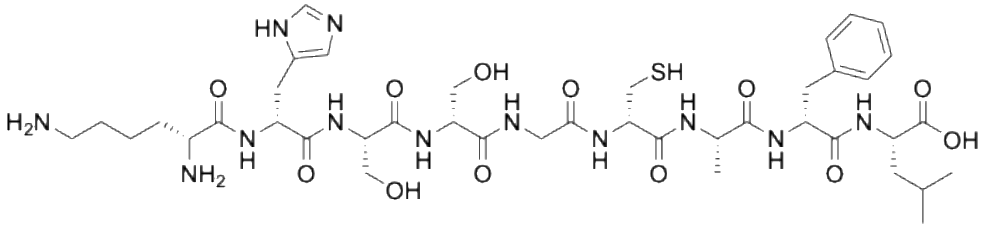

Shepherdin

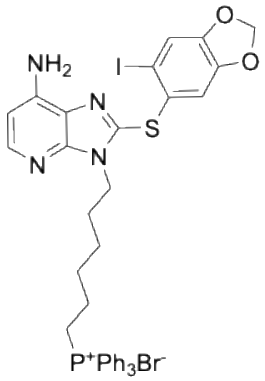

SMTIN-P01

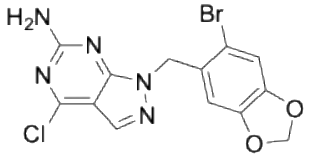

DN401

Abbreviations

17-AAG	17-N-allylamino-17-dimethoxygeldanamycin
17-AAGH$_2$	17-allylaminodimethoxygeldanamycin hydroquinone
17-DMAG	17-dimethylamino-17-dimthoxygeldanamycin
Aβ	β-amyloid
AD	Alzheimer's disease
AhR	aryl hydrocarbon receptor
CTD	C-terminal domain
DLT	dose-limiting toxicities
eHsp90	extracellular Hsp90
ER	endoplasmic reticulum
FDA	Food and Drug Administration
GDA	geldanamycin
GHKL	gyrase, Hsp90, histidine kinase, MutL
GIST	gastrointestinal stromal tumors
HDAC6	histone deacetylase 6
hERG	human Ether a-go-go Related Gene
HSE	heat shock element
HSF1	heat shock factor 1
Hsp	heat shock protein
Hsp90	90kDa heat shock protein
HSR	heat shock response
ICHCM	International Conference on the Hsp90 Chaperone Machine

MAPK	mitogen activated protein kinase
MD	middle domain
mHtt	mutated Huntington protein
NECA	N-ethylcarboxamidoadenosine
NTD	N-terminal domain
PD	Parkinson’s disease
PPI	protein-protein interactions
PU	purine scaffold
RDC	radicicol
TNF	tumor necrosis factor
TPP	triphenylphosphonium
TPR	tetratricopeptide repeat
TRAP1	tumor necrosis factor receptor associated protein 1
TRL	Toll-like Receptor

References

1. Miyata Y, Nakamoto H and Neckers L. The therapeutic target Hsp90 and cancer hallmarks. *Curr Pharm Des* 2013;**19**(3): 347-365.
2. Whitesell L and Lindquist SL. HSP90 and the chaperoning of cancer. *Nat Rev Cancer* 2005;**5**(10): 761-772.
3. Ritossa FM. A new puffing pattern induced by temperature shock an DNP in Drosophila. *Experientia* 1962;**18**(571-573.
4. Ritossa FM. Experimental activation of specific loci in ploytene chromosomes of drosophila. *Exp Cell Res* 1964;**35**(601-607.
5. Ritossa FM. New puffs induced by temperature shock, DNP and salicilate in salivary chromosomes of D. melanogaster. *Drosophilia Information Service* 1963;**37**(122-123.
6. McKenzie SL, Henikoff S and Meselson M. Localization of RNA from heat-induced polysomes at puff sites in Drosophila melanogaster. *Proc Natl Acad Sci U S A* 1975;**72**(3): 1117-1121.
7. Tissieres A, Mitchell HK and Tracy UM. Protein synthesis in salivary glands of Drosophila melanogaster: relation to chromosome puffs. *J Mol Biol* 1974;**84**(3): 389-398.
8. Bagatell R, Paine-Murrieta GD, Taylor CW, Pulcini EJ, Akinaga S, Benjamin IJ*, et al.* Induction of a heat shock factor 1-dependent stress response alters the cytotoxic activity of hsp90-binding agents. *Clin Cancer Res* 2000;**6**(8): 3312-3318.
9. Yufu Y, Nishimura J and Nawata H. High constitutive expression of heat shock protein 90 alpha in human acute leukemia cells. *Leuk Res* 1992;**16**(6-7): 597-605.
10. Prodromou C. The 'active life' of Hsp90 complexes. *Biochim Biophys Acta* 2012;**1823**(3): 614-623.
11. Yano M, Naito Z, Tanaka S and Asano G. Expression and roles of heat shock proteins in human breast cancer. *Jpn J Cancer Res* 1996;**87**(9): 908-915.
12. Kamal A, Thao L, Sensintaffar J, Zhang L, Boehm MF, Fritz LC*, et al.* A high-affinity conformation of Hsp90 confers tumour selectivity on Hsp90 inhibitors. *Nature* 2003;**425**(6956): 407-410.
13. Whitesell L, Mimnaugh EG, De Costa B, Myers CE and Neckers LM. Inhibition of heat shock protein HSP90-pp60v-src heteroprotein complex formation by benzoquinone ansamycins: essential role for stress proteins in oncogenic transformation. *Proc Natl Acad Sci U S A* 1994;**91**(18): 8324-8328.
14. Xu Y and Lindquist S. Heat-shock protein hsp90 governs the activity of pp60v-src kinase. *Proc Natl Acad Sci U S A* 1993;**90**(15): 7074-7078.
15. Xu Y, Singer MA and Lindquist S. Maturation of the tyrosine kinase c-src as a kinase and as a substrate depends on the molecular chaperone Hsp90. *Proc Natl Acad Sci U S A* 1999;**96**(1): 109-114.
16. Kim YS, Alarcon SV, Lee S, Lee MJ, Giaccone G, Neckers L*, et al.* Update on Hsp90 inhibitors in clinical trial. *Curr Top Med Chem* 2009;**9**(15): 1479-1492.
17. Schopf FH, Biebl MM and Buchner J. The HSP90 chaperone machinery. *Nat Rev Mol Cell Biol* 2017;**18**(6): 345-360.

18. Murphy MP and LeVine H, 3rd. Alzheimer's disease and the amyloid-beta peptide. *J Alzheimers Dis* 2010;**19**(1): 311-323.
19. Kalia LV and Kalia SK. alpha-Synuclein and Lewy pathology in Parkinson's disease. *Curr Opin Neurol* 2015;**28**(4): 375-381.
20. Stefanis L. alpha-Synuclein in Parkinson's disease. *Cold Spring Harb Perspect Med* 2012;**2**(2): a009399.
21. Csermely P, Schnaider T, Soti C, Prohaszka Z and Nardai G. The 90-kDa molecular chaperone family: structure, function, and clinical applications. A comprehensive review. *Pharmacol Ther* 1998;**79**(2): 129-168.
22. Sreedhar AS, Kalmar E, Csermely P and Shen YF. Hsp90 isoforms: functions, expression and clinical importance. *FEBS Lett* 2004;**562**(1-3): 11-15.
23. Prodromou C, Roe SM, O'Brien R, Ladbury JE, Piper PW and Pearl LH. Identification and structural characterization of the ATP/ADP-binding site in the Hsp90 molecular chaperone. *Cell* 1997;**90**(1): 65-75.
24. Meyer P, Prodromou C, Hu B, Vaughan C, Roe SM, Panaretou B*, et al.* Structural and functional analysis of the middle segment of hsp90: implications for ATP hydrolysis and client protein and cochaperone interactions. *Mol Cell* 2003;**11**(3): 647-658.
25. Minami Y, Kimura Y, Kawasaki H, Suzuki K and Yahara I. The carboxy-terminal region of mammalian HSP90 is required for its dimerization and function in vivo. *Mol Cell Biol* 1994;**14**(2): 1459-1464.
26. Jhaveri K, Taldone T, Modi S and Chiosis G. Advances in the clinical development of heat shock protein 90 (Hsp90) inhibitors in cancers. *Biochim Biophys Acta* 2012;**1823**(3): 742-755.
27. Garg G, Khandelwal A and Blagg BS. Anticancer Inhibitors of Hsp90 Function: Beyond the Usual Suspects. *Adv Cancer Res* 2016;**129**(51-88.
28. Yuno A, Lee MJ, Lee S, Tomita Y, Rekhtman D, Moore B*, et al.* Clinical Evaluation and Biomarker Profiling of Hsp90 Inhibitors. *Methods Mol Biol* 2018;**1709**(423-441.
29. Blair LJ, Genest O and Mollapour M. The multiple facets of the Hsp90 machine. *Nat Struct Mol Biol* 2019;**26**(2): 92-95.
30. Soga S, Akinaga S and Shiotsu Y. Hsp90 inhibitors as anti-cancer agents, from basic discoveries to clinical development. *Curr Pharm Des* 2013;**19**(3): 366-376.
31. Lee BL, Rashid S, Wajda B, Wolmarans A, LaPointe P and Spyracopoulos L. The Hsp90 Chaperone: (1)H and (19)F Dynamic Nuclear Magnetic Resonance Spectroscopy Reveals a Perfect Enzyme. *Biochemistry* 2019;**58**(14): 1869-1877.
32. Gorska M, Popowska U, Sielicka-Dudzin A, Kuban-Jankowska A, Sawczuk W, Knap N*, et al.* Geldanamycin and its derivatives as Hsp90 inhibitors. *Front Biosci (Landmark Ed)* 2012;**17**(2269-2277.
33. Huryn DM and Wipf P (2014). Chapter 3 - Natural Product Chemistry and Cancer Drug Discovery. Cancer Drug Design and Discovery (Second Edition). Neidle, S. San Diego, Academic Press, doi: https://doi.org/10.1016/B978-0-12-396521-9.00003-6**:** 91-120.
34. Biamonte MA, Van de Water R, Arndt JW, Scannevin RH, Perret D and Lee WC. Heat shock protein 90: inhibitors in clinical trials. *J Med Chem* 2010;**53**(1): 3-17.

35. Samuni Y, Ishii H, Hyodo F, Samuni U, Krishna MC, Goldstein S*, et al.* Reactive oxygen species mediate hepatotoxicity induced by the Hsp90 inhibitor geldanamycin and its analogs. *Free Radic Biol Med* 2010;**48**(11): 1559-1563.
36. Hanson BE and Vesole DH. Retaspimycin hydrochloride (IPI-504): a novel heat shock protein inhibitor as an anticancer agent. *Expert Opin Investig Drugs* 2009;**18**(9): 1375-1383.
37. Lee J, Grenier L, Holson E, Slocum K, Coco J, Ge J*, et al.* (2008). IPI-493, a potent, orally bioavailable Hsp90 inhibitor of the ansamycin class. EORTC-NCI-AACR-International Conference Geneva, Switzerland, doi.
38. Floris G, Sciot R, Wozniak A, Van Looy T, Wellens J, Faa G*, et al.* The Novel HSP90 inhibitor, IPI-493, is highly effective in human gastrostrointestinal stromal tumor xenografts carrying heterogeneous KIT mutations. *Clin Cancer Res* 2011;**17**(17): 5604-5614.
39. Chene P. ATPases as drug targets: learning from their structure. *Nat Rev Drug Discov* 2002;**1**(9): 665-673.
40. Chiosis G, Timaul MN, Lucas B, Munster PN, Zheng FF, Sepp-Lorenzino L*, et al.* A small molecule designed to bind to the adenine nucleotide pocket of Hsp90 causes Her2 degradation and the growth arrest and differentiation of breast cancer cells. *Chem Biol* 2001;**8**(3): 289-299.
41. Wright L, Barril X, Dymock B, Sheridan L, Surgenor A, Beswick M*, et al.* Structure-activity relationships in purine-based inhibitor binding to HSP90 isoforms. *Chem Biol* 2004;**11**(6): 775-785.
42. Lundgren K and Biamonte MA. CHAPTER 5 The Discovery of BIIB021 and BIIB028. *Inhibitors of Molecular Chaperones as Therapeutic Agents* 2014, doi: 10.1039/9781849739689-00158158-179.
43. Lundgren K, Zhang H, Brekken J, Huser N, Powell RE, Timple N*, et al.* BIIB021, an orally available, fully synthetic small-molecule inhibitor of the heat shock protein Hsp90. *Mol Cancer Ther* 2009;**8**(4): 921-929.
44. Shi X, Kiesman WF and Walker DG (2016). Development of Hsp90 Inhibitors for the Treatment of HER-2 Positive Solid Cancers. Comprehensive Accounts of Pharmaceutical Research and Development: From Discovery to Late-Stage Process Development Volume 1, American Chemical Society. **1239:** 69-100.
45. Caldas-Lopes E, Cerchietti L, Ahn JH, Clement CC, Robles AI, Rodina A*, et al.* Hsp90 inhibitor PU-H71, a multimodal inhibitor of malignancy, induces complete responses in triple-negative breast cancer models. *Proc Natl Acad Sci U S A* 2009;**106**(20): 8368-8373.
46. Fadden P, Huang KH, Veal JM, Steed PM, Barabasz AF, Foley B*, et al.* Application of chemoproteomics to drug discovery: identification of a clinical candidate targeting hsp90. *Chem Biol* 2010;**17**(7): 686-694.
47. Huang KH, Veal JM, Fadden RP, Rice JW, Eaves J, Strachan JP*, et al.* Discovery of novel 2-aminobenzamide inhibitors of heat shock protein 90 as potent, selective and orally active antitumor agents. *J Med Chem* 2009;**52**(14): 4288-4305.
48. Cheung KM, Matthews TP, James K, Rowlands MG, Boxall KJ, Sharp SY*, et al.* The identification, synthesis, protein crystal structure and in vitro biochemical evaluation of a new 3,4-diarylpyrazole class of Hsp90 inhibitors. *Bioorg Med Chem Lett* 2005;**15**(14): 3338-3343.

49. Brough PA, Aherne W, Barril X, Borgognoni J, Boxall K, Cansfield JE*, et al.* 4,5-diarylisoxazole Hsp90 chaperone inhibitors: potential therapeutic agents for the treatment of cancer. *J Med Chem* 2008;**51**(2): 196-218.
50. Eccles SA, Massey A, Raynaud FI, Sharp SY, Box G, Valenti M*, et al.* NVP-AUY922: a novel heat shock protein 90 inhibitor active against xenograft tumor growth, angiogenesis, and metastasis. *Cancer Res* 2008;**68**(8): 2850-2860.
51. Jensen MR, Schoepfer J, Radimerski T, Massey A, Guy CT, Brueggen J*, et al.* NVP-AUY922: a small molecule HSP90 inhibitor with potent antitumor activity in preclinical breast cancer models. *Breast Cancer Res* 2008;**10**(2): R33.
52. Wang Y, Trepel JB, Neckers LM and Giaccone G. STA-9090, a small-molecule Hsp90 inhibitor for the potential treatment of cancer. *Curr Opin Investig Drugs* 2010;**11**(12): 1466-1476.
53. Woodhead AJ, Angove H, Carr MG, Chessari G, Congreve M, Coyle JE*, et al.* Discovery of (2,4-dihydroxy-5-isopropylphenyl)-[5-(4-methylpiperazin-1-ylmethyl)-1,3-dihydrois oindol-2-yl]methanone (AT13387), a novel inhibitor of the molecular chaperone Hsp90 by fragment based drug design. *J Med Chem* 2010;**53**(16): 5956-5969.
54. Murray CW, Carr MG, Callaghan O, Chessari G, Congreve M, Cowan S*, et al.* Fragment-based drug discovery applied to Hsp90. Discovery of two lead series with high ligand efficiency. *J Med Chem* 2010;**53**(16): 5942-5955.
55. Nakashima T, Ishii T, Tagaya H, Seike T, Nakagawa H, Kanda Y*, et al.* New molecular and biological mechanism of antitumor activities of KW-2478, a novel nonansamycin heat shock protein 90 inhibitor, in multiple myeloma cells. *Clin Cancer Res* 2010;**16**(10): 2792-2802.
56. Cavenagh J, Oakervee H, Baetiong-Caguioa P, Davies F, Gharibo M, Rabin N*, et al.* A phase I/II study of KW-2478, an Hsp90 inhibitor, in combination with bortezomib in patients with relapsed/refractory multiple myeloma. *Br J Cancer* 2017;**117**(9): 1295-1302.
57. Bussenius J, Blazey CM, Aay N, Anand NK, Arcalas A, Baik T*, et al.* Discovery of XL888: a novel tropane-derived small molecule inhibitor of HSP90. *Bioorg Med Chem Lett* 2012;**22**(17): 5396-5404.
58. Haarberg HE, Paraiso KH, Wood E, Rebecca VW, Sondak VK, Koomen JM*, et al.* Inhibition of Wee1, AKT, and CDK4 underlies the efficacy of the HSP90 inhibitor XL888 in an in vivo model of NRAS-mutant melanoma. *Mol Cancer Ther* 2013;**12**(6): 901-912.
59. Menezes DL, Taverna P, Jensen MR, Abrams T, Stuart D, Yu GK*, et al.* The novel oral Hsp90 inhibitor NVP-HSP990 exhibits potent and broad-spectrum antitumor activities in vitro and in vivo. *Mol Cancer Ther* 2012;**11**(3): 730-739.
60. Ohkubo S, Kodama Y, Muraoka H, Hitotsumachi H, Yoshimura C, Kitade M*, et al.* TAS-116, a highly selective inhibitor of heat shock protein 90alpha and beta, demonstrates potent antitumor activity and minimal ocular toxicity in preclinical models. *Mol Cancer Ther* 2015;**14**(1): 14-22.
61. Shimomura A, Yamamoto N, Kondo S, Fujiwara Y, Suzuki S, Yanagitani N*, et al.* First-in-Human Phase I Study of an Oral HSP90 Inhibitor, TAS-116, in Patients with Advanced Solid Tumors. *Mol Cancer Ther* 2019;**18**(3): 531-540.

62. Kurokawa Y, Doi T, Sawaki A, Komatsu Y, Ozaka M, Takahashi T*, et al.* (2017). Phase II study of TAS-116, on oral inhibitor of heat shock protein (HSP90), in metastatic or unresectable gastrointestinal stromal tumor refractory to imatinib, sunitinib, and regorafenib. ESMO 2017 Congress. Madrid, Spain, Annals of Oncology. **28:** v521-v538.
63. Donnelly A and Blagg BS. Novobiocin and additional inhibitors of the Hsp90 C-terminal nucleotide-binding pocket. *Curr Med Chem* 2008;**15**(26): 2702-2717.
64. Schulte TW, Akinaga S, Soga S, Sullivan W, Stensgard B, Toft D*, et al.* Antibiotic radicicol binds to the N-terminal domain of Hsp90 and shares important biologic activities with geldanamycin. *Cell Stress Chaperones* 1998;**3**(2): 100-108.
65. Soti C, Racz A and Csermely P. A Nucleotide-dependent molecular switch controls ATP binding at the C-terminal domain of Hsp90. N-terminal nucleotide binding unmasks a C-terminal binding pocket. *J Biol Chem* 2002;**277**(9): 7066-7075.
66. Yun BG, Huang W, Leach N, Hartson SD and Matts RL. Novobiocin induces a distinct conformation of Hsp90 and alters Hsp90-cochaperone-client interactions. *Biochemistry* 2004;**43**(25): 8217-8229.
67. Marcu MG, Chadli A, Bouhouche I, Catelli M and Neckers LM. The heat shock protein 90 antagonist novobiocin interacts with a previously unrecognized ATP-binding domain in the carboxyl terminus of the chaperone. *J Biol Chem* 2000;**275**(47): 37181-37186.
68. Chatterjee BK, Jayaraj A, Kumar V, Blagg B, Davis RE, Jayaram B*, et al.* Stimulation of heat shock protein 90 chaperone function through binding of a novobiocin analog KU-32. *J Biol Chem* 2019;**294**(16): 6450-6467.
69. Rahimi MN and McAlpine SR. Protein-protein inhibitor designed de novo to target the MEEVD region on the C-terminus of Hsp90 and block co-chaperone activity. *Chem Commun (Camb)* 2019;**55**(6): 846-849.
70. Terracciano S, Russo A, Chini MG, Vaccaro MC, Potenza M, Vassallo A*, et al.* Discovery of new molecular entities able to strongly interfere with Hsp90 C-terminal domain. *Sci Rep* 2018;**8**(1): 1709.
71. Cox MB and Miller CA, 3rd. Cooperation of heat shock protein 90 and p23 in aryl hydrocarbon receptor signaling. *Cell Stress Chaperones* 2004;**9**(1): 4-20.
72. Byrd KM, Subramanian C, Sanchez J, Motiwala HF, Liu W, Cohen MS*, et al.* Synthesis and Biological Evaluation of Novobiocin Core Analogues as Hsp90 Inhibitors. *Chemistry* 2016;**22**(20): 6921-6931.
73. Cohen SM, Mukerji R, Samadi AK, Zhang X, Zhao H, Blagg BS*, et al.* Novel C-terminal Hsp90 inhibitor for head and neck squamous cell cancer (HNSCC) with in vivo efficacy and improved toxicity profiles compared with standard agents. *Ann Surg Oncol* 2012;**19 Suppl 3**(S483-490.
74. Samadi AK, Zhang X, Mukerji R, Donnelly AC, Blagg BS and Cohen MS. A novel C-terminal HSP90 inhibitor KU135 induces apoptosis and cell cycle arrest in melanoma cells. *Cancer Lett* 2011;**312**(2): 158-167.
75. Subramanian C, Kovatch KJ, Sim MW, Wang G, Prince ME, Carey TE*, et al.* Novel C-Terminal Heat Shock Protein 90 Inhibitors (KU711 and Ku757) Are Effective in Targeting Head and Neck Squamous Cell Carcinoma Cancer Stem cells. *Neoplasia* 2017;**19**(12): 1003-1011.

76. White PT, Subramanian C, Zhu Q, Zhang H, Zhao H, Gallagher R*, et al.* Novel HSP90 inhibitors effectively target functions of thyroid cancer stem cell preventing migration and invasion. *Surgery* 2016;**159**(1): 142-151.
77. Zhao J, Zhao H, Hall JA, Brown D, Brandes E, Bazzill J*, et al.* Triazole Containing Novobiocin and Biphenyl Amides as Hsp90 C-Terminal Inhibitors. *Medchemcomm* 2014;**5**(9): 1317-1323.
78. Langer T, Rosmus S and Fasold H. Intracellular localization of the 90 kDA heat shock protein (HSP90alpha) determined by expression of a EGFP-HSP90alpha-fusion protein in unstressed and heat stressed 3T3 cells. *Cell Biol Int* 2003;**27**(1): 47-52.
79. Condelli V, Crispo F, Pietrafesa M, Lettini G, Matassa DS, Esposito F*, et al.* HSP90 Molecular Chaperones, Metabolic Rewiring, and Epigenetics: Impact on Tumor Progression and Perspective for Anticancer Therapy. *Cells* 2019;**8**(6):
80. Hanahan D and Weinberg RA. Hallmarks of cancer: the next generation. *Cell* 2011;**144**(5): 646-674.
81. Li W, Sahu D and Tsen F. Secreted heat shock protein-90 (Hsp90) in wound healing and cancer. *Biochim Biophys Acta* 2012;**1823**(3): 730-741.
82. Marzec M, Eletto D and Argon Y. GRP94: An HSP90-like protein specialized for protein folding and quality control in the endoplasmic reticulum. *Biochim Biophys Acta* 2012;**1823**(3): 774-787.
83. Eletto D, Dersh D and Argon Y. GRP94 in ER quality control and stress responses. *Semin Cell Dev Biol* 2010;**21**(5): 479-485.
84. Biswas C, Ostrovsky O, Makarewich CA, Wanderling S, Gidalevitz T and Argon Y. The peptide-binding activity of GRP94 is regulated by calcium. *Biochem J* 2007;**405**(2): 233-241.
85. Van PN, Peter F and Soling HD. Four intracisternal calcium-binding glycoproteins from rat liver microsomes with high affinity for calcium. No indication for calsequestrin-like proteins in inositol 1,4,5-trisphosphate-sensitive calcium sequestering rat liver vesicles. *J Biol Chem* 1989;**264**(29): 17494-17501.
86. Felts SJ, Owen BA, Nguyen P, Trepel J, Donner DB and Toft DO. The hsp90-related protein TRAP1 is a mitochondrial protein with distinct functional properties. *J Biol Chem* 2000;**275**(5): 3305-3312.
87. Song HY, Dunbar JD, Zhang YX, Guo D and Donner DB. Identification of a protein with homology to hsp90 that binds the type 1 tumor necrosis factor receptor. *J Biol Chem* 1995;**270**(8): 3574-3581.
88. Hua G, Zhang Q and Fan Z. Heat shock protein 75 (TRAP1) antagonizes reactive oxygen species generation and protects cells from granzyme M-mediated apoptosis. *J Biol Chem* 2007;**282**(28): 20553-20560.
89. Masgras I, Sanchez-Martin C, Colombo G and Rasola A. The Chaperone TRAP1 As a Modulator of the Mitochondrial Adaptations in Cancer Cells. *Front Oncol* 2017;**7**(58.
90. Sciacovelli M, Guzzo G, Morello V, Frezza C, Zheng L, Nannini N*, et al.* The mitochondrial chaperone TRAP1 promotes neoplastic growth by inhibiting succinate dehydrogenase. *Cell Metab* 2013;**17**(6): 988-999.
91. Xiang F, Ma SY, Lv YL, Zhang DX, Song HP and Huang YS. Tumor necrosis factor receptor-associated protein 1 regulates hypoxia-induced apoptosis through a

mitochondria-dependent pathway mediated by cytochrome c oxidase subunit II. *Burns Trauma* 2019;**7**(16.
92. Grbovic OM, Basso AD, Sawai A, Ye Q, Friedlander P, Solit D*, et al.* V600E B-Raf requires the Hsp90 chaperone for stability and is degraded in response to Hsp90 inhibitors. *Proc Natl Acad Sci U S A* 2006;**103**(1): 57-62.
93. Dickey CA, Kamal A, Lundgren K, Klosak N, Bailey RM, Dunmore J*, et al.* The high-affinity HSP90-CHIP complex recognizes and selectively degrades phosphorylated tau client proteins. *J Clin Invest* 2007;**117**(3): 648-658.
94. Evans CG, Wisen S and Gestwicki JE. Heat shock proteins 70 and 90 inhibit early stages of amyloid beta-(1-42) aggregation in vitro. *J Biol Chem* 2006;**281**(44): 33182-33191.
95. Ansa-Addo EA, Thaxton J, Hong F, Wu BX, Zhang Y, Fugle CW*, et al.* Clients and Oncogenic Roles of Molecular Chaperone gp96/grp94. *Curr Top Med Chem* 2016;**16**(25): 2765-2778.
96. Robert J, Menoret A and Cohen N. Cell surface expression of the endoplasmic reticular heat shock protein gp96 is phylogenetically conserved. *J Immunol* 1999;**163**(8): 4133-4139.
97. Amoroso MR, Matassa DS, Sisinni L, Lettini G, Landriscina M and Esposito F. TRAP1 revisited: novel localizations and functions of a 'next-generation' biomarker (review). *Int J Oncol* 2014;**45**(3): 969-977.
98. Peterson LB, Eskew JD, Vielhauer GA and Blagg BS. The hERG channel is dependent upon the Hsp90alpha isoform for maturation and trafficking. *Mol Pharm* 2012;**9**(6): 1841-1846.
99. Renouf DJ, Velazquez-Martin JP, Simpson R, Siu LL and Bedard PL. Ocular toxicity of targeted therapies. *J Clin Oncol* 2012;**30**(26): 3277-3286.
100. Neckers L and Workman P. Hsp90 molecular chaperone inhibitors: are we there yet? *Clin Cancer Res* 2012;**18**(1): 64-76.
101. Rosser MF and Nicchitta CV. Ligand interactions in the adenosine nucleotide-binding domain of the Hsp90 chaperone, GRP94. I. Evidence for allosteric regulation of ligand binding. *J Biol Chem* 2000;**275**(30): 22798-22805.
102. Duerfeldt AS, Brandt GE and Blagg BS. Design, synthesis, and biological evaluation of conformationally constrained cis-amide Hsp90 inhibitors. *Org Lett* 2009;**11**(11): 2353-2356.
103. Shen G and Blagg BS. Radester, a novel inhibitor of the Hsp90 protein folding machinery. *Org Lett* 2005;**7**(11): 2157-2160.
104. Wang M, Shen G and Blagg BS. Radanamycin, a macrocyclic chimera of radicicol and geldanamycin. *Bioorg Med Chem Lett* 2006;**16**(9): 2459-2462.
105. Immormino RM, Metzger LEt, Reardon PN, Dollins DE, Blagg BS and Gewirth DT. Different poses for ligand and chaperone in inhibitor-bound Hsp90 and GRP94: implications for paralog-specific drug design. *J Mol Biol* 2009;**388**(5): 1033-1042.
106. Duerfeldt AS, Peterson LB, Maynard JC, Ng CL, Eletto D, Ostrovsky O*, et al.* Development of a Grp94 inhibitor. *J Am Chem Soc* 2012;**134**(23): 9796-9804.
107. Yang Y, Liu B, Dai J, Srivastava PK, Zammit DJ, Lefrancois L*, et al.* Heat shock protein gp96 is a master chaperone for toll-like receptors and is important in the innate function of macrophages. *Immunity* 2007;**26**(2): 215-226.

108. Crowley VM, Khandelwal A, Mishra S, Stothert AR, Huard DJ, Zhao J*, et al.* Development of Glucose Regulated Protein 94-Selective Inhibitors Based on the BnIm and Radamide Scaffold. *J Med Chem* 2016;**59**(7): 3471-3488.
109. Stothert AR, Suntharalingam A, Huard DJ, Fontaine SN, Crowley VM, Mishra S*, et al.* Exploiting the interaction between Grp94 and aggregated myocilin to treat glaucoma. *Hum Mol Genet* 2014;**23**(24): 6470-6480.
110. Stothert AR, Suntharalingam A, Tang X, Crowley VM, Mishra SJ, Webster JM*, et al.* Isoform-selective Hsp90 inhibition rescues model of hereditary open-angle glaucoma. *Sci Rep* 2017;**7**(1): 17951.
111. Crowley VM, Huard DJE, Lieberman RL and Blagg BSJ. Second Generation Grp94-Selective Inhibitors Provide Opportunities for the Inhibition of Metastatic Cancer. *Chemistry* 2017;**23**(62): 15775-15782.
112. Khandelwal A, Crowley VM and Blagg BSJ. Resorcinol-Based Grp94-Selective Inhibitors. *ACS Med Chem Lett* 2017;**8**(10): 1013-1018.
113. Patel PD, Yan P, Seidler PM, Patel HJ, Sun W, Yang C*, et al.* Paralog-selective Hsp90 inhibitors define tumor-specific regulation of HER2. *Nat Chem Biol* 2013;**9**(11): 677-684.
114. Jiang F, Guo AP, Xu JC, You QD and Xu XL. Discovery of a Potent Grp94 Selective Inhibitor with Anti-Inflammatory Efficacy in a Mouse Model of Ulcerative Colitis. *J Med Chem* 2018;**61**(21): 9513-9533.
115. Ernst JT, Liu M, Zuccola H, Neubert T, Beaumont K, Turnbull A*, et al.* Correlation between chemotype-dependent binding conformations of HSP90alpha/beta and isoform selectivity-Implications for the structure-based design of HSP90alpha/beta selective inhibitors for treating neurodegenerative diseases. *Bioorg Med Chem Lett* 2014;**24**(1): 204-208.
116. Putcha P, Danzer KM, Kranich LR, Scott A, Silinski M, Mabbett S*, et al.* Brain-permeable small-molecule inhibitors of Hsp90 prevent alpha-synuclein oligomer formation and rescue alpha-synuclein-induced toxicity. *J Pharmacol Exp Ther* 2010;**332**(3): 849-857.
117. Ernst JT, Neubert T, Liu M, Sperry S, Zuccola H, Turnbull A*, et al.* Identification of novel HSP90alpha/beta isoform selective inhibitors using structure-based drug design. demonstration of potential utility in treating CNS disorders such as Huntington's disease. *J Med Chem* 2014;**57**(8): 3382-3400.
118. Khandelwal A, Kent CN, Balch M, Peng S, Mishra SJ, Deng J*, et al.* Structure-guided design of an Hsp90beta N-terminal isoform-selective inhibitor. *Nat Commun* 2018;**9**(1): 425.
119. Plescia J, Salz W, Xia F, Pennati M, Zaffaroni N, Daidone MG*, et al.* Rational design of shepherdin, a novel anticancer agent. *Cancer Cell* 2005;**7**(5): 457-468.
120. Altieri DC, Stein GS, Lian JB and Languino LR. TRAP-1, the mitochondrial Hsp90. *Biochim Biophys Acta* 2012;**1823**(3): 767-773.
121. Siegelin MD. Inhibition of the mitochondrial Hsp90 chaperone network: a novel, efficient treatment strategy for cancer? *Cancer Lett* 2013;**333**(2): 133-146.
122. Seo YH. Organelle-specific Hsp90 inhibitors. *Arch Pharm Res* 2015;**38**(9): 1582-1590.

123. Lee C, Park HK, Jeong H, Lim J, Lee AJ, Cheon KY*, et al.* Development of a mitochondria-targeted Hsp90 inhibitor based on the crystal structures of human TRAP1. *J Am Chem Soc* 2015;**137**(13): 4358-4367.
124. Park HK, Jeong H, Ko E, Lee G, Lee JE, Lee SK*, et al.* Paralog Specificity Determines Subcellular Distribution, Action Mechanism, and Anticancer Activity of TRAP1 Inhibitors. *J Med Chem* 2017;**60**(17): 7569-7578.

Chapter 3
A Novel C-Terminal Hsp90 Inhibitor KU758 Synergizes Efficacy in Combination with BRAF or MEK Inhibitors and Targets Drug-Resistant Pathways in BRAF-Mutant Melanomas[3]

Abstract

Melanoma remains the most aggressive and fatal form of skin cancer, despite several FDA-approved targeted chemotherapies and immunotherapies for use in advanced disease. Of the 100,350 new patients diagnosed with melanoma in 2020 in the U.S., more than half will develop metastatic disease leading to a 5-year survival rate <30%, with a majority of these developing drug-resistance within the first year of treatment. These statistics underscore the critical need in the field to develop more durable therapeutics as well as those that can overcome chemotherapy-induced drug resistance from currently approved agents. Fortunately, several of the drug-resistance pathways in melanoma including the proteins in those pathways rely in part on Hsp90 chaperone function. This presents a unique and novel opportunity to simultaneously target multiple proteins and drug-resistant pathways in this disease via molecular chaperone inhibition. Taken together, we hypothesize that our novel C-terminal Hsp90 inhibitor, KU758, in combination with current standard of care targeted therapies (e.g. vemurafenib and cobimetinib) can both synergize melanoma treatment efficacy in BRAF-mutant tumors, as well as target and overcome several major resistance pathways in this

[3] This chapter in under revision in *Melanoma Research* and completed in collaboration with Chitra, Subramanian, Nina Zhang, Ton Wang, Barbara N. Timmermann, Brian S.J. Blagg, and Mark S. Cohen.

disease. Using *in vitro* proliferation and protein-based Western Blot analyses, our novel inhibitor, KU758 potently inhibited melanoma cell proliferation (without induction of the heat-shock-response) *in vitro* and synergized with both BRAF and MEK inhibitors in inhibition of cell migration and protein expression from resistance pathways. Overall, our work provides early support for further translation of C-terminal Hsp90 inhibitor and MAPK pathway inhibitor combinations as a novel therapeutic strategy for BRAF-mutant melanomas.

Introduction

Despite Food and Drug Administration (FDA) approval of several targeted chemotherapies and immunotherapies, melanoma remains the most aggressive and fatal skin cancer. Melanoma incidence is rising yearly with 100,350 new U.S. cases expected in 2020 [1]. Of the patients diagnosed, >50% will present with metastatic disease decreasing their 5-year survival rate to ~25% [1]. This indicates the critical need for novel, more-durable drugs and therapeutic approaches for these patients. Although several approved therapies – namely mitogen activated protein kinase (MAPK) pathway and immune checkpoint inhibitors – are reasonably effective early-on, the majority of patients develop drug resistance within the first year of treatment [2,3].

A common clinical approach to mitigate resistance utilizes drug combinations that simultaneously target multiple pathways. Combination therapy using lower drug doses also has the potential to decrease toxicities while improving overall efficacy [4]. In 2014, the FDA approved the combination of MAPK pathway inhibitors (MAPKi) targeting BRAF (e.g. vemurafenib) and MEK (e.g. cobimetinib) in patients with unresectable advanced BRAF-mutant melanomas. A year later, the PD-1 (programmed cell death protein-1) and CTLA-4 (cytotoxic T-lymphocyte associated protein-4) monoclonal antibodies were approved as first-line immunotherapies in metastatic BRAF-wildtype patients [5]. While initial patient responses were promising, emergence of drug-resistance in both approaches highlights the need for development of more-durable therapies.

Targeting the 90-kDa heat shock protein (Hsp90) provides an attractive anticancer therapeutic approach as inhibition of chaperone function can target multiple cancer-promoting kinase pathways simultaneously. As chaperones, Hsps play a crucial role in

cellular proteostasis, and more specifically the heat shock response (HSR), by maintaining protein folding, stabilization, and activation of a myriad of substrates, referred to as clients [6-8]. Hsp clientele are involved in several cellular pathways/processes including steroid hormone receptors, protein kinases/phosphatases for signal transduction, cell cycle regulation, and gene transcription regulators[9]. Hsp90's role in cancer was elucidated in the 1990s by Whitesell and colleagues after observing that oncogenic cell morphology in *v-src* transformed fibroblasts was reversed with the treatment of geldanamycin (GDA), a benzoquinone ansamycin antibiotic [10]. Since then, numerous N-terminal Hsp90 inhibitors have been developed and tested in clinical cancer trials. This ongoing interest is best explained by Hsp90's "central node" role in chaperoning client proteins involved in all the processes/hallmarks that contribute to and maintain the initiation and progression of cancer [11,12]. While no Hsp90 inhibitors (Hsp90i) to date are FDA approved as monotherapies, numerous clinical studies show their efficacy and anti-cancer potency. Currently 94% of Hsp90i in clinical trials target Hsp90's N-terminal domain and induce the HSR with upregulation of Hsp70. This leads to needing higher Hsp90 concentrations to maintain cellular inhibition – a potential contributor to dose-limiting toxicities observed in these trials [13]. To address this, we developed novel compounds that target the C-terminal as a unique approach for Hsp90 inhibition that does not stimulate the HSR as robustly. Our group has recently shown that C-terminal inhibitors (CT-Hsp90i) are effective in breast cancers, adrenocortical cancers, and head and neck squamous cell carcinomas and targeting cancer stem cells (CSC) by decreasing CSC markers and downregulating invasion/migration and epithelial-to-mesenchymal transition both *in vitro* and *in vivo* [14-16]. Taken together, we hypothesize

that combining a MAPKi (BRAF or MEK) with a new CT-Hsp90i could synergize anticancer-effect and provide a novel rational therapeutic strategy for metastatic melanoma patients. Such a combination should downregulate major BRAF-resistance pathways and dampen the effect(s) of several cancer hallmarks. We evaluate here our novel CT-Hsp90i, KU758, alone and in combination with a BRAFi/MEKi for its ability to inhibit melanoma cell proliferation, migration, and target melanoma cellular processes critical in the maintenance of resistance.

Methods

Cell Culture and Reagents

For cell culture, unless otherwise noted, DNA-fingerprint validated human melanoma cell lines harboring a $BRAF_{V600E}$-mutation (UACC-257 and UACC-62) were maintained in T-75 flasks (Thermo Fisher Scientific, Waltham, MA) in high glucose and L-glutamine Dulbecco's Modified Eagle's Medium (Thermo Fisher Scientific, Waltham, MA) supplemented with 10% FBS (Sigma-Aldrich, St. Louis, MO) and 1% penicillin/streptomycin (Thermo Fisher Scientific). Cell lines were incubated at 37°C in 5% CO2. The same protocol was followed to culture a human fetal fibroblast (FF) cell line as a control. Cells were washed with 1X phosphate buffer solution (PBS), then detached using Trypsin-EDTA (Sigma-Aldrich, St. Louis, MO). Drug compounds used included: BRAF inhibitor (BRAFi) vemurafenib (Ve) (Selleck Chemicals, Houston, TX), MEK inhibitor (MEKi), cobimetinib (Cb) (AdooQ Bioscience, Irvine, CA), novel CT-Hsp90i KU758 obtained from Dr. Brian S.J. Blagg (Univ. of Notre Dame, Notre Dame, ID), N-terminal Hsp90i (NT-Hsp90i) XL888 (AdooQ Bioscience, Irvine, CA), and natural product

Hsp90i withalongolide A 4,19,27-triacetate (WGA-TA) obtained from Dr. Barbara Timmermann (Kansas Univ., Lawrence, KS).

Cell Viability Assay

Cell lines were plated in polystyrene, clear flat-bottom 96-well plates (Thermo Fisher Scientific, Waltham, MA) at 1,500 cells/well and adhered overnight. Cells were treated in serial concentrations of each inhibitor and left to incubate for 24hrs. To determine cell viability, ATP was quantified using a CellTiter-Glo® Luminescent Cell Viability Assay (Promega, Madison, WI) following the manufacturer's instructions. The luminescence was read using a BioTek Synergy Neo plate reader and Gen5 software (BioTek, Winooski, VT). The values collected were imported into GraphPad Prism (GraphPad Prism Software, Inc., La Jolla, CA) to obtain dose-response curves and calculate the half maximal inhibition concentration (IC_{50}) of each drug in all cell lines. Cell viability for FF cells was determined using an MTS assay. Cells were plated in 96-well plates at 6,000 cells/well. MTS reagent (Owen's reagent) was added to each well after 24hrs treatment period. Absorbance and IC_{50} values were read and calculated, respectively, as stated above.

Combination Assay

Cells were plated in 96-well plates, as aforementioned, then treated with a BRAFi or MEKi plus a Hsp90i or BRAFi plus MEKi for a total of seven combinations. The drug concentrations used were based on the IC_{50} values of each compound and cells were treated with each inhibitor at a range of concentrations (e.g. 1/4x, 1/2x, and 1x IC_{50}) for 24hrs. The plating and CellTiter-Glo® protocols described above were used for combination assays. Following luminescence reading, values were analyzed using the

CompuSyn software (Compusyn, Inc., Paramus, NJ), based on the Chou-Talalay theorem, to calculate the combination index (CI) of each treatment and determine synergistic combinations (e.g. CI<1). Surface maps of combination effects were plotted using Combenefit software (Cancer Research UK Cambridge Institute) to illustrate extent of biological (viability as percent of control) and synergistic/antagonistic (coloring of map) effects.

Immunoblot Analysis

Cell lines were cultured to 70% confluency, then treated for 24hrs with a drug alone or two in combination – concentrations used: 0.5μM KU758, 0.1μM WGA-TA, 0.3μM XL888, 0.125μM Cb, and 50μM Ve. Next, cells were collected, then lysed via suspension in a lysis buffer cocktail containing 2μL/mL PR protease inhibitor, 1μL/mL 100M phenylmethane sulfonyl fluoride, 2μL/mL 0.5M NaF, and 10μL/mL 100M Na3VO4 followed by sonication (Qsonica Sonicators, Newtown, CT). After centrifuging (Eppendorf, Hamburg, Germany) samples for 20mins at 4°C and 14,000rpm, protein supernatant was collected then quantified using a BSA protein standard assay (Thermo Fisher Scientific, Waltham, MA) following manufacturer's instructions. Protein samples were prepped with 5X loading dye, loaded in equal amounts, and separated using SDS-PAGE. The Precision Plus Protein Dual Color Standards (Bio-Rad Laboratories, Hercules, CA) was used as a protein ladder. Briefly, SDS-PAGE gels were transferred to nitrocellulose blotting membranes (GE Healthcare Life Sciences, Pittsburgh, PA), washed with PBS and PBS-Tween20, and probed overnight in primary antibodies (Cell Signaling Technologies, Inc., Danvers, MA). Next blots were probed with appropriate horseradish peroxidase-linked anti-rabbit or anti-mouse secondary antibodies (Cell Signaling Technologies, Inc.,

Danvers, MA), washed again, and enhanced chemiluminescence horseradish peroxidase substrate [SuperSignal West Pico PLUS or Femto (Thermo Fisher Scientific, Waltham, MA)] was used to visualize nitrocellulose blots with a digital image using a ChemiDoc Imaging System (BioRad, Hercules, CA). β-actin was used as a loading control. ImageJ software (National Institutes of Health, Bethesda, MD) was used to perform densitometry of protein bands. Immunoblot quantification (densitometry) of a given protein band is described as a normalized, relative value to the corresponding β-actin expression.

Migration Assays

Cells were plated in polystyrene, clear flat-bottom 6-well plates at 250,000 cells/well and adhered overnight. A pipette tip was used to scratch a clear vertical line in well. Culture media was removed, and wells were washed with PBS to remove cell debris. Images of each well were captured in triplicate using the EVOS FLc microscope and camera (Thermo Fisher Scientific, Waltham, MA). Fresh cell culture media was added to each well, then treated with each inhibitor alone and in combination with Ve or Cb using the determined synergistic drug combination concentrations (see above), for a total of 12 treatment conditions and one untreated control. Cells incubated at 37°C in 5% CO2 until untreated cells migrated and covered previously scratched area (24hrs). Images of each well were recaptured in triplicate. For each well, we calculated the percent of the scratch zone covered by migrated cells at t=24hrs (higher percentage indicates more cell migration).

Additionally, Boyden chambers with 8.0µM pore size and PET track-etched membranes were used (Falcon, Tewksbury, MA). Cells were seeded at 50,000 cells/chamber in serum-free DMEM media. Chambers were submerged into polystyrene,

clear flat-bottom 24-well plate wells with 20% FBS DMEM media and left to migrate for 24hrs at 37°C in 5% CO2. After 24hrs, each chamber was removed from the well, then fixed with formalin for 15mins and stained with 1% crystal violet, 20% methanol dye for 30mins. Chambers were washed and images captured using an EVOS FLc microscope and camera at 10X magnification. To quantify cell migration, images were used to count cells after 24hrs treatment.

Statistical Analysis

All *in vitro* experiments were replicated in triplicate. Significance was determined using Student's t-test (*$p < 0.05$ and **$p < 0.001$). Dose-response curves were normalized to untreated control for all inhibitors and used to calculate IC_{50} values with 95% confidence intervals in GraphPad Prism, as stated above. Data is presented as mean values with standard deviation error bars. SPSS version 25 (IBM, Almont NY) was used to verify all statistical calculations.

Results

KU758 Selectively and Potently Inhibits Growth of BRAF-Mutated Melanocytes

Before characterizing the combinational effect of KU758+MAPKi on resistance pathways and cancer hallmarks, it was pertinent to determine the potency and selectivity of KU758 in melanocytes. To evaluate this, we performed a proliferation assay (CellTiter-Glo®) and compared the IC_{50} values of 3 different Hsp90i: our novel CT-Hsp90i (KU758), the NT-Hsp90i (XL888), and the natural product inhibitor (WGA-TA). All *in vitro* cell viability assays were performed in UACC-257 and UACC-62 human BRAF-mutant melanocytes and FF cell line controls. The IC_{50} of KU758 was consistent across both

BRAF-mutant cell lines (360-430 nM) and this was comparable to XL888 and WGA-TA. The IC_{50} of the BRAFi (Ve) and MEKi (Cb) are also listed in **Figure** 3-1. As a non-malignant control, fetal fibroblasts (FF cells) were treated with all three Hsp90i. Each inhibitor demonstrated a cancer-specific selectivity over normal cells from 10-fold (KU758) to 300-fold (XL888) (

).

KU758 Synergizes with MAPK Pathway Inhibitors

Combination therapy with targeted small molecular inhibitors, such as Ve with Cb, is one standard treatment for metastatic melanoma patients with a $BRAF_{V600E/K}$-mutation status. Combination therapy success can be predicted by the extent of synergism, or lack thereof, between the two compounds of interest and is quantified by calculating the combination index (CI) of a given drug combination. A CI<1, especially <0.5 indicates synergistic combinations, while a CI=1 is an additive effect, and a CI>1 indicates an antagonistic effect [4,17]. To identify the combination effect of our novel CT-Hsp90i, KU758, and a MAPKi (Ve or Cb) on proliferation in BRAF-mutant melanocytes (UACC-257), we determined the CI of several drug combinations (**Table** 3-1). Cells were treated with Ve or Cb and KU758, XL888, or WGA-TA for seven inhibitor combinations (including Ve+Cb) at a range of concentrations based on the IC_{50} values. The response to combination treatment was measured as the percentage of viable cells compared to control (**Figure** 3-2). KU758 synergized with Ve and Cb, in seven out of nine combinations with six having a robust synergy (CI<0.5 for three K758+Ve combinations and CI>0.4 for three KU758+Cb combinations typically at 0.5µM KU758; dark blue and cyan coloring of the surface plots; **Table** 3-1). The most synergistic combinations of WGA-TA+Cb and XL888+Cb were at 0.125µM Cb and 50µM Ve, so these concentrations were used for all subsequent studies. Similar to KU758, WGA-TA, synergized with BRAFi and MEKi at several drug concentrations, but with only one CI<0.5 (**Figure** 3-2**, Table** 3-1). Unlike the other Hsp90i, XL888+Cb synergized with relatively mid-to-low CIs, whereas CIs in XL888+Ve combinations were predominantly >1 suggesting some antagonism

(**Figure** 3-2**, Table** 3-1). Since BRAFi and MEKi combinations are already FDA approved for use in BRAF-mutant metastatic melanoma patients, combination assays of Ve+Cb were performed and CIs were calculated for comparison. As expected, almost all (94%) Ve+Cb combinations, between the two cell lines, were synergistic (**Figure** 3-2**, Table** 3-1). To demonstrate replication of the synergistic combinational effect observed with KU758+MAPKi in UACC-257, experiments were repeated in UACC-62 (Error! Reference source not found.**,** Error! Reference source not found.) and similar synergistic effects were noted. To confirm the inhibitor combinations were effective at promoting cell death, protein expression of PARP and its cleaved product were measured (Western Blot) and quantified utilizing Image-J software densitometry (compared to ß-actin). All combinations synergistically increased the expression of cleaved PARP compared to each treatment of each drug alone ($p < 0.05$) (**Figure** 3-2).

Major Resistance Pathway Proteins are Targeted with KU758 Combinations

After determining the potency/selectivity of KU758 in melanocytes, and its synergy in combination with a MAPKi, we next evaluated this combination effect on two major BRAFi-resistance signaling pathways in melanoma (MAPK/Erk and PI3K/Akt pathways). We hypothesized that since Hsp90 serves as the molecular chaperone for several proteins involved in these two resistant pathways, then utilization of Hsp90i+MAPKi will lead to subsequent downregulation of these kinase drivers from the resistant pathways. To investigate this effect on resistant-pathway protein expression levels, we performed immunoblot analysis, then quantified the change in protein expression. Melanocytes treated with XL888+Cb or WGA-TA+Cb showed a 2- to 3-fold significant increase in expression of Raf1, ($p<0.001$). However, with XL888+Ve or WGA-TA+Ve combinations,

expression of Raf1 was almost entirely ablated. In all instances, there was a significant change in protein expression compared to Cb or Ve alone ($p<0.05$), but not with an Hsp90i as a single agent (**Figure** 3-3). In KU758+Ve and KU758+Cb treated cells, there was a significant decrease to Raf1 expression when compared to KU758-only treatment ($p<0.05$) (**Figure** 3-3). Next, we immunoblotted for p-Erk, a kinase downstream of Raf1. In XL888+Cb and XL888+Ve combinations, the phosphorylated kinase was almost entirely knocked downed ($p<0.01$); while it was significantly knocked down with WGA-TA+Cb, WGA-TA+Ve, and KU758+Cb ($p<0.01$**; Figure** 3-3). For p-Akt expression there was a 3- and 5-fold increase in cells treated with Cb or WGA-TA alone, respectively. Combinations of Hsp90i+MAPKi showed more significant knockdown than any drug alone with KU758+Cb having the highest knockdown of expression (95% vs. control), but with significant decreases also observed with the WGA-TA and X888 combinations with Ve or Cb (all with $p<0.01$ vs. controls; **Figure** 3-3).

Migration is Decreased with Hsp90i+MAPKi Combinations

Since KU758+Ve and KU758+Cb combinations target key melanoma resistance pathways, we next investigated this combination effect on cell migration, since it contributes to the potential of a melanoma's ability to move from one tissue into an adjacent one [18]. Extent of cell migration *in vitro* is also a reasonable surrogate method to predict metastatic potential and its associated cellular processes. We hypothesized that KU758+MAPKi combinations would effectively decrease melanocyte migration since the proteins directly involved with these processes are also Hsp90 clients.

To determine the effect of Hsp90i alone and in combinations with Ve or Cb on cell migration (and indirectly on metastatic potential), we utilized scratch and Boyden chamber

assays. For each treatment condition in the scratch assay, scratch distance at t=0hrs and t=24hrs was measured, then calculated as percent of cells migrated at 24hrs and significance values reflect the quantified change – lower percent migration is desired suggesting little to no migration. After 24hrs, untreated/control cells migrated to occupy 99% of the scratched area representing significant cell migration ($p<0.001$). Ve and Cb single-agent treatments resulted in 83% and 54% cell migration, respectively ($p<0.05$ vs. control), KU758-alone, KU758+Ve, and KU758+Cb resulted in 27%, 20% and 16% cell migration, respectively (all $p<0.01$). Similar decreases in migration were observed with XL888 and WGA-TA alone and in combination with a MAPKi (**Figure 3-4**). These effects were then confirmed in our second cell line, UACC-62 (Error! Reference source not found.**)**. Immunoblot analysis showed that expression of E-cadherin (an important determinant of tumor progression, serving as a suppressor of migration) in KU758 and MAPKi single-agent treated cells was low ($p<0.05$) but its protein expression was significantly increased in combination treatments indicating an increase in suppression of migration (KU758+Ve and KU758+Cb, $p<0.05$) (**Figure 3-4**). Finally, we utilized Boyden chambers to quantify the number of cells that migrated from a serum-free media environment to a nutrient-rich one with 20% FBS after inhibitor treatment for 24hrs (**Figure 3-4**). All inhibitors alone significantly interfered with the migration of cells compared to untreated/control ($p<0.001$). In combination, only KU758+Ve, KU758+Cb and XL888+Ve showed a significant decrease in migration compared to each drug alone ($p<0.01$).

The HSR is not Activated in KU758 Treated Cells vs. XL888

Finally, it was crucial to distinguish the effect of Hsp90i+MAPKi combinations on the HSR as 94% of Hsp90i (including XL888) target the N-terminal domain, which many experts believe stimulates a HSR with upregulation of pro-survival proteins (Hsp32 and Hsp70) requiring subsequent higher Hsp90i doses to overcome and ultimately leading to dose-limiting toxicities. As we have shown in other models [14-16], targeting Hsp90's C-terminal domain does not upregulate the HSR so we should observe less HSR activation with KU758 and KU758+MAPKi combinations.

To test this, we quantified by Western Blot the change of expression of key Hsps – Hsp90, Hp70, Hsp32, and HSF1 in melanoma cells treated with Hsp90i alone or in combination with Ve or Cb. In all single-agent and combination treatments, Hsp90 expression was not significantly altered and remained consistent throughout (**Figure** 3-5). XL888 alone on in combinations significantly increased expression of both Hsp32 ($p<0.01$ vs. control) and Hsp70 (16-fold increase vs. control; $p<0.01$). Compared to XL888, Hsp32 and Hsp70 expression was significantly decreased in KU758 treated cells ($p<0.05$). Lastly HSF1, a transcription factor required for Hsp32/70 expression, was decreased vs controls by KU758(47% decrease), its combinations, WGA-TA+Cb, and XL888+Cb (all $p<0.05$; **Figure** 3-5).

Discussion

Since 2011, the standard treatment for metastatic melanoma patients with activating BRAF-mutations (V600E/K) has been BRAF+MEK inhibitor combination therapy, such as vemurafenib and cobimetinib (Ve+Cb). While this combination has good

efficacy initially, the majority of patients acquire drug-resistance within the first year of therapy resulting in disease progression [2]. This underscores the major clinical need to develop novel therapeutic strategies in melanoma with longer durability. The lack of durability of current targeted therapies is due primarily to drug resistance; two of the most prevalent resistance mechanisms resulting from BRAF-inhibition include the MAPK/Erk pathway and the PI3K/Akt pathway. In drug-resistant melanoma, these resistance pathways propagate the hallmarks of cancer and their associated processes. Since Hsp90 chaperones proteins involved in all of the hallmarks of cancer, including melanoma drug-resistance pathways, inhibiting Hsp90 function would simultaneously down-regulate multiple resistance and cancer-propagating pathways, making it an attractive therapeutic strategy [19,20]. This therapeutic approach using Hsp90 inhibition has been explored in numerous clinical trials targeting the Hsp90 N-terminal ATP binding site. N-terminal Hsp90i pan-inhibit all four Hsp90 isoforms leading to a HSR, that in turn upregulates several pro-survival processes in the cell including induction of Hsp70 levels. To overcome these pro-survival effects, higher doses of Hsp90 inhibitor are required, and as noted in clinical trials these NT-Hsp90i trials have been plagued with dose-limiting toxicities resulting in a lack of progression to FDA approval. In an attempt to overcome this Hsp90i limitation, our research team developed novel Hsp90i that target the C-terminal region of the molecular chaperone. These have been shown to be equally potent to NT-Hsp90i and selective against multiple cancers, but do not induce a significant HSR or upregulation of Hsp70 expression, and do not show any significant dose-limiting toxicity *in vivo* [14-16].

In this set of experiments, we demonstrate that our novel CT- Hsp90i, KU758, has similarly efficacy and potency to the NT-Hsp90i, XL888, yet is more synergistic in combination with Ve or Cb, without activating the HSR and with significantly lower Hsp70 expression modulation. In our first experiment, we demonstrate that our CT-Hsp90i, KU758, had similar efficacy, potency, and melanoma-selectively to an XL888, an NT-Hsp90i used in several clinical trials. Our 24hrs cell viability assays showed that the IC50 of KU758 in melanocytes was 0.4µM, which was comparable to the IC_{50} for XL888 (0.3µM) and WGA-TA (0.1µM). Additionally, these Hsp90i had 10- to 300-fold selectivity for melanocytes compared to the FF control cells. At 72hrs, these IC_{50} values continued to lower (data not shown), indicating increased potency when cells were exposed to each drug for a longer period of time.

After demonstrating that the three Hsp90i had similar potency and melanoma selectivity, it was crucial to identify whether they exhibited a synergistic combination effect in the presence of a MAPKi, such as vemurafenib or cobimetinib. Optimal combinations of our Hsp90i+Ve or Hsp90i+Cb had CI<1 indicating synergism, whereas additive or antagonistic combinations had CIs equal to or far greater than 1, respectively. Our compound, KU758, not only synergized with Ve and Cb, but with relatively lower CIs compared to the other two Hsp90i. It is important to note that all of the combination experiments were conducted using the highest concentration (at or near the respective compound's IC_{50}) of Ve, but not Cb. The reason for this is that despite KU758 synergizing with Ve at 12.5µM, 25µM, and 50µM, WGA-TA and XL888 only synergized at the highest concentration. Therefore, in order to keep as many variables consistent across all Hsp90i combinations, 50µM Ve was used for all corresponding treatments. A common

observation in all of our Hsp90i+Ve or Hsp90i+Cb was that more synergism was noted in Cb-combinations compared to Ve-combinations. One potential explanation for this could be that since Cb targets MEK, the downstream effector of Ve's target, BRAF, there is potentially a greater suppressive effect on the MAPK pathway with more distal targeting. One of the reasons MEKi were developed was to abrogate compensatory activation of the MAPK pathway resulting in the pathway's downregulation and this is noted especially in combination with a BRAFi [2].

After identifying that KU758 was effective, potent, and synergized with Ve and Cb, we took a mechanistic approach to understand and determine the effects of KU758+MAPKi combinations on known melanoma resistance pathways. We showed that in certain Cb-combinations there was an increase of Raf1 expression, while in Ve-combinations there was an almost complete decrease. This could in part be explained by the fact that Ve innately targets Raf1 and through this there is an overall decrease in its expression. Moreover, although Raf1 is a client of Hsp90, WGA-TA and XL888 Cb-combinations do not synergize to an extent where they result in knockdown of the protein product. On the contrary, both KU758 combinations decreased Raf1 perhaps due to a more synergistic effect. Further downstream of Raf1, there was varying p-Erk expression as the result of Hsp90i combinations. The most notable being in all XL888+Ve and WGA-TA+Ve combinations with almost complete knock down of p-Erk expression. In KU758+Ve, the lack of substantial p-Erk decrease could potentially be the effect of an alternative kinase, outside of the MAPK pathway, that activates MEK [2]. Additionally, in another drug-resistant melanoma pathway (PI3K/Akt), p-Akt was almost completely knocked down in KU758+Cb treated cells. This supports our hypothesis that synergistic

combinations of KU758+MAPKi help to mitigate compensatory signaling pathways in drug-resistant melanomas. All the Hsp90i tested demonstrated some synergy when combined with BRAF/MEK inhibitors and mitigated protein expression levels of key regulators from melanoma drug-resistant pathways.

Next we determined the effects of these inhibitor-combinations on cell migration, an important hallmark of cancer. While each Hsp90i showed moderate inhibition of melanocyte migration in scratch assays (with KU758 having the most inhibition), this effect was more significant when combined with a MAPKi. Evaluating cell migration results, each Hsp90i decreased cell migration significantly compared to untreated cells, and this inhibition was synergistically enhanced with KU758+MAPKi and XL888+MAPKi combinations. Compared to the current standard-of-care melanoma treatment combination (Ve+Cb), our Hsp90i+MAPKi combinations had superior effects on cell migration. This may be due to the role Hsp90i has in mitigating MAPKi drug-resistant pathways simultaneously leading to a more potent therapeutic effect on migration. E-cadherin (tumor suppressor that plays a role in the transition of stable to invasive tumors) expression is lost in melanocytes [21,22]. Down-regulation of the protein subsequently leads to a decrease in cell-adhesion molecules, and thus, increased cell motility and migration and metastatic spread. In our KU758 combinations, E-cadherin expression was significantly increased from controls, again underscoring the effectiveness and synergism of the Hsp90i+MAPKi combination on this cancer hallmark of cell migration/metastatic potential.

A distinction between each Hsp90i (and respective combinations with Ve and Cb) was its effect on the HSR. This HSR was significantly lower in the CT-Hsp90i KU758 than

the NT-Hsp90i XL888. KU758 does not increase the expression of Hsp32, a major pro-survival Hsp, and rescued protein expression in KU758+Ve or KU758+Cb compared to Ve or Cb alone. This highlighted that unlike XL888, XL888+MAPKi and Ve+Cb combinations, KU758 does not activate the HSR or significantly increase Hsp32 or Hsp70 protein expression levels. This finding is significant since the HSR induction observed with NT-Hsp90i is thought by many to be a major contributing factor to their dose-limiting toxicities and failures in clinical trials. Since KU758 did not induce this HSR and its pro-survival effects, it may have clinical advantages and lower toxicity than the N-terminal inhibitors and warrants future translational studies to better evaluate this potential.

In conclusion, these studies demonstrate early proof-of-concept that the novel CT-Hsp90i KU758 is an effective therapy to target BRAF-mutated melanomas with potency similar to XL888, an NT-Hsp90i tested in clinical trials. This therapy is potent and selective against melanoma cells. It not only synergizes with BRAF and MEK inhibitors to decrease melanoma proliferation, but also induces apoptosis through PARP cleavage, inhibits cell migration, and mitigates two important drug-resistance pathways; all without inducing the HSR, which has potential clinical advantages with lower toxicity concerns than previously tested NT-Hsp90i. Also given the advantages of KU758 in mitigating major melanoma drug-resistance pathways, this treatment approach could have more durability in the clinic than current options and would address an important treatment gap. As such, this data supports further translational testing of KU758 in metastatic melanomas *in vivo* to determine its future clinical potential and ideal combinational approach with MAPKi for optimal clinical synergy and benefit.

Tables

Table 3-1 Combination effect of Hsp90i+MAPKi.

The CIs are listed for each inhibitor combination treatment in UACC-257 between (A) Hsp90i+MAPKi, as well as (B) Ve+Cb. Synergistic combination boxes are colored according to relative value: CI<0.5 (blue), 0.5<CI<1.0 (green).

A)

		KU758			WGA-TA			XL888		
	(μM)	**0.125**	**0.25**	**0.5**	**0.025**	**0.5**	**0.1**	**0.075**	**0.15**	**0.3**
Ve	**12.5**	1.530	0.678	0.837	39.115	6.954	1.380	45.500	5.936	3.132
	25	1.497	0.492	0.566	4.916	1.787	0.868	21.717	3.653	2.465
	50	0.747	0.183	0.088	0.547	0.689	0.479	0.862	0.652	0.938
Cb	**0.125**	1.234	0.762	0.369	1.960	1.404	0.948	0.815	0.310	0.349
	0.25	1.371	0.592	0.371	1.999	1.139	1.132	0.846	0.497	0.512
	0.5	0.927	0.675	0.214	2.058	1.334	1.205	1.028	0.741	0.689

B)

		Cb		
	(μM)	**0.125**	**0.25**	**0.5**
Ve	**12.5**	0.953	0.887	1.463
	25	0.227	0.324	0.649
	50	0.195	0.343	0.622

Figures

Figure 3-1 Melanocyte viability and IC50 after Hsp90i or MAPKi treatment.

All inhibitors exhibited efficacy in BRAF-mutant melanocyte (UACC-257 and UACC-62) death after 24hrs treatment with a range of potencies (IC50 value). A) The dose-response curves of all three Hsp90i show similar potencies in the sub-micromolar range (~0.1-0.4 µM) – ascending IC50: WGA-TA (green) < XL888 (blue) < KU758 (orange). B) Melanocytes were treated with the BRAFi Ve (dark grey) and MEKi Cb (light grey) at several concentrations and the dose-response curves indicate higher potency of Cb over Ve. All inhibitor IC50 concentrations are listed below dose-response curves in micromolar with 95% confidence interval.

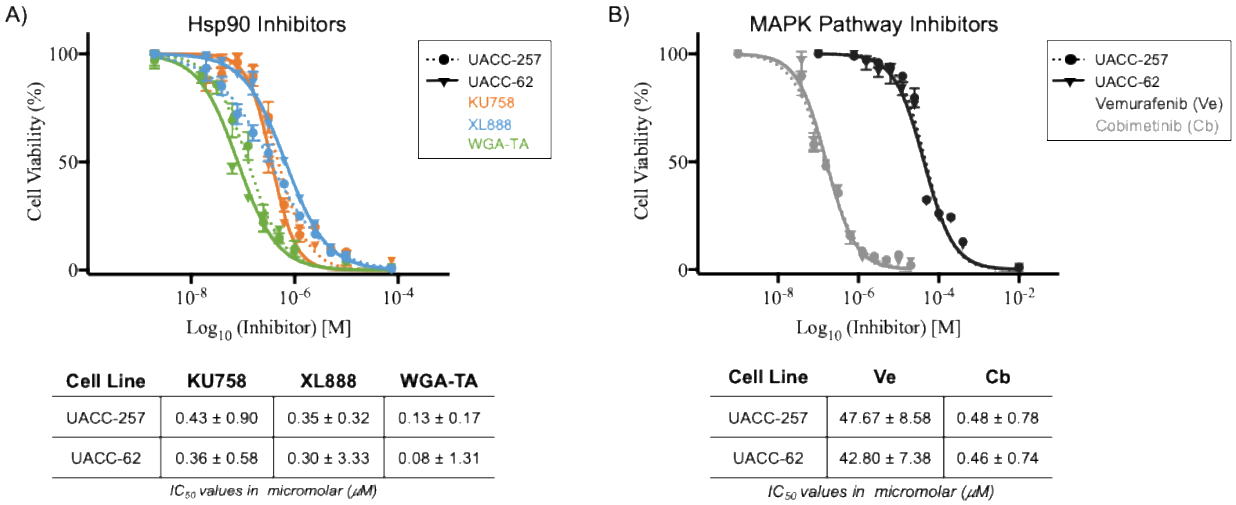

Cell Line	KU758	XL888	WGA-TA
UACC-257	0.43 ± 0.90	0.35 ± 0.32	0.13 ± 0.17
UACC-62	0.36 ± 0.58	0.30 ± 3.33	0.08 ± 1.31

IC_{50} values in micromolar (µM)

Cell Line	Ve	Cb
UACC-257	47.67 ± 8.58	0.48 ± 0.78
UACC-62	42.80 ± 7.38	0.46 ± 0.74

IC_{50} values in micromolar (µM)

Figure 3-2 Responses to Hsp90i+MAPKi combinations.

A) All Hsp90i, (listed left to right) KU758, WGA-TA, and XL888, showed a decrease in UACC-257 cell viability after treatment with Ve (top) or Cb (bottom). Each plot shows the percent of cell viability relative to control and illustrates the corresponding combination effect (e.g. synergistic, additive, or antagonistic) on a color spectrum. The most synergistic combinations were observed in KU758+Ve and KU758+Cb. All six Hsp90i+MAPKi combination abbreviations are tabulated. B and C) The expression of cleaved PARP increased in all inhibitor combinations compared to each drug alone.

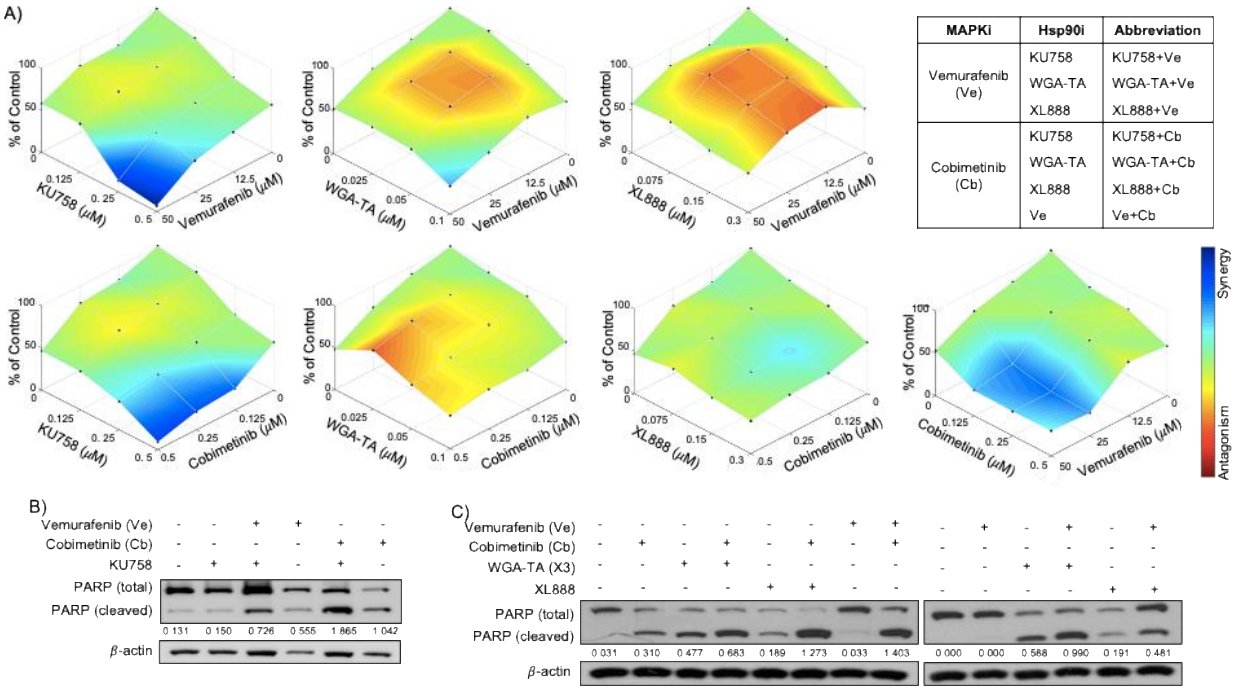

MAPKi	Hsp90i	Abbreviation
Vemurafenib (Ve)	KU758	KU758+Ve
	WGA-TA	WGA-TA+Ve
	XL888	XL888+Ve
Cobimetinib (Cb)	KU758	KU758+Cb
	WGA-TA	WGA-TA+Cb
	XL888	XL888+Cb
	Ve	Ve+Cb

Figure 3-3 Hsp90i+MAPKi combination effect on key resistance pathways.

A) In KU758 treated cells, alone or plus MAPKi, p-Akt expression decreased from untreated (control). Each combination decreased p-Akt to a greater extent than each inhibitor alone, especially KU758+Ve ($p<0.001$). Raf1 expression decreased in KU758+Ve, Cb, and KU758+Cb compared to control and each inhibitor alone ($p<0.05$). Ve, KU758+Ve, and Cb combinations increased p-Erk, while KU758+Cb effectively decreased the expression ($p<0.05$). B) p-Akt expression decreased in all Ve- and Cb-combinations, for WGA-TA and XL888, when compared to each inhibitor alone ($p<0.05$). Raf1 expression increased in WGA-TA, WGA-TA+Cb, XL888, and XL888+Cb. p-Erk expression was knocked down in WGA-TA+Ve and XL888+Ve combinations ($p<0.001$).

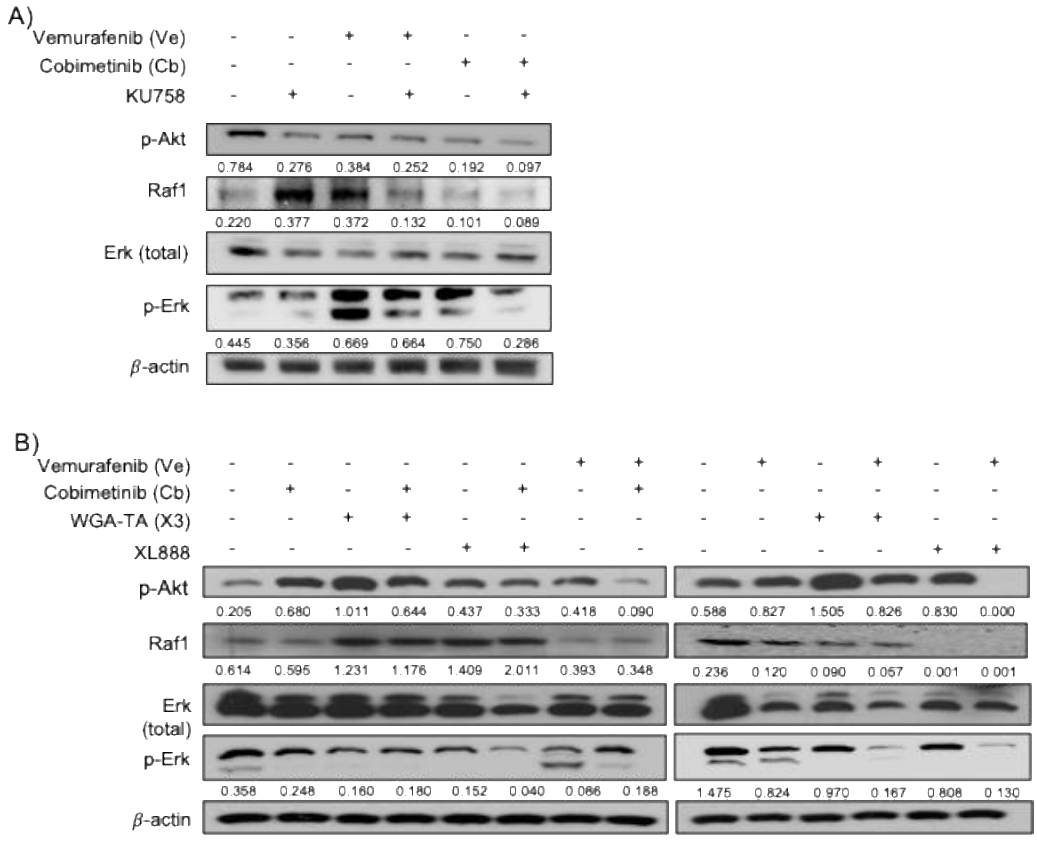

Figure 3-4 Changes to cell migration after exposure to Hsp90i combinations.

A) KU75+MAPKi combinations decreased cell migration compared to inhibitors alone and is represented by fewer cells crossing the scratched area (red line). B) The percent of cell migration at 24hrs was calculated with the most significant cell migration (>30%) was observed in untreated, Ve, Cb, and WGA-TA treated cells ($p<0.05$). All other treatments mitigated cell migration into the scratched areas. C) The number of migrated cells across the membrane were counted. All treatments significantly decreased cell migration compared to untreated ($p<0.001$). KU758+Ve and KU758+Cb decreased cell migration to a greater extent than each inhibitor alone ($p<0.05$). XL888+Ve and XL888+Cb exhibited similar decrease ($p<0.05$).

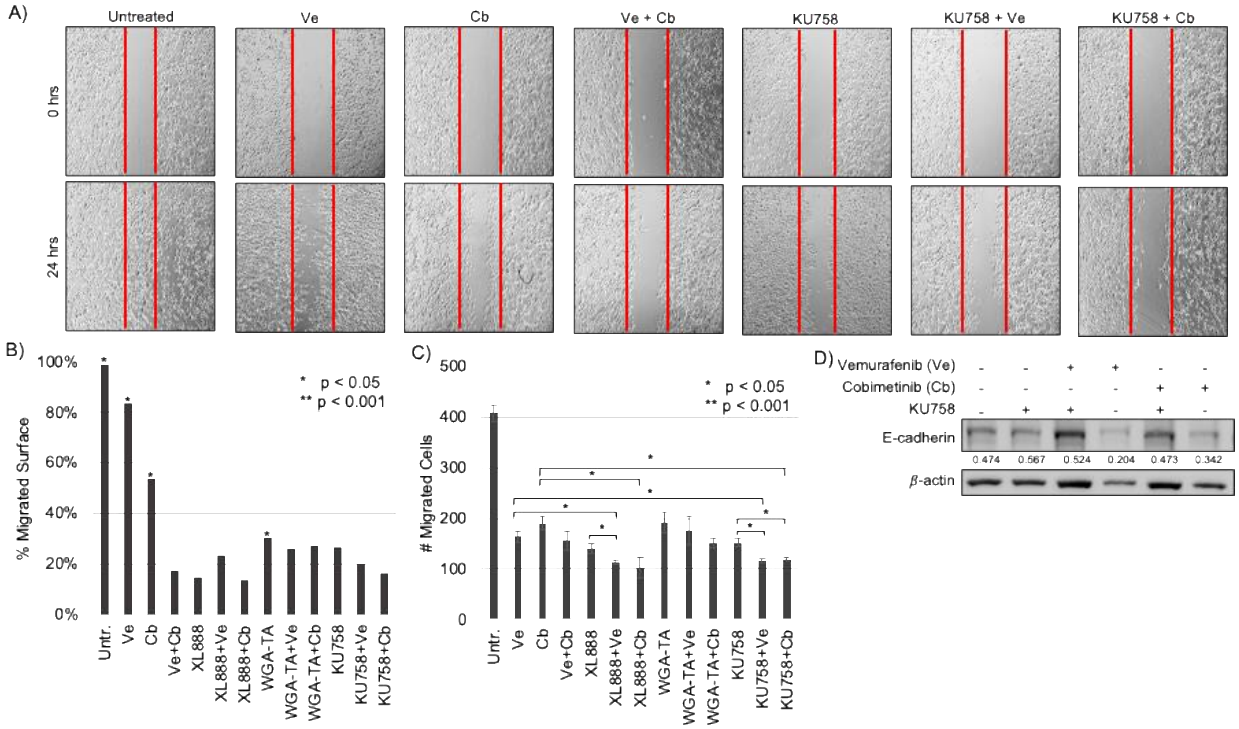

Figure 3-5 Effect of Hsp90i combinations on the HSR.

A) There was no significant change to HSF1 or Hsp90 expression in all KU758 and KU758+MAPKi cells. Expression of Hsp70 increased in all treatments compared to untreated (control), especially in Ve alone ($p<0.05$). Hsp32 increased in Ve and Cb treatments alone but decreased in KU758+Ve and KU758+Cb ($p<0.05$). B-E) Hsp70 expression increased in WGA-TA+MAPKi and XL888+MAPKi ($p<0.05$). No change to Hsp90 expression from control after inhibitor treatment. Hsp32 expression showed the most drastic increase in XL888 and XL88+MAPKi treated cells ($p<0.05$). *$p<0.01$; **$p<0.001$

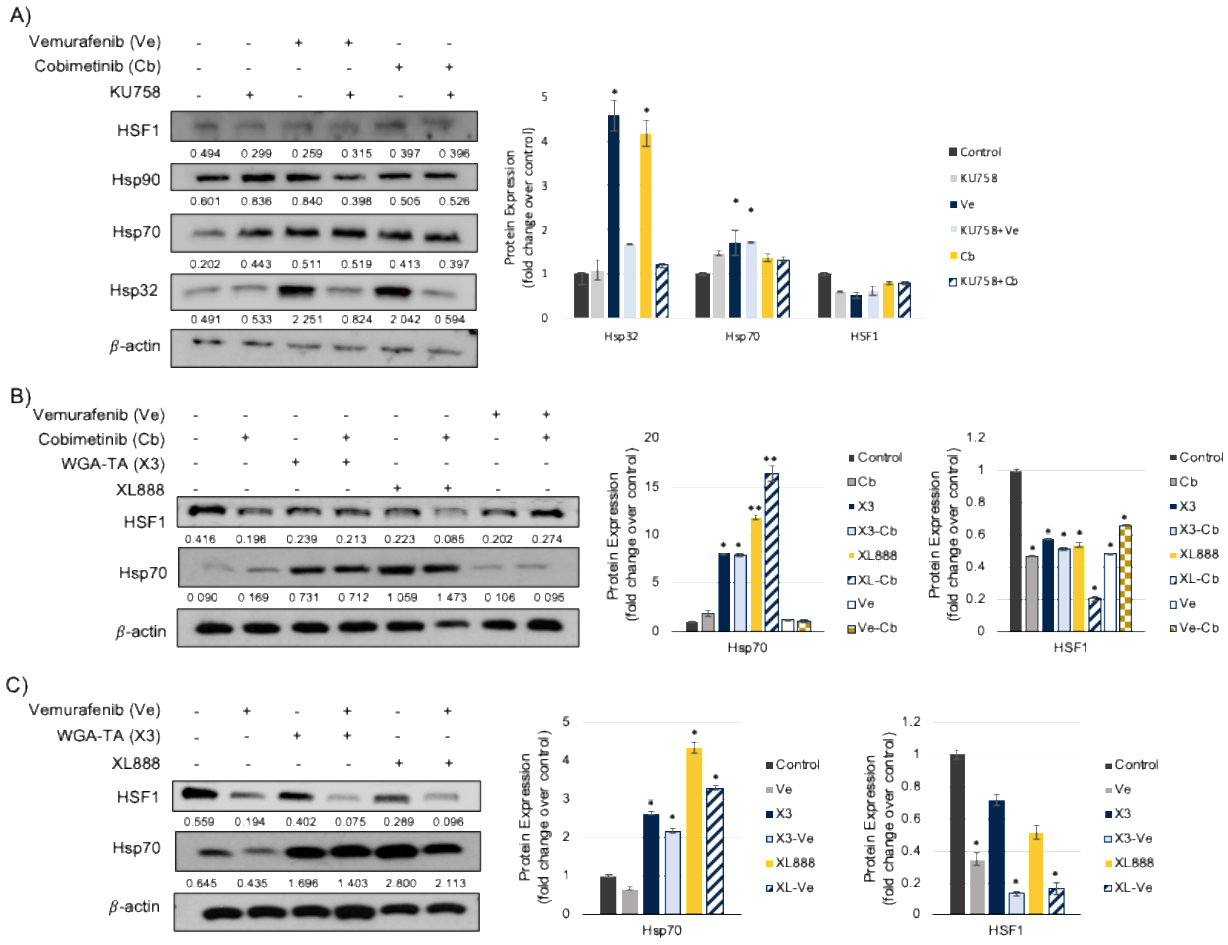

Figure 3-5 continued

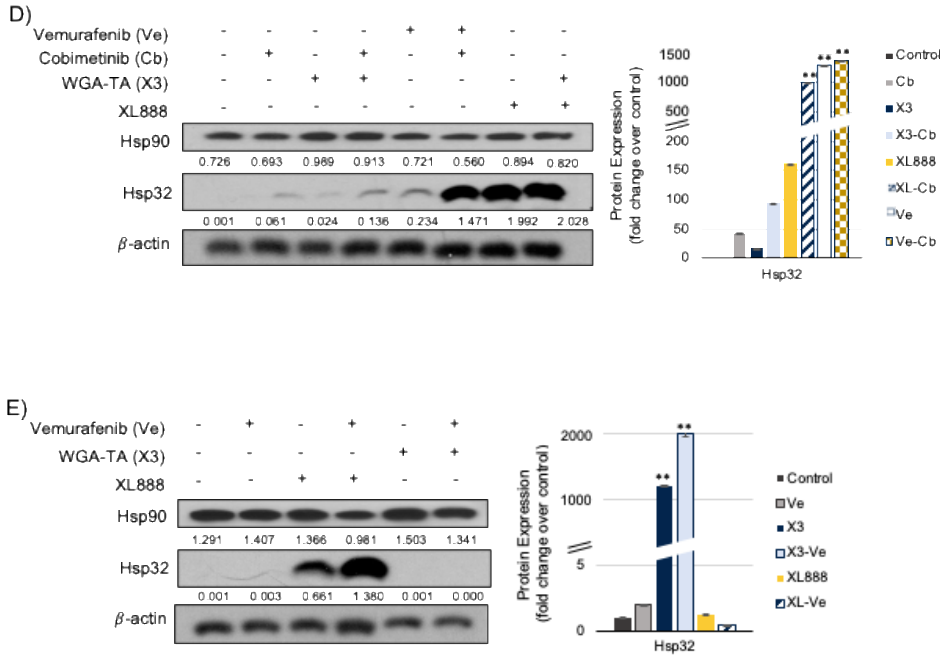

Abbreviations

BRAFi	BRAF inhibitor
Cb	cobimetinib
CI	combination index
CT-Hsp90i	C-terminal Hsp90i
FF	fetal fibroblasts
Hsp90i	Hsp90 inhibitor
IC_{50}	half-maximal inhibition concentration
MEKi	MEK inhibitor
NT-Hsp90i	N-terminal Hsp90i
PBS	phosphate buffer solution
Ve	vemurafenib
WGA-TA	withalongolide A 4,19,27-triacetate

References

1. Siegel RL, Miller KD and Jemal A. Cancer statistics, 2020. *CA Cancer J Clin* 2020;**70**(1): 7-30.
2. Sanchez JN, Wang T and Cohen MS. BRAF and MEK Inhibitors: Use and Resistance in BRAF-Mutated Cancers. *Drugs* 2018;**78**(5): 549-566.
3. Sharma P, Hu-Lieskovan S, Wargo JA and Ribas A. Primary, Adaptive, and Acquired Resistance to Cancer Immunotherapy. *Cell* 2017;**168**(4): 707-723.
4. Bayat Mokhtari R, Homayouni TS, Baluch N, Morgatskaya E, Kumar S, Das B*, et al.* Combination therapy in combating cancer. *Oncotarget* 2017;**8**(23): 38022-38043.
5. Eggermont AMM, Crittenden M and Wargo J. Combination Immunotherapy Development in Melanoma. *Am Soc Clin Oncol Educ Book* 2018;**38**(197-207.
6. Ritossa FM. A new puffing pattern induced by temperature shock an DNP in Drosophila. *Experientia* 1962;**18**(571-573.
7. Ritossa FM. New puffs induced by temperature shock, DNP and salicilate in salivary chromosomes of D. melanogaster. *Drosophilia Information Service* 1963;**37**(122-123.
8. Ritossa FM. Experimental activation of specific loci in ploytene chromosomes of drosophila. *Exp Cell Res* 1964;**35**(601-607.
9. Csermely P, Schnaider T, Soti C, Prohaszka Z and Nardai G. The 90-kDa molecular chaperone family: structure, function, and clinical applications. A comprehensive review. *Pharmacol Ther* 1998;**79**(2): 129-168.
10. Whitesell L, Mimnaugh EG, De Costa B, Myers CE and Neckers LM. Inhibition of heat shock protein HSP90-pp60v-src heteroprotein complex formation by benzoquinone ansamycins: essential role for stress proteins in oncogenic transformation. *Proc Natl Acad Sci U S A* 1994;**91**(18): 8324-8328.
11. Hanahan D and Weinberg RA. Hallmarks of cancer: the next generation. *Cell* 2011;**144**(5): 646-674.
12. Hanahan D and Weinberg RA. The hallmarks of cancer. *Cell* 2000;**100**(1): 57-70.
13. Sanchez JN, Carter TR, Cohen MS and Blagg BS. Old and New Approaches to Target the Hsp90 Chaperone. *Curr Cancer Drug Targets* 2019, doi: 10.2174/1568009619666191202101330
14. Subramanian C, Kovatch KJ, Sim MW, Wang G, Prince ME, Carey TE*, et al.* Novel C-Terminal Heat Shock Protein 90 Inhibitors (KU711 and Ku757) Are Effective in Targeting Head and Neck Squamous Cell Carcinoma Cancer Stem cells. *Neoplasia* 2017;**19**(12): 1003-1011.
15. Subramanian C, Grogan PT, Wang T, Bazzill J, Zuo A, White PT*, et al.* Novel C-terminal heat shock protein 90 inhibitors target breast cancer stem cells and block migration, self-renewal, and epithelial-mesenchymal transition. *Mol Oncol* 2020, doi: 10.1002/1878-0261.12686
16. Wang T, Subramanian C, Blagg BSJ and Cohen MS. A novel heat shock protein 90 inhibitor potently targets adrenocortical carcinoma tumor suppression. *Surgery* 2020;**167**(1): 233-240.
17. Chou TC. Theoretical basis, experimental design, and computerized simulation of synergism and antagonism in drug combination studies. *Pharmacol Rev* 2006;**58**(3): 621-681.

18. Friedl P and Alexander S. Cancer invasion and the microenvironment: plasticity and reciprocity. *Cell* 2011;**147**(5): 992-1009.
19. Jaeger AM and Whitesell L. Hsp90: Enabler of Cancer Adaptation. *Annual Review of Cancer Biology* 2018;**3**(275-297.
20. Miyata Y, Nakamoto H and Neckers L. The therapeutic target Hsp90 and cancer hallmarks. *Curr Pharm Des* 2013;**19**(3): 347-365.
21. Danen EH, de Vries TJ, Morandini R, Ghanem GG, Ruiter DJ and van Muijen GN. E-cadherin expression in human melanoma. *Melanoma Res* 1996;**6**(2): 127-131.
22. Pecina-Slaus N. Tumor suppressor gene E-cadherin and its role in normal and malignant cells. *Cancer Cell Int* 2003;**3**(1): 17.

Chapter 4 : Summary and Perspectives

Summary and Significance

For this doctoral dissertation, I researched therapeutic resistance mechanisms in *BRAF*-mutant (*BRAF*+) melanoma through various preclinical *in vitro* studies that targeted the 90-kDa heat shock protein (Hsp90) molecular chaperone. Specifically, I tested the hypothesis that several resistance-promoting processes require Hsp90 function and, therefore, could be targeted with an Hsp90 inhibitor (Hsp90i) to simultaneously knockdown multiple resistance pathways and oncogenic processes. This body of work is significant because I investigated a unique therapeutic combination strategy utilizing a novel C-terminal Hsp90i (CT-Hsp90i) plus standard mitogen-activated protein kinase (MAPK) pathway inhibitors (MAPKi) targeted therapy in *BRAF*+ melanoma. Furthermore, using a CT-Hsp90i alone or in combination with MAPKi, I was able to target not only the key therapeutic resistance pathways in *BRAF*+ melanoma cell lines but also critical heat shock proteins (Hsps) involved in heat shock response (HSR) activation.

Since 2011, the FDA approved several effective small molecule MAPKi (e.g., BRAF/MEK inhibitors [BRAFi/MEKi]) in combination as a first-line treatment for unresectable late-stage *BRAF*+ melanoma. However, the lack of durability of these agents still pose a significant clinical limitation to their reliability [1]. Conversely, Hsp90 inhibition while not an FDA-approved therapy in melanoma, has been a therapeutic strategy supported by over 170 clinical trials completed, terminated, or in progress [2].

Moreover, from the 18 Hsp90 inhibitors in the clinical pipeline, nearly all are N-terminal Hsp90i (NT-Hsp90i). These inhibitors frequently require dose-escalation to maintain their therapeutic efficacy and result in dose-limiting toxicities (DTLs) likely in-part related to their activation of the HSR. For these reasons and limited chemotherapy options in advanced melanoma patients, there is a need for more durable targeted therapies. Optimization of current Hsp90i is a novel and rational approach to create transformative scientific and clinical advancements for unresectable late-stage *BRAF*+ melanoma patients. Taken together, this formed the cornerstone of my doctoral research studies.

First, I presented comprehensive insights on BRAFi/MEKi use and resistance not only in melanoma, but several other cancers driven by *BRAF*-mutations. Next, I discussed the current clinical pipeline of Hsp90 inhibitors, especially in oncology. I also outlined the rationale for isoform-selective inhibition and introduced Hsp90i development and use in other disease states. Finally, I demonstrated robust synergy of a novel CT-Hsp90i, KU758, in combination with BRAFi/MEKi (e.g., Ve/Cb) to target two resistance pathways effectively (e.g., MAPK/Erk and phosphatidylinositol 3-kinase (PI3K)/Akt), mitigate cell migration, and downregulate key Hsps involved in HSR activation (Error! Reference source not found.). Here, I also incorporate key published literature in the field to provide my final perspectives and recommendations for future work investigating therapeutic resistance in *BRAF*+ melanoma and rationale for advancing Hsp90i through the clinical pipeline and into approved therapeutic options for advanced melanoma patients.

Future Directions

While my experiments and research to-date have provided insights into a novel preclinical combination strategy in *BRAF*+ melanoma cell lines using a CT-Hsp90i, there remain several unanswered questions. What cellular pathways, outside of MAPK/Erk and PI3K/Akt, warrant further investigation in $BRAF_+$ melanoma? Why do CT-Hsp90i affect the cell differently than NT-Hsp90i? What pharmacokinetic (PK) and pharmacodynamic (PD) attributes of NT-Hsp90i are worth integrating into new Hsp90i? Why do NT-Hsp90i lead to several DTLs in patients, but not preclinically *in vivo*? What biomarkers report Hsp90 inhibition or toxicity accurately? Can CT-Hsp90i be used as a pharmacological tool to positively modulate the immune response? It is imperative to continue posing these questions, among others, and seeking out research-supported answers to contribute to the discovery and development of transformative achievements in this field. To be at the forefront of advancing the science and translatability of these novel molecules into the clinic, a better understanding of the genetic and epigenetic changes of these tumors and their key driving or resistant pathways is required. As such, incorporating precision medicine approaches and deep sequencing of these tumors will provide additional key data and guide *in vitro* and *in vivo* combination strategies, including those with immune checkpoint inhibitors (e.g., CTLA-4 and PD-1 inhibitors), and better translate more successful treatments into the clinic.

Understanding PK and PD profiles of CT-Hsp90i to optimize therapeutic use

Regardless of there being nearly 200 clinical trials that test Hsp90i in humans, significant strides are needed for these small molecule inhibitors to receive FDA approval

[2]. For example, it is recognized by many in the cancer field that Hsp90 is a rationale drug target to simultaneously select for multiple signaling pathways [3-5]. Still, toxicity profiles of these drug candidates in clinical trial participants remain too high to allow progression of these drugs through FDA approval and commercialization [6,7]. In Chapter 2 of this dissertation, I elaborate more on this point. I reviewed the clinical landscape of Hsp90i to give a well-informed perspective on why these compounds have been so challenging to achieve FDA approval to-date – most notably, DTLs resulting from the inherent PD (e.g., selectivity) of these small molecule inhibitors in the clinical pipeline [8,9].

Currently, 94% of Hsp90i in clinical trials competitively bind at the N-terminal ATP-binding site of the chaperone and are pan-inhibitors of the heterochaperone complex [2]. Additionally, they are not selective for a particular Hsp90 isoform. The non-selective nature of NT-Hsp90i may contribute to their toxicity because they inhibit the function of all four Hsp90 isoforms (e.g., Hsp90α, Hsp90β, Grp94, and TRAP1) in essential compartments throughout the cell (e.g., cytoplasm, endoplasmic reticulum, and mitochondria) [2]. Fortunately, medicinal chemistry and related drug discovery efforts by our collaboration with Dr. Brian S.J. Blagg have allowed for the optimization of the Hsp90 inhibition to selectively target specific isoforms of the molecular chaperone [2,9]. Several groups, including ours, are actively improving the PD of Hsp90i to have more isoform-selectivity, as mentioned above, to mitigate off-target effects. Chapter 2 covered a full review of these advancements. Despite the effort for improvement, it will be critical to characterize a full PK profile of these compounds, especially for CT-Hsp90i, like KU758,

and identify more specific PD biomarkers of Hsp90 inhibition to be able to better track toxicity and effectiveness of inhibition clinically.

In vivo model to examine PK of CT-Hsp90i

I propose for the future to translate my *in vitro* studies presented in this work, specifically in Chapter 3, into an *in vivo* mouse model to provide valuable PK/PD insights of the CT-Hsp90i KU758. After characterizing the KU758 PK profile, comparing it with the PK/PD profiles of an NT-Hsp90i, such as XL888, will be critical to providing essential evidence of similarities and discrepancies between the two types of inhibitors. This analysis could unveil insights into drug metabolism and how DLTs develop with NT-Hsp90i compared to CT-Hsp90i or isoform-selective Hsp90i.

The current understanding is that CT-Hsp90i may have several favorable biological effects over NT-Hsp90i. For example, a study from our lab showed promising *in vivo* effects of two CT-Hsp90i, KU711 and KU757, in a head and neck squamous cell carcinoma (HNSCC) model compared to an NT-Hsp90i [10]. In this study, using a HNSCC buccal orthotopic xenograft model with MDA-1986 cells, our lab demonstrated a decrease in tumor volume, prolonged survival, and no significant changes to body weight in CT-Hsp90i treated mice compared to an NT-Hsp90i (17-N-allylamino-17-demethoxy-geldanamycin; 17-AAG) or controls. Additionally, histopathology evaluation of the liver, kidney, and proliferation marker, Ki67, showed an improved toxicity profile (e.g., less toxicity) with CT-Hsp90i treatment compared to untreated controls or 17-AAG. Together, this data highlights the beneficial potential CT-Hsp90i, like KU758, over NT-Hsp90i, warranting additional translational preclinical investigation and development.

In a similar manner, I hypothesize that CT-Hsp90i therapy with a drug like KU758 in a *BRAF*+ melanoma orthotopic xenograft mouse model would demonstrate improved efficacy *in vivo* for three key reasons. First, KU758 shares its core chemical structure with KU711 and KU757; as all three compounds are novobiocin core analogs [2,10]. For the development of these KU-compounds, researchers maintained biologically active components of the novobiocin core while altering minimal structural elements, such as (thio)urea and side chain components, to build a library of similar analog compounds and optimize their pharmacological effect [10,11]. Second, *in vitro* biological effects of CT-Hsp90i, such as decreased cancer cell migration and reduced expression of HSR-related proteins, remain reproducible across various cancer models [12,13]. Collectively these *in vitro* findings and others underscore that similar CT-Hsp90i (KU711, 757, 758, etc.) effectively target the same biological pathways, and therefore, provides a basis for expecting relatively similar phenotypic effects to result in an *in vivo* model. Lastly, KU758 decreased tumor size and showed no toxicity in a triple-negative breast cancer orthotopic xenograft, which supports *in vivo* safety in a murine model [12].

Despite their potential, several gaps still exist in our knowledge of CT-Hsp90i that will need to be addressed prior to further clinical development. Future studies must take a more in-depth look into the *in vivo* effects of these inhibitors, beyond just improved animal survival and histopathology surrogates of toxicity. For example, in addition to the outcomes measured above in KU711 or KU757 treated HNSCC, in Subramanian *et al.*, determining clinically relevant PK will be necessary to assess the therapeutic effect, half-life, and optimal dosing to maximize efficacy and avoid toxicity in a *BRAF*+ melanoma *in vivo* model.

A comprehensive *in vivo* study should not only investigate KU758 as a monotherapy but also in combination with BRAFi/MEKi, such as vemurafenib (Ve) and cobimetinib (Cb), respectively. The results from Chapter 3 showed that KU758 synergizes with both Ve and Cb. These combinations had more favorable effects on targeting resistance pathways and mitigating cell migration than each compound alone. I would expect this same synergy to translate in an *in vivo* model, and for the combination treatments to be advantageous over single-agent intervention. Finally, an *in vivo* efficacy investigation will compare findings of KU758 and KU758+BRAFi/MEKi treated mice to XL888 and XL888+BRAFi/MEKi treated animals to demonstrate if the CT-Hsp90i has efficacy and toxicity benefits over the NT-Hsp90i.

Various studies, both preclinical and clinical, tested an NT-Hsp90i (e.g., XL888 or AT13387) in combination with BRAFi/MEKi in *BRAF*+ melanoma (ClinicalTrials.gov NCT01657591; NCT02721459) [14-16]. In preclinical studies, the emergence of therapeutic resistance *in vitro* and *in vivo* to BRAFi/MEKi was circumvented and delayed by introducing an NT-Hsp90i. These data support the rationale for combined targeted therapy of Hsp90i+BRAFi/MEKi in *BRAF*+ melanoma and continuation of Chapter 3 findings. Interestingly, a Phase I trial reported therapeutic activity of XL888+Ve in *BRAF*+ melanoma treatment-naïve patients with tolerable side-effects and few grade 3/4 toxicities (ClinicalTrials.gov NCT01657591). The results of this Phase I trial further support that Hsp90 inhibition is a rational anti-cancer therapeutic strategy in melanoma that would be enhanced further with a lower toxicity profile. Despite meeting the primary endpoints (e.g., identify the maximum tolerated dose (MTD) and recommended Phase II dose (RP2D)), the researchers and clinicians of the study recommended further investigation of

Hsp90i+BRAFi, especially with a MEKi. The same research group completed a Phase I study investigating XL888+Ve+Cb in October 2019, with the final results still to be reported (ClinicalTrials.gov NCT02721459). Hsp90i+BRAFi/MEKi remains a rationale anti-cancer therapeutic approach with an opportunity to continue the development of CT-Hsp90i, such as KU758, to decrease off-target effects leading to potential DTLs. In the following section, I will propose and discuss ways to address and improve this shortcoming in the context of PD.

Hsp90 inhibition and PD biomarkers

Since the discovery of geldanamycin as an inhibitor of Hsp90, there were significant advancements in the field to circumvent off-target effects, most notably and recently being the development of domain-specific and isoform-selective inhibitors. As mentioned in the previous section and Chapter 2, pan-inhibitors of the molecular chaperone can and often lead to DTLs in the clinic [2]. We understand that DTLs here likely resulted from the dose-escalation observed in these trials that was required to maintain therapeutic efficacy [17-19]. In the future, it will be critical to achieve durable therapeutic levels of an Hsp90i that have low or limited toxicity profiles for it to receive FDA approval. Biomarkers are vital tools used to measure not only a drug's biological response(s) and activity but also its selectivity [20]. Related to their utility in Hsp90 inhibition, there is a need to improve current biomarkers to provide more accurate on-target reporting of this inhibition *in vivo* and in patients.

First, it is critical to consider and evaluate the biomarkers used in preclinical research and clinical trials. An accepted and relevant biological signature of effective Hsp90 inhibition is the increased expression of 70-kDa heat shock protein (Hsp70), an

Hsp90 co-chaperone, and decreased expression of select Hsp90 client proteins [21]. A practical preclinical example of this biomarker reporting is in Chapter 3, where I immunoblotted for Hsp70 and Hsp32 and showed no upregulation of HSR-related proteins in KU758-treated (e.g., alone or in combination with BRAFi/MEKi) cells compared to cells treated with XL888 or WGA-TA which demonstrated a more robust HSR. Additionally, I demonstrated Hsp90 client protein knockdown in key resistance pathways (e.g., MAPK/Erk and PI3K/Akt) with both CT- and NT-Hsp90i.

In clinical trials, the Hsp70 expression profile remains the gold standard for PD analysis of Hsp90 inhibition [9]. For example, peripheral blood mononuclear cells (PBMCs) are collected from patients and analyzed for changes in Hsp70 expression [22]. A caveat of using Hsp70 expression levels as a biomarker of effective Hsp90 inhibition is that the increase of Hsp70 expression is also indirectly indicative of Hsp90i toxicity. Hsp70 has an essential cytoprotective role within cells, especially malignant ones [23]. An increase in Hsp70 expression following Hsp90i administration is often accompanied by an increased dose of the Hsp90i to reach therapeutic efficacy and contributing to DLTs [9]. In this scenario, while an increase in Hsp70 expression does denote effective Hsp90 inhibition, it also exemplifies its role to protect the cancer cell from the cytotoxic effects of that Hsp90 inhibition. Therefore, an increase of Hsp70 expression is often used as a surrogate to indicate toxicities. This limitation prompts us with a pivotal opportunity to identify more useful and accurate biomarkers that indicate Hsp90 inhibition or predict Hsp90i toxicity.

Before identifying ways to optimize biomarker reporting of Hsp90 inhibition, it is crucial to understand why studies thus far have used Hsp70 expression to measure

Hsp90i activity. In the cytoplasm, Hsp90 is transiently bound to heat shock factor 1 (HSF1), a stress-induced regulator of several Hsps, including Hsp90 and Hsp70 [24]. For example, Hsp expression levels increase in stressed cells, such as cells in a malignant state. The process HSF1 follows is not entirely defined, but broadly, HSF1 dissociates from Hsp90, becomes phosphorylated, and aggregates to form HSF1-trimers. The trimer translocates to the nucleus where it binds to its genetic regulatory element, heat shock element (HSE), resulting in increased expression of several Hsps – collectively referred to as HSR activation [25]. Additionally, Hsp90i binding to the molecular chaperone disrupts the Hsp90/HSF1 complex, such that HSF1 follows the same process noted above, leading to the upregulation of HSR-mediating Hsps. Therefore, an increase of Hsp70 expression correlates with effective Hsp90 inhibition [21,24].

Since HSF1 dissociation from Hsp90 leads to increased expression of more than one Hsp, not just Hsp90, this supports why a more accurate biomarker of molecular chaperone inhibition is needed. There are many steps between Hsp90 inhibition and increased HSR-activated Hsp expression. One important aspect of identifying a reliable biomarker for Hsp90 inhibition involves acquiring a better understanding of the immediate effects of Hsp90i that occur before the onset of the HSR. In Chapter 3, I demonstrated similar biological results in KU758 (CT-Hsp90i) and XL888 (NT-Hsp90i) treated cells, but with some nuances, especially a decreased induction of HSR in the former. I propose that future *in vivo* studies should take a more in-depth look into these differences, especially related to changes in Hsp90 client protein expression that occur early after exposure to an Hsp90i. Additionally, analyzing changes to protein-protein interactions could provide aid in refining novel Hsp90i biomarkers [26]. It will also be essential to distinguish

biomarkers that may be unique for NT-Hsp90i and CT-Hsp90i in the preclinical setting that are based mechanistically on differences between the two classes of inhibitors. This would be ideal to find as it would allow for better *in vivo* PK/PD and toxicity analysis.

Finally, while refining biomarker(s) of Hsp90 inhibition is a logical strategy, researchers could use an alternative approach to address increased Hsp70 expression as an indicator of toxicity. For example, by disrupting Hsp70's cytoprotective role, it could ultimately improve the utility of Hsp90i in humans, while maintaining Hsp70 as a biomarker solely for effective Hsp90 inhibition. The blockade of Hsp70 upregulation could aid in decreasing the need for dose-escalation of Hsp90i, and theoretically mitigate potential DTLs. Many groups have identified Hsp70 inhibition as a strategy to combat its cytoprotective role in the cell, but an obstacle that remains is avoiding off-target effects. As with any targeted therapeutic development, one important goal is to increase its specificity and decrease off-target effects. In a cancer model, Hsp70 blockade would need to be specific to malignant cells and not normal cells, as inhibiting Hsp70 in all cells could lead to numerous detrimental and toxic effects. Technical methods available to use to further investigate this biological effect of blocking Hsp70 expression in the setting of Hsp90 inhibition might include using pharmacological intervention (e.g., inhibitors of Hsp70), RNA interference (e.g., shRNA, siRNA), or other gene knockout and loss-of-function studies [27-31].

Exploiting a genetic approach to improve therapeutic strategies in BRAF+ melanoma

In Chapter 1 of this dissertation, I discussed the current clinical landscape and indication of BRAFi/MEKi use in *BRAF*+ malignancies. I also elaborated on primary (intrinsic) and secondary (acquired) resistance mechanisms many patients experience

when taking BRAFi/MEKi. For example, *BRAF*-wildtype (*BRAF*$_{WT}$) melanoma patients are intrinsically resistant to BRAFi because the inhibitors have a pharmacophore specific for the V600E codon in the mutated form of the protein [1]. Interestingly, it has been reported that several *BRAF*$_{WT}$ patients exhibited transactivation of the MAPK pathway when given a BRAFi [32]. Secondary resistance is more challenging to convey concisely since there are various modes of acquired resistance. One predominant mechanism of resistance to BRAFi is the upregulation of the PI3K/Akt pathway to compensate for the MAPK pathway blockade and provide an alternative mode for cell proliferation and growth. The *in vitro* work I presented in Chapter 3 takes a first step towards identifying if CT-Hsp90i can effectively overcome this resistance in *BRAF*$_{+}$ melanoma. In an *in vitro* model, I demonstrated that KU758 combinations with either a BRAFi or MEKi (e.g., KU758+Ve, KU758+Cb) targeted two key BRAFi resistance pathways effectively. Future studies should investigate the downstream effect of KU758 combinations on these pathways; MAPK/Erk and PI3K/Akt pathways. Additionally, a more clinically relevant *in vivo* model should be created by transplanting patient-derived tumor cells from BRAFi/MEKi-resistant melanoma patients into immunodeficient mice (e.g., patient-derived xenograft [PDX] model) and then treating these drug-resistant PDX tumors with KU758+Ve or KU758+Cb or KU758+Ve+Cb to evaluate the efficacy of inhibitor combinations to mitigate and overcome this drug resistance.

While the *in vivo* studies mentioned above will need to be completed to better understand the translational application of CT-Hsp90i with BRAFi/MEKi, there is also an opportunity to take a more pointed approach to target and overcome resistance pathways/processes. In the following subsection, I will present recommendations to

continue this body of work utilizing precision medicine tools that harness patient-specific genomic data and analyses. Specifically, I will discuss genetic analysis of melanoma tumors in The Cancer Genome Atlas (TCGA) program and how these data could complement, and advance results noted from Chapter 3.

TCGA perspective and analysis

TCGA is a 12-year genomic-based initiative sponsored by the National Cancer Institute (NCI) aimed to enhance our understanding of 33 different types of malignancies, improve drug discovery, and transform the clinical management of several malignancies and diseases [33,34]. The data generated provides insights into the molecular basis of cancer, refined tumor subtype classification, and novel therapeutic targets. Additionally, the NCI offers various computational tools for researchers to revisit, visualize, and analyze the genomic data collected. For melanomas specifically, tumor and biological samples were collected and analyzed from 470 patients [35].

In the context of this dissertation, I was interested in identifying which genes were altered most in *BRAF*+ melanoma patients to refine my mechanistic approach and provide a rational genetic approach to continue my work from Chapter 3. It is important to note that there are three other genomic classifications (*RAS*-mutant*, NF1*-mutant*,* and triple wild-type) of cutaneous melanoma [36]. However, for this body of work and future recommendations, I will focus on the *BRAF*+ signature. To determine gene changes, I utilized a next-generation clustered heatmap (NG-CHM) of the TCGA skin cutaneous melanoma (TCGA-SKCM) data via The Cancer Proteome Atlas portal [37]. The NG-CHM illustrated increases/decreases of messenger RNA (mRNA) expression of 3,520 genes in 470 patients, organized into rows and columns, respectively (Error! Reference source

not found.). The NG-CHM categorized rows into three groups based on gene variability within melanoma and clustered columns into four groups hierarchically. For supplemental analysis, I utilized the TCGA – cBioPortal for Cancer Genomics [38].

The TCGA-SCKM data showed that 52.2% of patients had a mutated form of the BRAF kinase, and of these individuals, 84.1% expressed the V600E codon (e.g., $BRAF_{V600E}$). The remaining 15.9% of patients expressed an alternative missense mutation or indel at codon 600 [37]. All missense mutations of *BRAF* caused copy number gain or amplification of the gene, which is a significant contributor to BRAFi-resistance [39]. See **Figure** 4-1 for the filter/search criteria of TCGA-SKCM patients.

Within the NCI Genomic Data Commons portal, it reports that 100% of patients received pharmacological therapy, but does not indicate which therapeutic agent(s) or if therapeutic resistance occurred [35]. Because of this omission on the portal=--, raw data was accessed to determine which late-stage $BRAF_{+}$ melanoma received BRAFi/MEKi treatment. The raw data reported the therapeutic agents received in only 57% of the total patient cohort (268/470 patients). Of the patients reported, 14 $BRAF_{+}$ patients received BRAFi/MEKi as a mono- or combination therapy, and therefore were relevant to the context of this dissertation (Error! Reference source not found.). Despite being only a small percentage of the entire cohort, analysis of these 14 patients will provide beginning insights into the $BRAF_{+}$ melanoma patient population. A caveat to this “snapshot” analysis is the need for a much larger patient cohort with this treatment regimen to ensure statistical power and translatability of findings noted in the cohort to treatment strategies. In the future, these studies could be performed, similar to the analysis here, once all therapeutic agent data is populated and integrated into the NCI data portal.

Next, I identified changes to mRNA expression in the cohort of 14 *BRAF*+ patient samples to distinguish which pathways and oncogenic processes might contribute to melanoma tumor-maintenance, especially therapeutic resistance. To filter through the 3,520 genes, I utilized the three NG-CHM pre-generated categories, illustrated as red, blue, and purple on the left-most side of the heat map next to the dendrogram **(**Error! Reference source not found.)**.** The heat map categorized each as highly variable (1,650 genes; red), cancer interesting gene (1,520 genes; blue), or a highly variable/cancer interesting (346 genes; purple). For all subsequent analysis, the cancer interesting gene subset was considered to eliminate variability in mRNA expression data amongst the 14 patients. I identified 132 cancer interesting genes that were also Hsp90 clients [40]. See **Figure** 4-1 for the filter/search criteria of TCGA-SKCM genes. Of note, several of these cancer interesting genes altered in the 14 *BRAF*+ patients were genes involved in DNA damage/repair pathways. The list of these genes includes ATM, BRCA1, BRCA2, FANCA, MRE11A, PCNA, and RAD52. Additionally, several genes involved in epigenetic mechanisms were also in the list of Hsp90 clients and cancer interesting genes. These included DNMT1, EZH2, HDAC6, KAT5, KDM2A, KDM4C, and SMYD3. See Error! Reference source not found. for complete list of 132 cancer interesting genes/Hsp90 clients from the TCGA-SKCM data. Upon further heatmap and quantitative analysis there were slight dissimilarities amongst the patient cohort, in terms of mRNA expression patterns (**Figure** 4-2). The quantified data plots the relative mRNA expression of each group of genes (e.g., DNA damage/repair or epigenetic modifier) for all 14 patients. The median values and interquartile ranges are displayed to account for outliers within the data. All values do not show any significant changes from baseline.

As mentioned above, the small cohort size of only 14 samples is a significant barrier to identifying translatable conclusions however even this small “snapshot” of data analysis provides some early insights into this melanoma patient population of interest. In order to better evaluate novel therapeutic and resistance-mitigating strategies the use of a larger data set, for example an extension of this 14-patient snapshot, will help to determine which genes are significantly changed amongst the patient population. The current mRNA expression quantification (**Figure** 4-2) of the DNA damage/repair and epigenetic modifier genes does not suggest any specific key players that contribute to resistance to BRAFi/MEKi. However, use of a larger dataset in conjunction with an additional analytical method, such as fixed gene set enrichment analysis, could identify biological pathways, processes, and networks implicated in these resistance mechanisms [41]. Not only would this provide added value and refinement to our understanding of BRAFi/MEKi resistance in melanoma patients, but also increase the significance of our findings. Ultimately, the aim of these genetic analyses would be to identify a key pathway or network that is highly dependent on Hsp90 function, therefore rendering it susceptible to Hsp90 inhibition by small molecules, like CT-Hsp90i.

The snapshot analysis above and in **Figure** 4-2 suggests that DNA damage/repair pathways and epigenetic mechanisms are key contributors to patients becoming refractory to targeted therapeutic interventions. Given that the altered proteins in these pathways are all clients of Hsp90 support the role that an Hsp90i could positively coordinate these processes towards mitigating or overcoming therapeutic resistance to BRAFi/MEKi. A recent study showed that suppression of two major DNA repair pathways enhances MAPK inhibitor efficacy in Ras pathway-driven melanomas [42]. Interestingly,

researchers utilized HDAC inhibitors (HDACi) to promote this biological effect. The use of HDACi in this context supports the rationale to simultaneously target multiple resistance/oncogenic processes. Future work in *BRAF*+ melanomas should continue to look at the biological effects, especially on DNA damage/repair and epigenetic mechanisms, of CT-Hsp90i, like KU758, alone and in combination with BRAFi/MEKi or possibly an HDACi. Using CT-Hsp90i as a pharmacological tool to identify these changes will determine if inhibiting chaperone function coordinately suppresses resistance-promoting pathways outside of the MAPK/Erk and PI3K/Akt pathways. This finding will be key in advancing our knowledge of more diverse underlying mechanisms of resistance to ultimately improve therapeutic strategies used to treat *BRAF*+ melanoma patients.

Hsp90 inhibition and immunomodulation

In 2011, the first fully humanized monoclonal antibody (mAb) that targeted an immune checkpoint receptor was approved by the FDA for use in melanoma patients. This mAb, ipilimumab (trade name Yervoy; Bristol Myers Squibb) binds to and inhibits cytotoxic T lymphocyte-associated antigen 4 (CTLA-4) resulting in activation of the immune response [43]. Over the past decade, additional CTLA-4 inhibitors were also FDA approved for use in melanoma and various other cancers. Alongside this clinical development, another immune checkpoint was utilized to target and activate the immune response – programmed cell death protein 1 (PD-1). Anti-PD-1 therapies (e.g., humanized mAb inhibitors of PD-1) of this T cell receptor, like pembrolizumab (trade name Keytruda; Merck) and nivolumab (Opdivo; Bristol Myers Squibb), were FDA approved in 2014 [43].

Together these immunotherapies resulted in break-through treatment options for melanoma patients, but similar to targeted therapies, like BRAFi/MEKi, therapeutic resistance often emerges. Fortunately, efforts have been taken to overcome this resistance by combining CTLA-4 and PD-1 inhibitors [44]. Still, on average, approximately only 50% of patients will achieve a significant response to therapy and eventually relapse within 2 years [45]. This clinical shortcoming highlights the opportunity for novel approaches to target resistance-promoting processes. Interestingly, a recent study showed the ability to overcome resistance to immunotherapies by targeting metabolism processes in melanoma cells [45]. Furthermore, this work by Imbert et al. further supports the rationale to target multiple cancer cell processes at once.

Hsp90 poses as an ideal anti-cancer target to positively modulate the immune response towards anti-cancer effects, especially when combined with immunotherapies. Several research groups, including ours, have initiated studies that evaluate the therapeutic potential of this combination approach. For example, CTLA-4 and PD-1 responses were enhanced via upregulation of a few *IFIT* genes in melanoma cells following Hsp90 inhibition [46]. Additionally, in an *in vitro* breast cancer model, our preliminary results showed that CT-Hsp90i and β-selective Hsp90i treated cells can decrease the secretion of pro-inflammatory cytokines suggesting the ability to overcome immunosuppressive effects. Lastly, our lab performed a pilot *in vivo* study evaluating the use of Hsp90i in combination with immunotherapy and showed benefit compared to untreated control. Taken together, these beginning insights support future work assessing the potential of Hsp90 in combination with immunotherapies to determine its clinical feasibility and translation into practice.

Overall Conclusions

Collectively, this dissertation demonstrates the utility of targeting the molecular chaperone, Hsp90, and MAPK-resistant pathways to improve preclinical therapeutic strategies for *BRAF*+ melanoma patients. The work presented here gives a detailed perspective of BRAFi/MEKi used in *BRAF*+ cancers, like melanoma and insights into a unique targeted approach to mitigate and/or overcome drug resistance in these malignancies. Specifically, I described the current preclinical and clinical pipelines of Hsp90i development for the treatment of various cancers, then evaluated original research investigating the efficacy of Hsp90i+MAKPi combinations (e.g., KU758+Ve; KU758+Cb) in *BRAF*+ melanoma cell lines. In these data, I showed that KU758 synergizes with a MAPKi and cooperatively targets resistance pathways/oncogenic processes while mitigating HSR induction. Taken together, targeting Hsp90, especially at the C-terminus, provides an alternative approach and added value to current melanoma therapies. Furthermore, from these findings, in addition to the genetic analysis, it is evident that Hsp90 serves as a central node in regulating several vital processes in melanoma cells. Future work will build upon this *in vitro* work to implement a combined pharmacologic and genetic approach along with key *in vivo* studies to distinguish a more precise mechanism by which Hsp90i elicit their key biologic effects in drug-resistant melanomas.

Abbreviations

17-AAG	17-N-allylamino-17-demethoxy-geldanamycin
$BRAF_{+}$	*BRAF*-mutant
BRAFi	BRAF inhibitor
$BRAF_{WT}$	BRAF-wildtype
Cb	cobimetinib
CT-Hsp90i	C-terminal Hsp90i
CTLA-4	cytotoxic T lymphocyte-associated antigen 4
DLT	dose-limiting toxicities
FDA	Food and Drug Administration
HNSCC	head and neck squamous cell carcinoma
HSE	heat shock element
HSF1	heat shock factor 1
Hsp	heat shock protein
Hsp70	70-kDa heat shock protein
Hsp90	90-kDa heat shock protein
Hsp90i	Hsp90 inhibitor
HSR	heat shock response
MAPK	mitogen-activated protein kinase
MEKi	MEK inhibitor
mAb	monoclonal antibody
mRNA	messenger RNA
MTD	maximum tolerated dose

NCI	National Cancer Institute
NG-CHM	next-generation clustered heatmap
NT-Hsp90i	N-terminal Hsp90i
PBMC	peripheral blood mononuclear cells
PD	pharmacodynamic
PD-1	programmed cell death protein 1
PDX	patient-derived xenograft
PI3K	phosphatidylinositol 3-kinase
PI3K	phosphatidylinositol 3-kinase
PK	pharmacokinetic
RP2D	recommended phase 2 dose
shRNA	short hairpin RNA
siRNA	small interfering RNA
SKCM	skin cutaneous melanoma
TCGA	The Cancer Genome Atlas
Ve	vemurafenib

Figures

Figure 4-1 Selection criteria for patients and genes of interest from TCGA-SKCM heatmap

The TCGA-SKCM heatmap displayed a total of 470 patients and 3,520 genes. A) Patients with transcriptome profiles were sorted based on the presence, or lack thereof, of an activating *BRAF* mutation (e.g., *BRAF*$_{+}$). 245 patients presented with *BRAF*$_{+}$ and 224 without (*BRAF*$_{WT}$). The subset of *BRAF*$_{+}$ patients were considered for further analysis. B) Genes were selected for based on Hsp90 clients and their variability within the study cohort. Gene variability was predetermined by the TCGA heatmap data as cancer interesting (1,520), highly variable (1,650), and a combination of both (346). Of the cancer interesting genes, 132 were also Hsp90 clients and used for further evaluation.

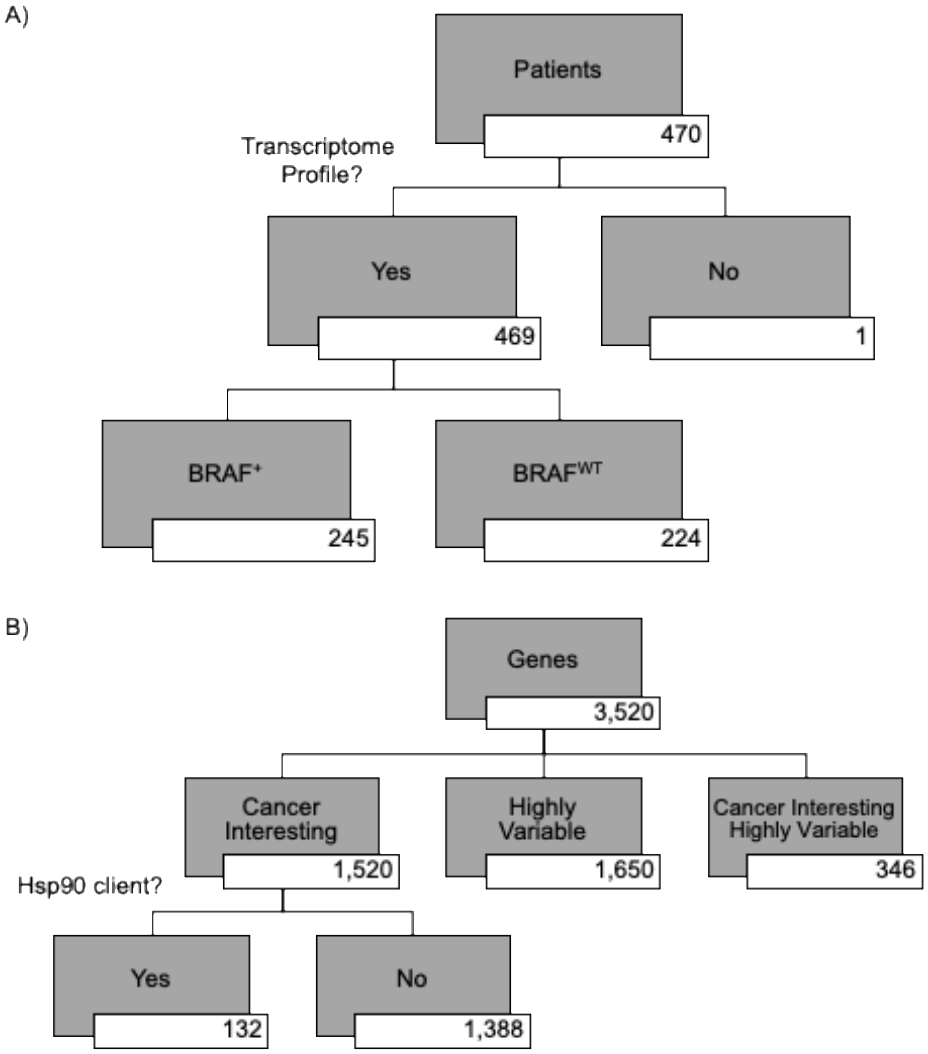

Figure 4-2 Heatmaps of mRNA expression in 14 BRAF+ Patients

Data from the TCGA-SKCM heatmap was used to refine analysis. A) Heatmap of mRNA expression for 132 genes (e.g., cancer interesting genes and Hsp90 clients) from *14 BRAF+* patients. B) DNA damage/repair pathways and C) epigenetic mechanisms genes sorted from larger mRNA heatmap. Both include quantitative analysis of the relative mRNA expression data for each set of genes. Values are presented as the median and interquartile ranges to account for outliers. Genes are depicted as columns and patients as rows for all heatmaps. Heatmaps are not clustered.

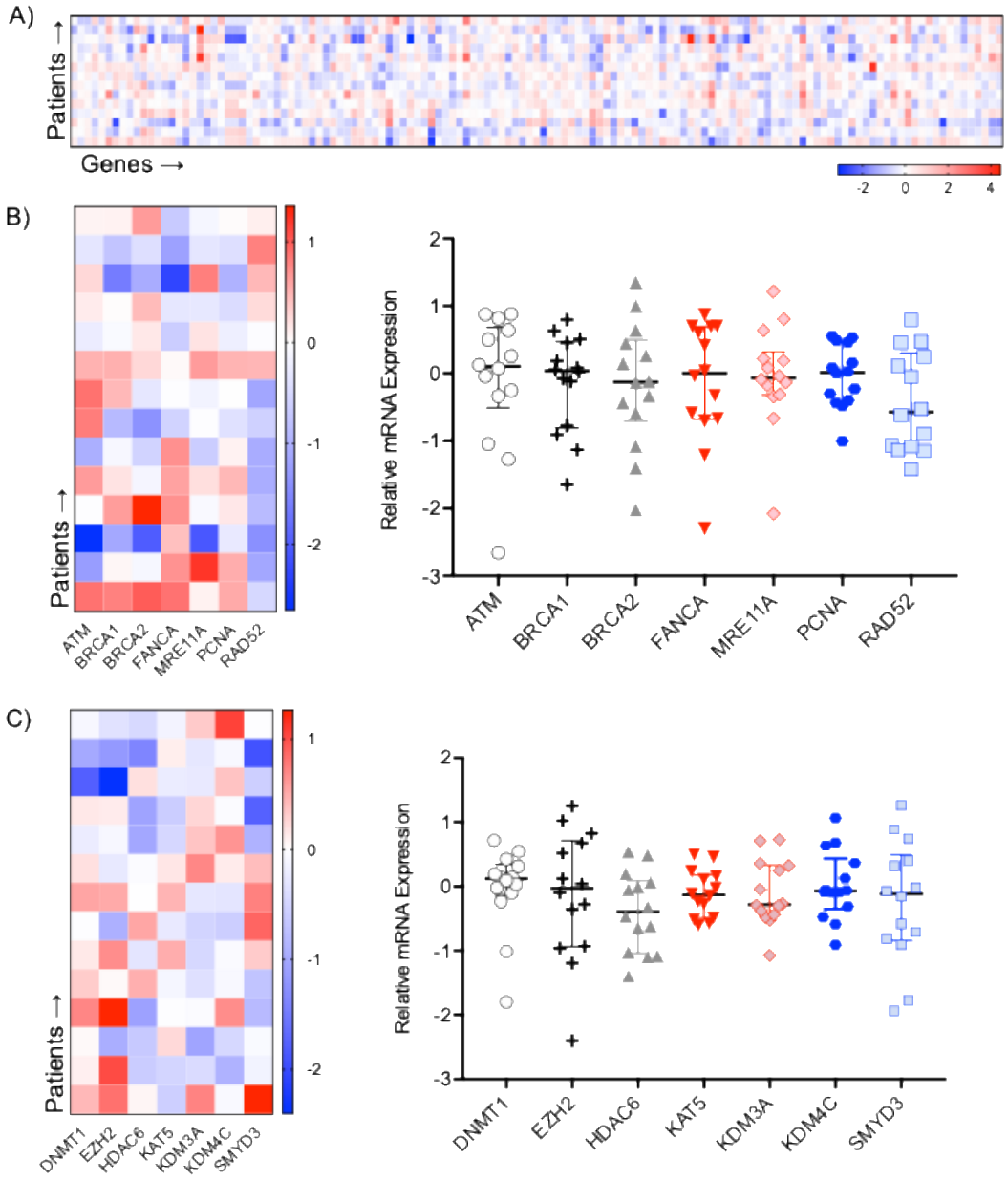

References

1. Sanchez JN, Wang T and Cohen MS. BRAF and MEK Inhibitors: Use and Resistance in BRAF-Mutated Cancers. *Drugs* 2018;**78**(5): 549-566.
2. Sanchez J, Carter TR, Cohen MS and Blagg BS. Old and New Approaches to Target the Hsp90 Chaperone. *Curr Cancer Drug Targets* 2019, doi: 10.2174/1568009619666191202101330
3. Jaeger AM and Whitesell L. Hsp90: Enabler of Cancer Adaptation. *Annual Review of Cancer Biology* 2018;**3**(275-297.
4. Miyata Y, Nakamoto H and Neckers L. The therapeutic target Hsp90 and cancer hallmarks. *Curr Pharm Des* 2013;**19**(3): 347-365.
5. Whitesell L and Lindquist SL. HSP90 and the chaperoning of cancer. *Nat Rev Cancer* 2005;**5**(10): 761-772.
6. Butler LM, Ferraldeschi R, Armstrong HK, Centenera MM and Workman P. Maximizing the Therapeutic Potential of HSP90 Inhibitors. *Mol Cancer Res* 2015;**13**(11): 1445-1451.
7. Kanamaru C, Yamada Y, Hayashi S, Matsushita T, Suda A, Nagayasu M*, et al.* Retinal toxicity induced by small-molecule Hsp90 inhibitors in beagle dogs. *J Toxicol Sci* 2014;**39**(1): 59-69.
8. Sanchez JN, Carter TR, Cohen MS and Blagg BS. Old and New Approaches to Target the Hsp90 Chaperone. *Curr Cancer Drug Targets* 2019, doi: 10.2174/1568009619666191202101330
9. Yuno A, Lee MJ, Lee S, Tomita Y, Rekhtman D, Moore B*, et al.* Clinical Evaluation and Biomarker Profiling of Hsp90 Inhibitors. *Methods Mol Biol* 2018;**1709**(423-441.
10. Subramanian C, Kovatch KJ, Sim MW, Wang G, Prince ME, Carey TE*, et al.* Novel C-Terminal Heat Shock Protein 90 Inhibitors (KU711 and Ku757) Are Effective in Targeting Head and Neck Squamous Cell Carcinoma Cancer Stem cells. *Neoplasia* 2017;**19**(12): 1003-1011.
11. Byrd KM, Subramanian C, Sanchez J, Motiwala HF, Liu W, Cohen MS*, et al.* Synthesis and Biological Evaluation of Novobiocin Core Analogues as Hsp90 Inhibitors. *Chemistry* 2016;**22**(20): 6921-6931.
12. Subramanian C, Grogan PT, Wang T, Bazzill J, Zuo A, White PT*, et al.* Novel C-terminal heat shock protein 90 inhibitors target breast cancer stem cells and block migration, self-renewal, and epithelial-mesenchymal transition. *Mol Oncol* 2020, doi: 10.1002/1878-0261.12686
13. White PT, Subramanian C, Zhu Q, Zhang H, Zhao H, Gallagher R*, et al.* Novel HSP90 inhibitors effectively target functions of thyroid cancer stem cell preventing migration and invasion. *Surgery* 2016;**159**(1): 142-151.
14. Eroglu Z, Chen YA, Gibney GT, Weber JS, Kudchadkar RR, Khushalani NI*, et al.* Combined BRAF and HSP90 Inhibition in Patients with Unresectable BRAF (V600E)-Mutant Melanoma. *Clin Cancer Res* 2018;**24**(22): 5516-5524.
15. Paraiso KH, Haarberg HE, Wood E, Rebecca VW, Chen YA, Xiang Y*, et al.* The HSP90 inhibitor XL888 overcomes BRAF inhibitor resistance mediated through diverse mechanisms. *Clin Cancer Res* 2012;**18**(9): 2502-2514.

16. Smyth T, Paraiso KHT, Hearn K, Rodriguez-Lopez AM, Munck JM, Haarberg HE*, et al.* Inhibition of HSP90 by AT13387 delays the emergence of resistance to BRAF inhibitors and overcomes resistance to dual BRAF and MEK inhibition in melanoma models. *Mol Cancer Ther* 2014;**13**(12): 2793-2804.
17. Cook N, Hansen AR, Siu LL and Abdul Razak AR. Early phase clinical trials to identify optimal dosing and safety. *Mol Oncol* 2015;**9**(5): 997-1007.
18. Iasonos A, Gönen M and Bosl GJ. Scientific Review of Phase I Protocols With Novel Dose-Escalation Designs: How Much Information Is Needed? *J Clin Oncol* 2015;**33**(19): 2221-2225.
19. Le Tourneau C, Lee JJ and Siu LL. Dose escalation methods in phase I cancer clinical trials. *J Natl Cancer Inst* 2009;**101**(10): 708-720.
20. Strimbu K and Tavel JA. What are biomarkers? *Curr Opin HIV AIDS* 2010;**5**(6): 463-466.
21. Banerji U, Walton M, Raynaud F, Grimshaw R, Kelland L, Valenti M*, et al.* Pharmacokinetic-pharmacodynamic relationships for the heat shock protein 90 molecular chaperone inhibitor 17-allylamino, 17-demethoxygeldanamycin in human ovarian cancer xenograft models. *Clin Cancer Res* 2005;**11**(19 Pt 1): 7023-7032.
22. Zhang H, Chung D, Yang YC, Neely L, Tsurumoto S, Fan J*, et al.* Identification of new biomarkers for clinical trials of Hsp90 inhibitors. *Mol Cancer Ther* 2006;**5**(5): 1256-1264.
23. Rérole AL, Jego G and Garrido C. Hsp70: anti-apoptotic and tumorigenic protein. *Methods Mol Biol* 2011;**787**(205-230.
24. Kijima T, Prince TL, Tigue ML, Yim KH, Schwartz H, Beebe K*, et al.* HSP90 inhibitors disrupt a transient HSP90-HSF1 interaction and identify a noncanonical model of HSP90-mediated HSF1 regulation. *Sci Rep* 2018;**8**(1): 6976.
25. Bagatell R, Paine-Murrieta GD, Taylor CW, Pulcini EJ, Akinaga S, Benjamin IJ*, et al.* Induction of a heat shock factor 1-dependent stress response alters the cytotoxic activity of hsp90-binding agents. *Clin Cancer Res* 2000;**6**(8): 3312-3318.
26. McDermott JE, Wang J, Mitchell H, Webb-Robertson BJ, Hafen R, Ramey J*, et al.* Challenges in Biomarker Discovery: Combining Expert Insights with Statistical Analysis of Complex Omics Data. *Expert Opin Med Diagn* 2013;**7**(1): 37-51.
27. Albakova Z, Armeev GA, Kanevskiy LM, Kovalenko EI and Sapozhnikov AM. HSP70 Multi-Functionality in Cancer. *Cells* 2020;**9**(3):
28. Behnsawy HM, Miyake H, Kusuda Y and Fujisawa M. Small interfering RNA targeting heat shock protein 70 enhances chemosensitivity in human bladder cancer cells. *Urol Oncol* 2013;**31**(6): 843-848.
29. Haley B and Roudnicky F. Functional Genomics for Cancer Drug Target Discovery. *Cancer Cell* 2020, doi: 10.1016/j.ccell.2020.04.006
30. Schlecht R, Scholz SR, Dahmen H, Wegener A, Sirrenberg C, Musil D*, et al.* Functional analysis of Hsp70 inhibitors. *PLoS One* 2013;**8**(11): e78443.
31. Yaglom JA, Wang Y, Li A, Li Z, Monti S, Alexandrov I*, et al.* Cancer cell responses to Hsp70 inhibitor JG-98: Comparison with Hsp90 inhibitors and finding synergistic drug combinations. *Sci Rep* 2018;**8**(1): 3010.

32. Poulikakos PI, Zhang C, Bollag G, Shokat KM and Rosen N. RAF inhibitors transactivate RAF dimers and ERK signalling in cells with wild-type BRAF. *Nature* 2010;**464**(7287): 427-430.
33. Hoadley KA, Yau C, Hinoue T, Wolf DM, Lazar AJ, Drill E*, et al.* Cell-of-Origin Patterns Dominate the Molecular Classification of 10,000 Tumors from 33 Types of Cancer. *Cell* 2018;**173**(2): 291-304.e296.
34. (2020). "The Cancer Genome Atlas Program." Retrieved June, 2020, from https://www.cancer.gov/about-nci/organization/ccg/research/structural-genomics/tcga.
35. (2020). "Genomic Data Commons Portal." Retrieved June, 2020, from https://portal.gdc.cancer.gov/.
36. Genomic Classification of Cutaneous Melanoma. *Cell* 2015;**161**(7): 1681-1696.
37. (2020). "The Cancer Proteome Atlas Portal." Retrieved June, 2020, from http://tcga.ngchm.net/.
38. (2020). "cBioPortal for Cancer Genomics." Retrieved June, 2020, from www.cbioportal.org; .
39. Stagni C, Zamuner C, Elefanti L, Zanin T, Bianco PD, Sommariva A*, et al.* BRAF Gene Copy Number and Mutant Allele Frequency Correlate with Time to Progression in Metastatic Melanoma Patients Treated with MAPK Inhibitors. *Mol Cancer Ther* 2018;**17**(6): 1332-1340.
40. Picard D. (2020). "Hsp90 Interactors." Retrieved June, 2020, from https://www.picard.ch/downloads/Hsp90interactors.pdf.
41. Creixell P, Reimand J, Haider S, Wu G, Shibata T, Vazquez M*, et al.* Pathway and network analysis of cancer genomes. *Nat Methods* 2015;**12**(7): 615-621.
42. Maertens O, Kuzmickas R, Manchester HE, Emerson CE, Gavin AG, Guild CJ*, et al.* MAPK Pathway Suppression Unmasks Latent DNA Repair Defects and Confers a Chemical Synthetic Vulnerability in BRAF-, NRAS-, and NF1-Mutant Melanomas. *Cancer Discov* 2019;**9**(4): 526-545.
43. Pardoll DM. The blockade of immune checkpoints in cancer immunotherapy. *Nat Rev Cancer* 2012;**12**(4): 252-264.
44. Chae YK, Arya A, Iams W, Cruz MR, Chandra S, Choi J*, et al.* Current landscape and future of dual anti-CTLA4 and PD-1/PD-L1 blockade immunotherapy in cancer; lessons learned from clinical trials with melanoma and non-small cell lung cancer (NSCLC). *J Immunother Cancer* 2018;**6**(1): 39.
45. Imbert C, Montfort A, Fraisse M, Marcheteau E, Gilhodes J, Martin E*, et al.* Resistance of melanoma to immune checkpoint inhibitors is overcome by targeting the sphingosine kinase-1. *Nat Commun* 2020;**11**(1): 437.
46. Mbofung RM, McKenzie JA, Malu S, Zhang M, Peng W, Liu C*, et al.* HSP90 inhibition enhances cancer immunotherapy by upregulating interferon response genes. *Nat Commun* 2017;**8**(1): 451.

Appendices

Figure A-1

Dose-response curves of each Hsp90i in FF cells are shown with corresponding 24 hrs IC_{50} values tabulated in micromolar concentrations.

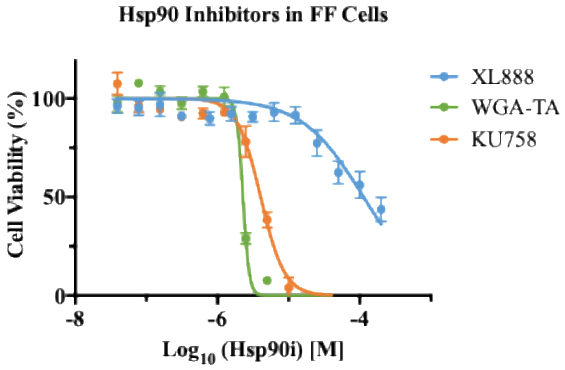

	IC50 (μM)
XL888	113.3
KU758	4.05
WGA-TA	2.28

Figure A-2

The combination effect of Hsp90 inhibitor combinations in UACC-62. Ve+Cb combination (FDA approved) is shown for comparison.

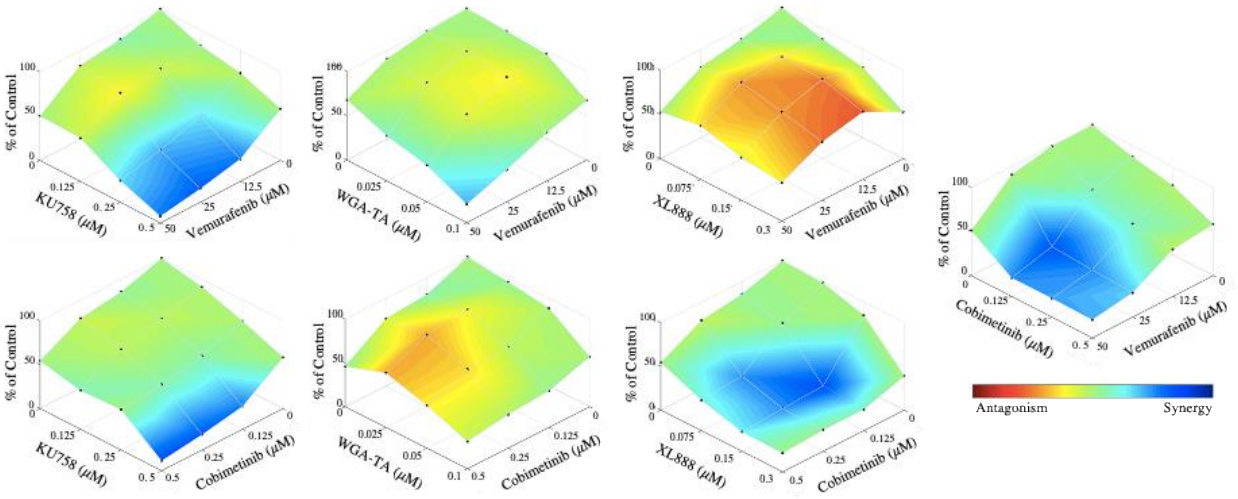

Figure A-3

The CI values are listed for each inhibitor combination treatment in UACC-62 between (A) Hsp90i and MAPKi, as well as (B) Ve+Cb. Synergistic combination boxes are colored according to relative CI value: CI value < 0.5 (blue), 0.5 < CI value < 1.0 (green).

A)

		KU758			WGA-TA			XL888		
	(μM)	**0.125**	**0.25**	**0.5**	**0.025**	**0.5**	**0.1**	**0.075**	**0.15**	**0.3**
Ve	**12.5**	1.445	0.428	0.291	116.814	0.353	0.070	8.166	7.199	2.580
	25	1.452	0.340	0.262	1.636	0.181	0.045	5.645	2.136	1.732
	50	0.815	0.248	0.185	0.231	0.074	0.037	0.725	0.536	0.757
Cb	**0.125**	1.166	0.735	0.315	1.198	1.557	1.701	0.895	0.236	0.342
	0.25	1.014	0.717	0.235	0.994	1.341	1.514	0.362	0.282	0.410
	0.5	0.723	0.883	0.202	0.887	1.063	1.326	0.522	0.364	0.471

B)

		Cb		
	(μM)	**0.125**	**0.25**	**0.5**
Ve	**12.5**	0.447	0.460	0.757
	25	0.086	0.152	0.272
	50	0.048	0.098	0.188

Figure A-4

Scratch and Boyden chamber assays in UACC-62. A) KU758 inhibitor combinations decreased cell migration (red lines indicate scratched cell-free area). B) quantification of the percent of cell migration at 24 hours after Hsp90i and MAPKi combinations. p values are recorded as significance between t = 0 and 24 hrs. C) The number of migrated cells after inhibitor single-agent and combination treatments.

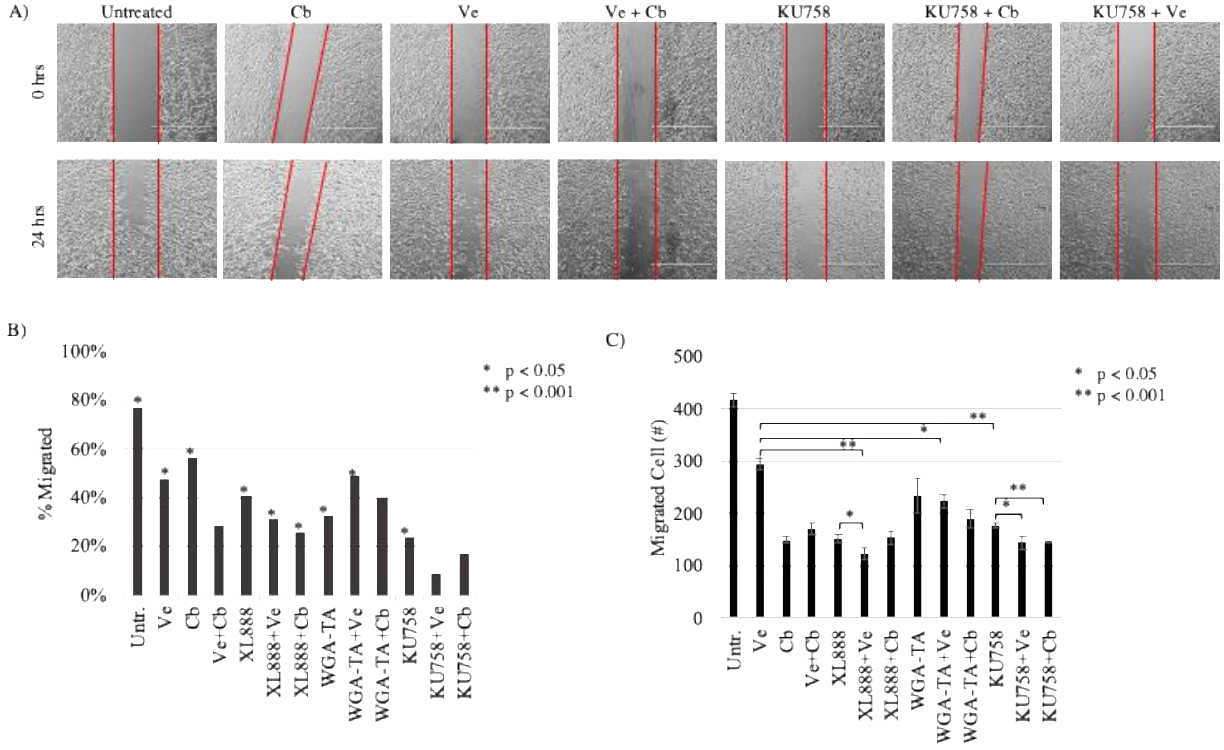

Figure A-5

Schematic of MAPK/Erk and PI3K/Akt pathways targeted by CT-Hsp90i. First-line BRAFi/MEKi are listed.

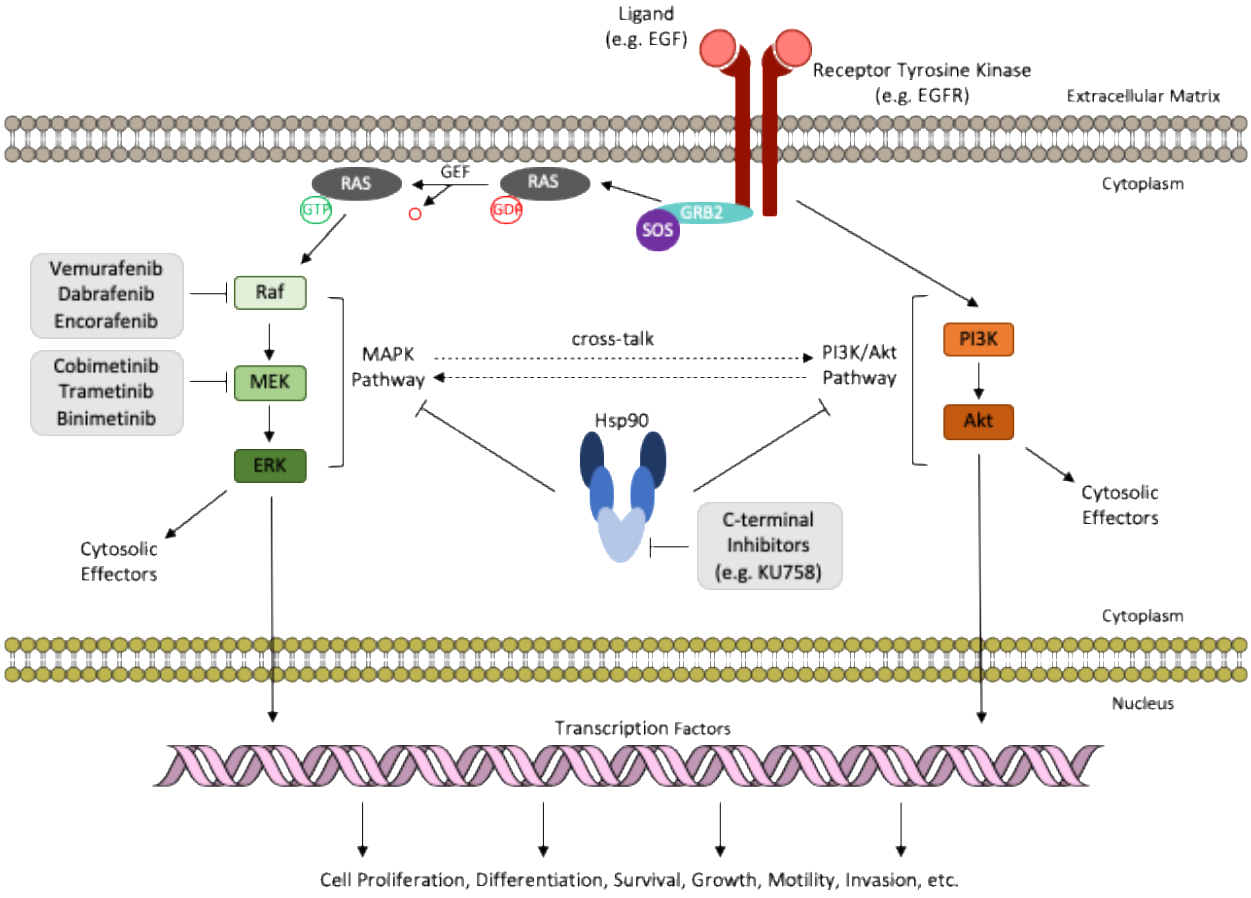

Figure A-6

mRNA expression data of melanoma patients accessed from TCGA-SKCM. Patient data was aggregated into four clusters in a hierarchical manner (columns) and genes into one of three categories (rows). Genes were defined as a cancer interesting gene, highly variable, or highly variable cancer interesting gene (e.g., left most column next to dendrogram illustrated as blue, red, or purple, respectively). Changes to RNA expression levels in melanoma patients are colored based on a matrix distribution of red to blue. Legend for all classifications shown at the bottom of the heatmap.

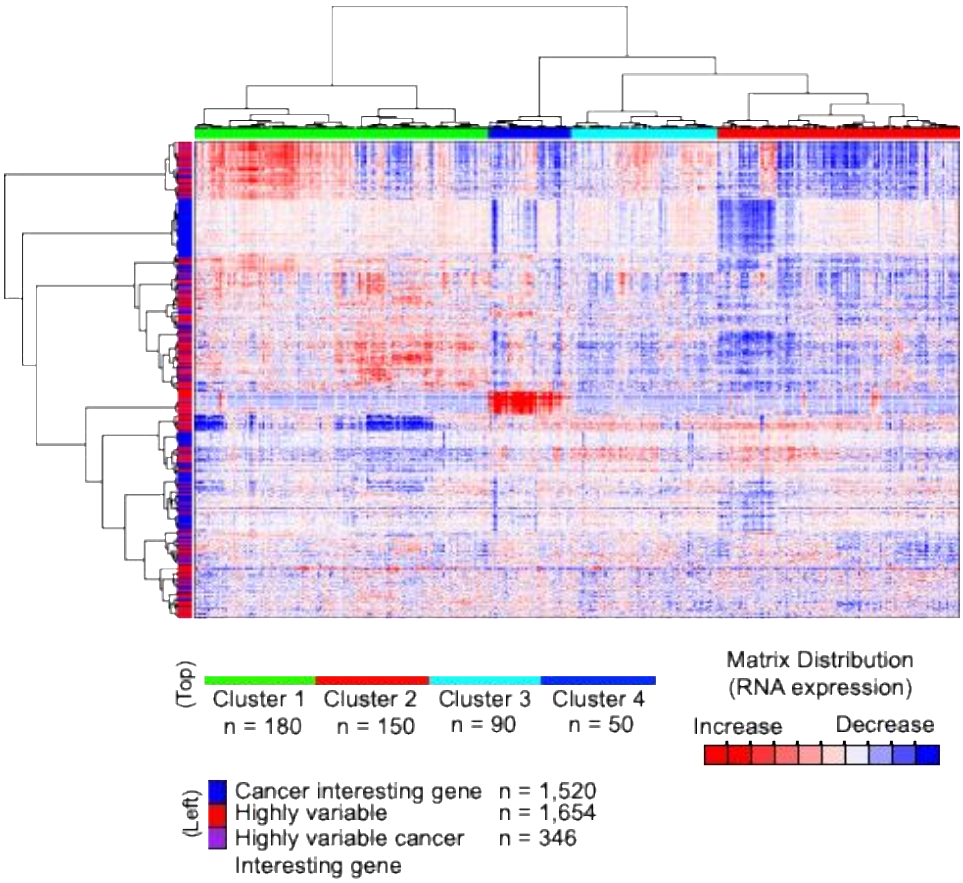

Table A-1

14 patients sorted from the NCI TCGA-SKCM heatmap data. Inclusion criteria: $BRAF_+$ signature and data available for therapeutic agent(s) used. Data does not include treatment regimen.

Patient Identifier	Therapeutic Agent(s)
TCGA-GN-A9SD-06A-11R-A40A-07	Vemurafenib
TCGA-EE-A29T-06A-11R-A18T-07	Vemurafenib
TCGA-WE-A8ZQ-06A-41R-A37K-07	Vemurafenib; dabrafenib
TCGA-WE-A8K6-06A-11R-A37K-07	Vemurafenib
TCGA-DA-A3F5-06A-11R-A20F-07	Vemurafenib
TCGA-EE-A2GS-06A-12R-A18S-07	Vemurafenib; dabrafenib
TCGA-WE-A8ZR-06A-11R-A37K-07	Vemurafenib
TCGA-EE-A29H-06A-12R-A18S-07	Vemurafenib
TCGA-EE-A29C-06A-21R-A18S-07	Dabrafenib
TCGA-FR-A728-01A-11R-A32P-07	Dabrafenib; trametinib
TCGA-ER-A2NG-06A-11R-A18T-07	Vemurafenib
TCGA-WE-AAA4-06A-12R-A38C-07	Vemurafenib; dabrafenib
TCGA-GN-A4U7-06A-21R-A32P-07	Vemurafenib
TCGA-EE-A3AD-06A-11R-A18S-07	BRAF inhibitor

Table A-2

132 genes sorted from the NCI TCGA-SKCM heatmap data. Inclusion criteria: cancer interesting gene and Hsp90 client. Genes listed in alphabetical order.

Gene Symbol			
ACVR1B	DYRK1B	LYN	RAD52
AKT1	EIF2AK2	MAFG	RAF1
AKT2	EML4	MAP2K5	REST
APAF1	EPHA1	MAP3K6	RET
ARAF	ERBB2	MAP4K2	RHOBTB1
ATF3	ERBB4	MAPK6	ROR2
ATM	ERG	MAPK7	RPS6KA1
AXIN1	EZH2	MATK	SIRT1
BCL2	FANCA	MAX	SKP2
BCL6	FBXW7	MDM2	SMYD3
BID	FES	MDM4	SRC
BLM	FGFR4	MIF	STAT3
BRAF	FGR	MLLT3	STAT5A
BRCA1	FLT3	MRE11A	STAT5B
BRCA2	FNIP1	MTA1	STK38L
BRMS1	FOXM1	MTOR	TBX22
BTK	FYN	MUC1	TGFB1
BTRC	GSK3B	MYC	TGFBR1
CAMK2B	HCK	NFIC	TIE1
CAMK2D	HDAC6	NOD1	TIMP2
CAMKK2	HMGA1	NOTCH1	TNFAIP3
CASP8	HMGCR	NTRK1	TP53
CDC25A	IRAK2	PCNA	TP53BP2
CDC25C	JAK1	PDGFB	TP53INP1
CDK1	KAT5	PDGFRB	TP53RK
CDK11B	KDM3A	PIM1	TPR
CDK4	KDM4C	PIM2	TRIM37
CSNK1A1	KEAP1	PIM3	TSG101
CUL1	KSR1	PKM2	TYRO3
CUL4B	LATS1	PLK1	VHL
DAPK1	LATS2	PPARG	WT1
DNMT1	LGALS3BP	PRDM1	WWP1
DYRK1A	LIMK1	PRKD1	YES1